R. & M. No. 3455

MINISTRY OF AVIATION

AERONAUTICAL RESEARCH COUNCIL

REPORTS AND MEMORANDA

Wind Tunnel Studies of Leading Edge Separation Phenomena on a Quarter Scale Model of the Outer Panel of the Handley Page "Victor" Wing, with and without Nose Droop

By R. A. WALLIS, M.ENG.

LONDON: HER MAJESTY'S STATIONERY OFFICE

1967

PRICE £1 6*s*. 9*d*. NET

Wind Tunnel Studies of Leading Edge Separation Phenomena on a Quarter-Scale Model of the Outer Panel of the Handley Page "Victor" Wing, with and without Nose Droop

By R. A. WALLIS, M.ENG.
DEPARTMENT OF SUPPLY, AUSTRALIA

Reports and Memoranda No. 3455
January, 1965

Summary,
Leading edge flows, present in the incidence range embracing the onset of general nose separation, have been studied experimentally. The effect of nose droop of these flows was established during the development of this device as a possible alternative to leading-edge flaps on the aircraft. Discrete air jets and vane type vortex generators were investigated in regard to both boundary-layer and hysteresis control. The influence of trailing-edge flaps on leading edge separation phenomena was also studied.

The concepts outlined in regard to the nature of nose stalling problems and the quantitative data presented should have application in respect to general wing design.

LIST OF CONTENTS

Section
1. Introduction
2. Test Objectives
3. Experimental Details
   - 3.1 Models
   - 3.2 Installation
   - 3.3 Scope of testing
   - 3.4 Air jet arrangements
   - 3.5 Vane type vortex generator arrangements
4. Definition of Separation Phenomena
5. Results
   - 5.1 Reynolds number effects
   - 5.2 Flow visualisation
     - 5.2.1 Original plain wing
     - 5.2.2 Original wing with lower surface air jets
     - 5.2.3 Original wing with lower and upper surface air jets
     - 5.2.4 Wing with plain drooped nose

*Replaces A.R.C. 19 227, 20 037 and 21 019.

5.2.5 Drooped nose wing with lower surface air jets
5.2.6 Drooped nose wing with lower and upper surface air jets
5.2.7 Drooped nose wing with trailing edge flaps
5.2.8. Flow studies of hysteresis
5.2.9 Effect of inboard leading-edge spoiler
5.2.10 Effect of pitot probe
5.3 Normal force coefficients
5.4 Pressure distributions
5.5 Minimum pressure coefficients
6. Discussion
6.1 Flow features
6.1.1 Separated vortex flows on swept wings in general
6.1.2 Flow at extreme tip
6.1.3 Inboard origin of separated flow vortex
6.1.4 Hysteresis
6.1.5 Leading edge droop
6.1.6 Trailing edge flaps
6.1.7. Spanwise control of separation
6.1.8 On flow separation
6.2 Application of test data to assessment of Victor wing modification
6.3 Design criteria
6.4 Usefulness of air jets
Acknowledgment
Notation
References
Tables 1 to 8

1. *Introduction*

The project had its origin in a request from Handley Page Ltd. for an assessment of the probable effectiveness of discrete air jets as a method of boundary-layer control on the 'Victor' bomber aircraft. This was associated with a desire to replace the leading edge flaps with a less complex device while retaining an equal degree of effectiveness as regards maximum lift and aircraft stability. The assessment (Ref. 1) was encouraging in its findings and as a consequence low-speed wind tunnel tests in the 13 ft. × 9 ft. wind tunnel at N.P.L. were planned.

When designing the model consideration was given to previous experience gained by the author in Australia. It was found that satisfactory results relating to nose stalling phenomena could be obtained only on models possessing moderately large chords; for the present tests the minimum chord was fixed at 3 ft. This limitation prohibits the testing of a complete half-span wing and hence the model is restricted to the outer panel of the wing; the panel has a leading edge sweep of 35° and comprises half the semi-span.

Wind tunnel data obtained by Handley Page Ltd. on a complete model show that the initial onset of general leading edge separation is associated with the outer panel of the wing. Since the object of the present tests is the maintenance of unseparated conditions on the critical part of the wing for local lift coefficients slightly in excess of those on the actual wing at the desired usable lift, tests on the part-span model are considered appropriate and valid. The difference in spanwise loading between the model and the complete wing is relatively unimportant in tests of this type.

From the aircraft point of view, however, it is important to ensure that, with the incidence of separation on the actual wing, the subsequent flow is such as to give a relatively gentle stall with adequate stability. Within the limitation imposed by the model, some qualitative comments are made in this paper concern-

ing the probable development of the stall on the actual wing in the proposed modified condition.

Experiments on the part-span model were conducted in three separate series within the period, May 1956 to June 1957. The specific objective of each series is outlined in the next Section.

The test results were originally published in three separate interim notes. The present report seeks to combine the dominant features of these papers into a single account from which certain general conclusions can be drawn.

2. *Test Objectives*

The initial testing was concerned with the development of the discrete air-jet device in an attempt to achieve a sufficient degree of boundary-layer control near the leading edge. There are two separate tasks which can be achieved by a device of this kind, namely,

(i) Use of a row of air jets midway between the stagnation point and the leading edge for the purpose of suppressing the laminar separation bubble and eliminating its undesirable consequences.

(ii) Installation of a row of air jets, on the suction surface, for the purpose of delaying turbulent separation in the vicinity of the aerofoil nose.

A measure of boundary-layer control was achieved with the device on the basic wing, that is without nose flaps, but this improvement was insufficient to meet the relatively ambitious target set. An analysis of the results revealed that the required pressure recoveries in the region of the leading edge were somewhat greater than those of the original Handley Page Ltd. estimates. A continuation of the work, however, was considered desirable.

In an endeavour to overcome the above difficulty, fixed nose droop was designed into the wing with a view to halving the estimated C_{pmin} that is peak suction coefficient, at the desired maximum usable lift.

Insufficient was known about the effects of fixed nose droop to engender confidence that a satisfactory solution could be obtained at the first attempt and hence two further series of tests were envisaged. The first of these two studies was planned to provide information on, (a) the accuracy of the method used in calculating leading-edge pressure distributions, (b) the nature of the leading-edge separation problem, and (c) the probable usefulness of discrete air jets as a means of boundary-layer control on a modified wing. The wind tunnel results were to be used in designing a second nose droop considered suitable for installation on the aircraft.

The improvement obtained with the first droop was so marked that Handley Page Ltd. decided to concentrate on fixed nose droop alone as an alternative to the existing hinged leading-edge flaps; the second droop was therefore designed with this in mind.

At the time of the wind tunnel tests on this latter re-designed leading edge, Handley Page Ltd. had no plans for further pre-flight experiments; this had a pronounced influence on the test schedule. In addition to checking the behaviour of the modified wing, preliminary information was sought on the effect of trailing edge flaps on the general nose separation properties of the wing. Other matters of interest included the high incidence behaviour of the curved tip, the influence of the aircraft pitot tube located near the tip, and the effect on the stall of the vane type vortex generators which exist on the actual aircraft for the delay of high-speed buffet. Limited experiments were carried out with discrete air jets and with vane type vortex generators in the vicinity of the leading edge; this work was aimed at reducing the large hysteresis encountered in the wind tunnel on the plain wing at the higher Reynolds numbers, and at maintaining orderly flow over the wing tips when general nose separation was present inboard. The use of boundary layer fences was also briefly investigated.

3. *Experimental Details*

3.1. *Models*

The basic wing is an exact quarter scale model of the outer Victor wing, Fig. 1, with the exception that no aileron is fitted. Wing thickness is 8 per cent at the root and 6 per cent at the tip when referred to the

chord length in the mainstream direction; the tip 'section' is defined in Fig. 1. The sections do not correspond exactly to any standard profile but are similar to NACA 'low drag' aerofoils. A small amount of camber is employed which increases as the tip is approached. In addition, the wing is twisted with decreasing incidence towards the tip.

The model was designed and built by Handley Page Ltd. The spars and selected ribs were made out of aluminium while the remainder of the model was of wooden construction with extensive use of plywood. The first 11 per cent of chord was detachable from the rest of the model and constructed so that compressed air up to 5 p.s.i. could be fed to the pressure box formed by the plywood skin and dummy spar member. Adequate ribs were used for the purpose of retaining the nose contour under pressure conditions.

For the second and third series of tests, the detachable nose was replaced by new units possessing the desired droop. The first droop was based on the NACA 220 camber line which is characterised by a camber restricted to the first 15 per cent of chord and a curvature which increases as the leading edge is approached. At 11 per cent chord the curvature is hardly perceptible and hence, since this point corresponds with the joint of the removable nose, no practical difficulties arise on this account. At the leading edge the tangent to the camber line makes an angle of over 20 deg with the basic chord line, for the amount of droop adopted.

The choice of droop was influenced to some degree by the general appearance of the modified nose. It was appreciated that excessive camber could introduce undesirable features into the low lift characteristics of the aircraft. As a consequence, the degree of camber used was restricted and, in order to obtain the full reduction in $C_{p\,\mathrm{min}}$, at the desired lift, the leading edge radius was increased.

The second droop consisted of a 2 per cent chord extension forward of the leading edge (*see* Fig. 2) and was designed so that the new nose shape faired into the existing contour, being completely external to it. These requirements were suggested by the desire to attach an additional skin to the nose flaps of an existing Victor aircraft in order to facilitate a simple flight test of the device. The droop and leading-edge radius of curvature were adjusted so that the computed values of $C_{p\,\mathrm{min}}$ at the desired usable lift were similar to those obtained on the previous drooped nose. The nose profiles at four spanwise stations for both droops are illustrated in Figs. 3 and 4.

Each drooped nose unit possessed a single pressure chamber as distinct from the basic nose unit which was partitioned along the chordline. In this latter case, the air supply to each of the two boundary-layer control applications listed in the introduction could be independently controlled.

The planform of the wing tip used in the second series of tests differed from the original shape. The decision on this matter was largely one of manufacturing expediency; for the type of test envisaged, tip shape was not considered to be of vital importance.

The suction surfaces of the modified wing tips were shaped so as to incorporate the fixed nose droop in a smoothed, faired manner. This led to unusual undersurface shapes near the leading edge but these did not produce any aerodynamic difficulties.

The modified leading edges were designed and constructed by Handley Page Ltd; this work included the aerodynamic design of the nose profiles.

In all three versions of the wing, flush surface static tubes are provided for the purposes of (i) estimating lift and (ii) determining the peak suctions at the leading edge and their accompanying adverse pressure gradients. Near the leading edge these tubes are very closely spaced in order to achieve the required degree of experimental accuracy. The spanwise locations of the stations, Figs. 1 and 2, chosen for this work are similar to those used by Handley Page Ltd. in the computation of pressure distributions on the Victor wing in its original configuration.

The trailing edge flaps on the Victor are of a Fowler type, but for a number of reasons it was impractical to reproduce this type of flap on the present model. Hence, in the third series of tests, the effect of flaps was simulated by split flaps of 20 per cent chord, deflected at 45 deg relative to the chord line. These were employed in two configurations, namely, part-span and full-span. For the type of information sought, these arrangements were considered to be sufficiently relevant.

3.2. *Installation*

The model was mounted vertically in the 13 ft × 9 ft N.P.L. wind tunnel on a rotatable base plate, the incidence being adjustable from outside the tunnel by means of a screw mechanism. The lift force tending to bend the wing about the root fixing was countered by means of a brace-wire and strut arrangement fixed at one end to the tunnel wall and attached at the other to a rib by means of a pin connection; the pin was co-axial with the turntable and was located at approximately the mid-point of the working section.

A removable skin panel on the lower surface of the wing facilitated the compressed air connections to the nose pressure-box and the installation of the pressure leads connecting the surface tubes to the manometer. These leads passed through the model ribs and the turntable to a multiple switch box. On the selection of a particular spanwise station, the corresponding pressures could be displayed on a 40-tube manometer.

The root chord of the model was taken as a datum and incidences have been measured with respect to it.

3.3. *Scope of Testing*

The major part of the work was in connection with the high incidence characteristics of the wing. However, the use of excessive fixed nose droop can adversely affect the low incidence behaviour of the wing; this problem was also studied experimentally but on a limited scale.

In addition to obtaining quantitative data on the local lift coefficients, obtainable prior to general nose separation, it is equally important to know the nature of the nose stall associated with any particular configuration, for the purposes of making an assessment and devising improvements. Hence flow visualisation studies with tufts and the well known titanium oxide/paraffin technique were undertaken at incidences before and after the onset of general nose separation. The white lines on the model facilitated comparative work.

The wind speeds and the mean chord Reynolds numbers pertaining to various aspects of the test programme are tabulated in Table 1.

In test cases involving the use of air jets and/or nose droop it is possible to carry out testing at a decreased Reynolds number without incurring the risk of operation too close to the critical Reynolds number. In addition, with the attainment of very large negative surface pressure coefficients, it is desirable to restrict wind speed in order to keep the experiments within the scope of the 90 in. high measuring manometer. These factors had an influence on the choice of the appropriate wind speed for any particular configuration.

3.4. *Air Jet Arrangements*

The location, size and type of air jet used in the various applications were, generally speaking, fixed largely as a result of past experience with the device (Refs. 2 and 3), although some further development did occur. As mentioned in Section 2, the jets fell into two general classes, namely, (a) lower surface (L.S.) jets for the suppression of laminar separation and (b) upper surface (U.S.) ones for controlling turbulent separation over the forward portion of the wing.

The arrangements adopted when carrying out tests aimed at assessing the merit of the device are listed in Tables 2 to 4.

All distances are measured along the surface, at right angles to the leading edge or parallel to it. Also, the holes inclined in the crossflow direction were drilled so that each jet issued from the surface in the direction of the wing root. The vortices so created were then of a co-rotating type which, on the wing surface, opposed the usual boundary-layer spanwise outflow.

The quantity of air used for each configuration with airjets operative was established from experimental curves of $\alpha_{N.S.}$ versus C_Q. These curves have a flat peak and hence it is difficult to ascertain a true optimum. The data presented in Table 5 for the test arrangements listed in Table 3 may be taken as

representative of near-optimum C_Q values for this type of air jet device.

The greater quantity of air used by the lower surface jets for the last two configurations was due to the use of a common pressure box for all jets. With a compartmented nose, the total C_Q for the last arrangement would be reduced to 0·00044.

Test experience to date has shown that C_Q is decreased with increasing Reynolds number and hence the above figures should be pessimistic. In the original assessment of C_Q for an air jet application to the Victor, a figure of 0·0005 was quoted (Ref. 1).

3.5. *Vane Type Vortex Generator Arrangements*

The two alternative arrangements of lower surface vanes tried in the final series of tests are given in Table 6.

In view of marked hysteresis effects present during the testing of the wind tunnel model fitted with the second nose droop, this device was developed for the purpose of providing a safeguard against this phenomenon during flight trials on the final nose droop. This step was taken as a result of the Handley Page Ltd. decision not to use air jets as a method of flow and hysteresis control in the present instance.

Although it was not expected that the existing upper surface vane type vortex generators, as used for suppressing shock-induced separation, would exercise any major influence on the nose separation properties of the wing, some testing was considered desirable. The vanes of $1\frac{7}{8}$ in. chord and $\frac{5}{16}$ in. height were spaced at intervals of 4.3 in. along the 25 per cent chord line. Each vane was set at an angle of 20 deg to the flight direction in such a sense as to produce vortices which oppose the boundary-layer outflow due to sweep. The most outboard vane was located $\frac{1}{2}$ in. inboard of the joint between the wing proper and the curved tip.

4. *Definition of Separation Phenomena*

Prior to presenting and discussing the results obtained, the phenomena associated with leading-edge separation will be briefly defined. It is well known that an adverse pressure gradient near the leading-edge of an aerofoil will cause separation of the laminar layer from the surface. When this separation first becomes apparent as the incidence is increased, the separating layer re-attaches itself to the surface along a line which is less than 1 per cent of the chord downstream of the separation line, provided the Reynolds number is not too low.

As incidence is further increased, a state is reached where a sudden breakdown in the flow around the aerofoil nose occurs. In the case of thin aerofoils, re-attachment of the flow as a turbulent layer usually occurs at a distance downstream of the leading-edge which is ten or more times greater than the length previously referred to.

The first separation phenomenon is referred to as a 'laminar separation bubble' and the second as 'general nose separation' or 'nose stalling'. The latter is the one with which this paper is mainly concerned.

From two-dimensional experimental studies (Ref. 4) it is known that the nature of the flow phenomenon giving rise to nose stalling is dependent on Reynolds number. At low Reynolds numbers, the onset of general separation with increasing incidence appears to be related to a breakdown of the momentum transfer mechanism at the downstream edge of the bubble. At moderate to high Reynolds numbers, turbulent separation from just downstream of the closed bubble initiates the collapse of the nose flow. For intermediate Reynolds numbers, both phenomena play an interrelated part. The actual Reynolds number defining the upper boundary of this intermediate region is a function of free stream turbulence, surface roughness and pressure gradient. Since the problem is closely related to the phenomenon of laminar boundary-layer transition large variations in the critical Reynolds number are inevitable, as confirmed by practice.

5 *Results*

The inclusion in this paper of all results presented in the interim notes would be impractical. A selection has been made and, in order to preserve continuity of thought on any particular aspect of the work, the preliminary discussion is included in the general presentation of experimental data relevant to the matter under study.

5.1. *Reynolds Number Effects*

As a measure of the scale effect $\alpha_{N.S.}$, the angle of incidence at which general nose separation first appears on the wing, is taken as a parameter. The results for all three test series are given in Figs. 5 to 7. By reducing incidence until the nose flow suddenly re-attaches itself to the surface, a measure of the flow hysteresis can be obtained; the angle of re-attachment, α_R, is also included in the preceding figures.

In the absence of the air jets or vanes, the appropriate curves demonstrate two very significant features. Firstly, $\alpha_{N.S.}$ rises sharply over a relatively narrow Reynolds number band and secondly, for the drooped nose cases shown, the hysteresis is considerable; no hysteresis data are available for the original model configuration.

An interesting phenomenon occurred within the speed range, 120 f.p.s. to 160 f.p.s., in the case of the original leading-edge, Fig. 5. Subsequent to the onset of general nose separation, flow unsteadiness occurs, evidenced by continual changes in the spanwise extent of the separation. The frequency with which this phenomenon moves along the leading edge is less than one per second. Static pressure distributions, with the characteristic region of constant pressure just downstream of the suction peak, provided evidence of a relatively large laminar separation bubble, prior to general nose separation, for speeds less than 120 f.p.s.; for speeds greater than 160 f.p.s. the bubble was approximately halved. A similar unsteady phenomenon was observed on a NACA 64A006 wing of 50 deg leading-edge sweep (Ref. 2) within the critical Reynolds number range.

In view of the great similarity between flow features in the present investigations and those in the experimental work which established the two distinct mechanisms initiating nose stalling (*see* Section 4), the foregoing Reynolds number features can be explained in terms of such phenomena. At the lower Reynolds numbers the usual theory of nose stalling applies, namely, the onset of instability in the laminar separation bubble. At the higher numbers, turbulent separation has a dominant initiating influence; strong support for this view is available from the oil film work described later. Therefore, for Reynolds numbers within the critical range, the changing nature of the nose separation phenomena could have a strong influence on the flow instability described above.

This tendency to instability was greatly reduced on the wings possessing fixed nose droop. Instead appreciable hysteresis was present; the degree increased with increasing Reynolds number throughout the critical range and then remained relatively constant up to the highest wind speeds employed. The significance of this hysteresis characteristic is discussed in detail in Section 6.1.4.

From past experience (Ref. 4) it is known that the laminar-separation bubble, and hence the problems associated with it, can be virtually eliminated by suitably placed lower surface air jets. When this device is employed, turbulent separation from near the leading-edge initiates general nose stalling as incidence is increased. Since elimination of the 'bubble' is the major function of the device, nose stalling incidences should be relatively constant with Reynolds number. The latter feature is clearly evident in Figs. 5 and 6; for the drooped nose cases the values closely approximate those for above-critical Reynolds number conditions on the plain wings.

From the results of Figs. 5 and 6 it can be inferred that the lower surface air jet device, because it has a similar effect to high Reynolds numbers on the laminar separation bubble, will show marked gains in $\alpha_{N.S.}$ only at the lower Reynolds numbers.

When upper surface air jets are used in conjunction with lower surface ones, the results are somewhat similar in regard to changes in $\alpha_{N.S.}$ with Reynolds number, Figs. 5 and 6. An exception exists for the case of the first droop nose, Fig. 5; at the lower Reynolds numbers, the use of two rows of upper surface air

jets resulted in a nose stall which lacked the clear-cut characteristic observed in other test cases. Hence too much significance should not be placed on the relative increase in $\alpha_{N.S.}$ at the lower Reynolds numbers.

Results for vane type vortex generator configurations show similar Reynolds number trends to those established with air jet arrangements.

5.2. *Flow Visualisation*

The two techniques used were briefly introduced in Section 3.3. Tufts were extensively employed during the tests involving surface pressure measurements and nose stalling studies. For a detailed analysis of wing flow, however, the titanium oxide/paraffin technique is vastly superior. Hence, with very few exceptions, the illustrations presented apply to the latter method of flow visualisation. In all instances the flow studies were confined to Reynolds numbers above the relevant critical values.

For the purpose of demonstrating the close agreement which exists between the two methods, three different examples are chosen from the first series of tests on the original nose. The complex flow illustrated by the oil technique can be traced in the tuft pattern, Fig. 8. In the second case, the pronounced spanwise deflection of one tuft is matched by a local region of high outflow in the case of the oil flow pattern, Fig. 9. Finally there is good agreement in the case of the separated flows shown in Fig. 10.

Local surface outflows, whether near the trailing or leading-edges, are indicative of the inability of the turbulent layer to transfer sufficient energy to the particles near the surface for the purpose of maintaining their downstream motion in the face of a severe adverse gradient. In other words, such outflows are an indication of approaching turbulent separation. As the trailing edge is closely approached the outflows become progressively larger. However, it is possible for outflows near the leading-edge to reach a maximum within a short distance and then experience a reduction in magnitude as the adverse pressure gradient eases at first slowly and then rapidly from the extreme value existing just downstream of the point of maximum velocity. This reduction is indicative of boundary-layer recovery, that is a movement away from the turbulent separation state. The two-dimensional data presented in Refs. 5 to 7 provide experimental support for this recovery argument. Considerable use will be made of the above feature in interpreting the flow patterns.

5.2.1. *Original plain wing*

The onset of general flow separation from the leading-edge was sudden and unattended by any noticeable outflows in the vicinity of the leading edge. Once separation occurred the spanwise extent of the leading-edge affected was appreciable suggesting that the critical region was located some little distance inboard of the tip. From Fig. 8 it will be seen that there are three distinct vortices at intervals along the leading-edge. The vortex over the extreme curved portion of the tip is believed to arise in the same manner as the vortex on a highly swept wing. The inboard vortex is identical to the type found on wings of fairly moderate sweep but an explanation for the intermediate vortex is not so readily found. With an additional incidence of 0·5 deg, the intermediate vortex remained fixed while the inner one moved further inboard to a point approximately 41 in. from the wing root. At 12 deg of incidence, however, severe buffeting was experienced making further tests impractical; this event could possibly be ascribed to a sudden and unsteady change in the vortex flows.

From the results described in Section 5.1 it would appear that the above tests were carried out at an above-critical Reynolds number. However, in view of the above unusual results, and with the data available from the next sub-section, some reservation is in order. The vertex of the intermediate vortex almost certainly marks the critical leading-edge region; the nature of the flow in this region before and after separation is, however, not clearly understood.

5.2.2. *Original wing with lower surface air jets*

The surface flow just prior to nose stalling, Fig. 9, indicates an outflow maximum between the 5 per cent and 10 per cent chord positions; downstream of approximately 15 per cent chord the outflow has disappeared. Since the main function of the air jets is the suppression of the laminar separation bubble, these flow patterns can be considered representative of the high Reynolds number case. Direct support for this statement is available in subsequent sub-sections.

With a small increase in incidence beyond 12 deg the flow separates from the nose due, it is believed, to the onset of turbulent separation in the critical region; this spanwise region is identical to the one assumed in the case of the plain wing. The intermediate vortex is no longer in evidence (*see* Fig. 11). In general the vortex pattern is more regular than for the case of the plain wing. Up to incidences of 13·5 deg there is no sign of heavy buffeting.

5.2.3. *Original wing with lower and upper surface air jets*

At an incidence of 13 deg, Fig. 12, just prior to the nose stall, the upper surface air jets appear to have re-energised the turbulent boundary layer in a very pronounced manner with the forward tufts possessing an inflow characteristic. General nose separation occurs, however, at an incidence of 13·25 deg. It was established that the problem of maintaining the leading-edge flow is related to flow conditions over the curved wing tip, as discussed in Section 6.1.2.

The flow pattern for 13·5 deg of incidence shows only one major vortex, Fig. 10. At a slightly greater incidence the flow at the extreme tip becomes noticeably more disturbed and slight buffeting commences.

5.2.4. *Wing with plain drooped nose*

The type of flow present is relatively independent of the actual droop nose tested and hence the phenomena are described in relation to the first droop only.

Appreciable outflows are present in the region of 15 per cent chord about 60 in. from the wing root, for an incidence of 18 deg, Fig. 13. This fixes the most critical region from the point of view of turbulent separation and demonstrates the effect of droop in moving the chordwise location of such a region further aft from the leading-edge. It will be observed that flow conditions at the extreme tip are satisfactory. Since the planform of this tip differs from the original one it might be supposed that the improvement is due to this modification; however, a return to the original tip planform, on the second droop nose model, did not re-introduce the problem. Hence the streamwise re-shaping of the tip sections in blending with the wing nose droop has apparently contributed to a more stable flow condition.

At an incidence immediately prior to the onset of general nose separation, Fig. 13 (18·75 deg), the outflows turn towards the leading edge and a region of relatively stagnant air appears just inboard of the tip. It is remarkable that relatively orderly flow and large suction peaks can be maintained in the face of such conditions.

When nose stalling occurs, however, there is a big change in the flow pattern. Buffeting is now present and there is some loss of lift near the tip. The inboard extremity of the general vortex flow is located in the region of 15 per cent chord and not in the close proximity of the leading edge [*see* Fig 13 (19 deg)]. Although not so pronounced as in the case of the original plain wing, the vortex springing from the leading-edge at station B is still in existence and once again no explanation is offered.

5.2.5. *Drooped-nose wing with lower surface air jets*

As in the preceding instance the comments will be confined to tests on the first droop. The main effect of the air jets is to delay slightly the onset of general nose separation.

With nose separation present at 19 deg, Fig. 14, that is the angle of attack for which a re-attachment of the flow with decreasing incidence is imminent, the flow is attached back to say 6 per cent chord with the exception of the leading edge region just inboard of station B; this is the critical region. Once separation is eliminated here, the flow is immediately re-attached to the whole upper surface. It is of interest to compare the flow patterns at this incidence with and without air jets operative, Figs. 13 and 14. The improved control over the boundary layer around the nose, when using air jets, is self evident; this feature is responsible for the greatly reduced hysteresis associated with the device. The reason for the differing spanwise extent of general flow separation on the wing is, however, not readily apparent.

5.2.6. *Drooped-nose wing with lower and upper surface air jets*

Air jets on the upper surface of the first droop-nose model have revitalized the turbulent boundary layer flow over the forward portion of the wing, even for a single row of jets, Fig. 15. When the flow eventually breaks down in a more or less general manner at $\alpha = 20{\cdot}5$ deg, separation does not reach forward to the leading edge.

The elimination of a critical region close to the leading edge has been accompanied by an increase in the outflows near the trailing edge. This is probably due to two factors, namely (a) an increase in boundary layer thickness due to increased mixing and (b) the unsuitability of the small scale superimposed mixing for the purpose of dealing effectively with momentum transfer in the thick turbulent layer at the rear of the aerofoil.

On increasing the incidence to 20·25 deg, Fig. 15, the outflow region has extended forward to the region of 10 per cent chord. At this incidence tufts indicate steady flow, the pressure distributions are qualitatively similar to those for unseparated flow, and buffet, in the accepted sense, is absent.

The surface flow, subsequent to nose stalling, is shown for $\alpha = 20{\cdot}5$ deg, Fig. 15. Buffet is now appreciable, the flow over the outer part of the wing is unsteady and the pressure distributions show a distinct nose separation. A comparison of the flows for incidences of 20·25 deg and 20·5 deg show appreciable differences only in the region of the vortex 'origin'. (On the basis of pressure distributions, however, the changeover is abrupt and clearly defined.) The similarity in the flow patterns near the trailing edge would suggest the predominance of the pressure gradients in dictating the direction of the surface flow in both cases.

In an attempt to reduce the outflows over the rear of the wing, a second row of jets at increased pitch was provided as far downstream as the pressure box of the model would permit. This added row delayed the forward movement of the outflows as will be seen in Fig. 16. It is believed that jets at 50 per cent chord with a pitch of approximately 2·5 in. would have been a far more appropriate arrangement.

When nose stalling occurs, Fig. 16 (20·75), the surface flow pattern resembles that experienced with the other test arrangements under similar conditions.

A point of interest is the manner in which the vortices arising from the front row of upper surface jets roll up to lose their identity in the vortices created by the aft jets. This is a feature which encourages the development of multiple air jet arrangements for the control of turbulent boundary layers when the adverse pressure gradient produces large changes in thickness over the surface in question. It will be noted that the flow over the tip extremity is reasonably good thus suggesting it is not a dominant factor in these droop nose tests.

5.2.7. *Drooped nose wing with trailing-edge flaps*

These tests were confined to the second droop nose configuration. Flow patterns for the no flap, part-span flap and full-span flap cases just prior to nose separation (α = 18·5 deg, 16·5 deg and 15 deg respectively) are shown in Figs. 17 to 19. The main feature is the negligible difference in regard to nature and location of the impending general nose separation phenomena. Another point of interest is the tendency of trailing-edge flaps to reduce the degree of outflow on the surface over the aft portion of the chord. The presence of split flaps tends to cause a slight acceleration rather than retardation of flow over this part of the surface and this feature could explain the observed result.

The degree of hysteresis present is not altered by the addition of the part-span flap. However, with the full-span flap the flow re-attaches at an angle 1·9 deg less than $\alpha_{N.S.}$ for 140 f.p.s. This reduced hysteresis is related to a less extensive spread of separation at the nose stalling incidence. The degree of spread was greatest for the no-flap case [*see* Fig. 17 (18·5 deg)].

5.2.8. *Flow studies of hysteresis*

The marked increase in hysteresis for the second droop nose model prompted a flow study of the phenomenon. A decrease in incidence from 18·5 deg to 16 deg reduces the spanwise extent of general nose separation by only 15 in. but the orderly vortex over the curved tip is re-established, Fig. 17. When with further decreases in incidence the 'origin' moves outboard to approximately midway between stations B and C, the flow suddenly re-attaches over the entire leading-edge.

Keeping in mind the flow characteristics which initiated the nose stall in the first instance, and giving consideration to the flow pattern at the vortex 'origin' in Fig. 17 (16 deg) it seems certain that the flow is separating from the leading-edge as a laminar layer with the inboard flow constituting a fairly stable turbulent layer which experiences a diminishing degree of interference as the chordwise distance from the leading-edge increases.

The function of lower surface air jets in greatly reducing the degree of hysteresis is related to their ability to facilitate transition in the laminar layer thus ensuring that turbulent separation is the most important single factor. When the wing stalls out, for the air jet case, the 'origin' does not move very far inboard of the critical region and hence re-attachment with reducing incidence is readily achieved.

5.2.9. *Effect of inboard leading-edge flow spoiler*

For longitudinal stability reasons, flow separation at the wing tips must be delayed while the stall spreads from inboard areas. The use of air jets or vortex generators provides a means of 'grading' the leading edge from the point of view of the degree of susceptibility to flow separation. By placing a spoiler at 3 per cent chord, over the inner 30 in. of the first droop nose wing, separation was forced in this region. The ability of an air jet arrangement to maintain the tip flow is demonstrated in Fig. 20. A similar result was obtained for the second droop nose model and, in addition, the undersurface vane type vortex generators were equally effective.

With increasing incidence there is a progressive spread of general nose separation outboard from the spoiler region; the tip flow is under positive control and not subject to sudden changes in flow pattern.

5.2.10. *Effect of pitot probe*

The manner in which pitot probes are attached to wing tips can affect the onset of nose stalling. In the case of the second droop nose model, it is apparent from Fig. 21 that the probe is producing an undesirable result. As a consequence the probe was re-located in a slightly underhung position and interference effects were eliminated.

5.3. *Normal Force Coefficients*

Normal force characteristics were obtained at each of the four spanwise stations from graphical integration of the surface static pressures. Results are presented in Figs. 22 to 29 for the original wing and for the second droop nose model, which can be considered representative of both droop configurations.

In some cases there is a tendency for the lift curve slope to increase at the higher incidences. This is thought to be related to the relatively orderly flows which are present over the outer wing region at these incidences. The effect is similar to the well known increase in lift which results from general nose separation on highly swept wings at incidence. Other points of interest include (a) the ability of air jets or vane type vortex generators to maintain lift increases with incidence despite the presence of the inboard flow spoiler and (b) the serious loss of lift during the period of recovery from a wing tip stall condition, Figs. 26 to 29, with decreasing incidence.

A number of normal force coefficient distributions for the wing are presented in Fig. 30. For comparison, the theoretical design curve for the outer portion of the complete Victor wing plus body is superimposed. Although the differences might appear serious enough to invalidate the tests, it will be shown later that such is not the case.

The addition of the full-span flap results in a large increase in the normal force coefficient for a given incidence. The spanwise distribution at an incidence of 14 deg has a form which is similar to that pertaining to the unflapped case. The distribution for the part-span configuration is of interest since a force reduction occurs along the whole wing when the outboard portion of the flap is removed. However, there is still an appreciable force increment with relation to the no-flap case for this outer portion of the wing.

5.4. *Pressure Distributions*

In the case of the first droop nose model, a detailed study was made of the effect which the droop produced in relation to chordwise pressure distributions. The manner in which the leading-edge suction peak develops is illustrated in Fig. 31; once established the growth is relatively rapid, Figs. 32 and 33. For a $C_{p\min}$ comparable with that for the original model, the rate and degree of pressure recovery in the case of the drooped nose are less, Fig. 32. These features would favour a downchord movement of the region critical to turbulent separation and a higher peak suction before the onset of flow separation; the results support these arguments. For incidences close to the nose stalling ones, however, the pressure distribution over the original and droop noses differ in degree, not basically.

The distribution of pressure on the lower surface, Fig. 34, assumes importance at low incidences. For incidences less than 4 deg there is a pronounced local separation with the flow re-attaching before reaching 20 per cent chord. This is surprising in view of the small suction peaks and adverse pressure gradients present. In the case of the second droop, the local separation is delayed at station C until the incidence has dropped to 0 deg. Reduced droop and the increased nose radius are responsible for this improvement.

This latter aspect of the droop nose investigation is of relevance for low incidence flight cases where speed is high and drag due to local separations is undesirable.

5.5. *Minimum Pressure Coefficients*

The numerical value of $C_{p\min}$ is a measure of the pressure recovery required and hence $C_{p\min}$ is one of the most important variables governing general nose separation. By controlling the spanwise variation of this parameter for a given wing lift coefficient, it is possible to initiate general leading-edge separation in the desired locality. Hence a detailed study of $C_{p\min}$ is of prime importance.

For a given aerofoil section there is a relationship between $C_{p\min}$, and C_{LL} which, to a first order, is not affected by three-dimensional influences. The relationships for all three series of tests are plotted in

Figs. 35 to 37; the effect of increasing wing thickness in reducing $C_{p\,min}$ for a given local lift is evident in the curves. (The wing varies in thickness from 6 per cent at the tip to 8 per cent at the root). The introduction of droop has resulted in a bodily shift of the plots to the right without altering the basic nature of the curves. There is, however, a suggestion of three-dimensional effects at station A for both droop nose cases.

The data presented in Fig. 35 clearly illustrate why the expectation in regard to nose stalling control, based on the assessment of Ref. 1, was not realised in practice for the original wing.

For a given C_N, the use of flap decreases the value of $C_{p\,min}$ at the critical station B, Fig. 38. This feature in the case of the part-span flap is related to the downwash field which extends well outboard of the flap termination.

At a given wing incidence, the section possessing the highest $C_{p\,min}$, is usually the one most susceptible to leading-edge separation. In Fig. 39, which presents the data for the second droop nose, station B appears as the most critical which, of course, agrees with the known facts. A cross plot of data for the three stations, Fig. 40, shows the relative independence to flap configuration of the critical station, a feature already established in the flow visualisation work.

The $C_{p\,min}$ attained at the critical station B just prior to nose stalling was increased slightly by the use of flap (*see* Fig. 38). The delay in the onset of turbulent separation as implied by this trend, is consistent with the reduced pressure recovery required in the vicinity of the leading edge; the application of flap increases the suction over the whole upper surface but near the leading edge this suction gain is relatively small.

6. *Discussion*

The discussion will be centred around (a) the basic flow problems associated with the control of general nose separation on thin swept wings, (b) the use of the test data in assessing the probable performance of the full-span Victor wing, and (c) the establishment of suitable design criteria. In some instances the comments are based on the author's experimental experience and overall understanding of the problems and hence not necessarily on fully documented proof. Some of the ideas are now widely known whilst others should be accepted as tentative only.

6.1. *Flow Features*

6.1.1. *Separated vortex flows on swept wings in general*

On highly swept wings at incidence, nose stalling leads to the well known type of leading-edge vortex which is characterised by (a) an increase in lift and (b) vorticity of an orderly nature. As a consequence, the forces acting on the wing are relatively steady which implies negligible buffeting. The type of surface pattern which results is illustrated in Fig. 41. (This photograph was taken by the staff of the N.P.L. Compressed Air Tunnel in connection with another investigation.)

The flow over a thin unswept wing at incidence is in contrast to the above. When nose separation occurs on such a wing, re-attachment takes place upstream of the trailing edge provided the incidence is not too great. In the separated region, particles move in a very disorderly manner.

On increasing the degree of sweep from zero, there is initially a mean outboard movement of the air particles in the leading-edge vortex flow with the particle motions remaining very irregular. With progressive increases in sweep, the particle paths become more regular as the mean outboard motion increases and as flow conditions associated with large sweep are approached. The final stages of the changeover to orderly vortex flow takes place over a relatively small range of sweep angles.

The type of vortex flow can usually be identified from the titanium oxide surface flow pattern. The strongly defined patterns of Fig. 41 signifies that the vortex flow is scrubbing right through to the surface and that the kinetic energy of the flow near the surface is high. This is a consequence of the known orderliness of the vortex flow associated with highly swept wings. Wings of moderate sweep possess a pattern in which liquid moving towards the leading edge is progressively turned in the direction of the vortex 'origin'. The speed at which the liquid moves is rapidly retarded during this process. This signifies that the

kinetic energy of the air particles is being rapidly exhausted thus allowing the pressure forces to exercise an increasing influence over the flow direction of the liquid. The inability of the vortex flow to transfer a worthwhile amount of the free stream momentum through to the surface flow could possibly be traced to the mixing losses associated with the disorderly nature of the vortex flow.

The Victor is an example of a moderately swept wing for which the flow patterns of Fig. 10 (13·5 deg and 14 deg) can be considered qualitatively representative. The flow unsteadiness which one associates with Fig. 10 (13·5 deg) is not sufficient to cause buffeting of any consequence. With increasing incidence [*see* Fig. 10 (14 deg)], the vortex flow in the vicinity of the tip loses all semblance of orderliness and this condition represents a complete stall at the tip. As illustrated in Fig. 22, a loss in local lift is experienced at this incidence.

Certain detailed aspects of the general nose separation problem will now be discussed.

6.1.2. *Flow at extreme tip*

In Section 5.2.3. reference is made to the difficulties which arise due to flow conditions at the extreme tip of the original wing; some characteristics of this flow will now be discussed.

The separated flow on the tip resembles that associated with highly swept wings, e.g. compare the surface flows of Figs. 8 (11 deg) and 11 (12·5 deg) with Fig. 41. At an early incidence this separation sets in at the very extremity of the wing and then moves forward along the curved leading edge with increasing incidence in much the same manner as the vortex flow progresses inboard on a highly swept wing.

The presence and development of this tip separation vortex can, in certain circumstances, initiate general nose separation. Attempts to improve the tip flow with air jets on the original wing were only mildly successful owing to the limited extent of the pressure box in the tip.

Similar difficulties due to the presence of the tip vortex were reported in Ref. 2.

It can be assumed that a separated flow vortex is present on all wing tips at moderate incidences irrespective of wing sweep or tip shape. However, since the vortex is an orderly one, the effect on the flow over the main wing may not be a detrimental one. During the tests connected with Ref. 2 a condition was noted, on a square tipped configuration, where with increasing incidence the flow just inboard of the tip separated from the leading edge over a small incidence range, and became re-attached to the leading edge for a similar incidence range before detaching again. It was surmised that the tip vortex possessed an action similar to that of a vortex generator and hence was exercising a small amount of boundary-layer control. The scale of the motion, however, was too large to permit worthwhile gains from such a vortex.

The presence of the separated flow vortex at the tip is normally of little consequence but assumes some importance when leading-edge boundary-layer control is attempted. No separation can occur at the tip in potential flow and hence it is of interest to postulate the type of flow which might be expected. Since there is a large spanwise gradient of lift in the vicinity of the tip, appreciable cross flows might be expected. At the trailing edge these cross flows constitute an intense vortex sheet which presumably rolls up in the wake.

The probable paths of air particles near the surface on the suction side are indicated in Fig. 42; these are based on surface patterns obtained when a limited amount of boundary-layer control was achieved over the forward part of the tip by means of air jets.

From the postulated flow directions, it appears that the flow over the tip leading-edge is, within a short distance, moving into a region of relatively high pressure or, in other words, moving against a severe adverse gradient. In practice, therefore, a boundary-layer separation readily occurs thus precipitating the roll-up of the vortex sheets before the trailing edge is reached.

The flow problem experienced on the original wing is not present on either of the droop nose models. It is suggested that the droop, which is continued into the tip, has moved the 'origin' of the vortex further outboard away from the critical region. In addition, the effect of droop in shifting the region critical to turbulent separation further downstream would also be of assistance. The smaller tip used on the first droop nose model produced an intense vortex of reduced overall diameter which is related to the increased leading-edge sweep angles of the curved tip. From visual studies this latter tip appeals as the more suitable one from a stall point of view.

6.1.3. *Inboard origin of separated flow vortex*

For brevity, the junction between unseparated and separated flows on the leading edge will be termed the vortex 'origin'. This definition should be used strictly in the above sense.

The flow in the region of the origin is an extremely complex one with the details varying from case to case. This can be traced to a rather complicated interaction between the various factors involved in the process of maintaining flow equilibrium. An attempt will be made to discuss some of the more obvious variables but it should be emphasised that the discussion is purely tentative.

The interaction of the vortex sheet, arising from general nose separation, with the inboard attached boundary layer is of prime importance. For the first part of this discussion, the Reynolds number will be assumed to be greater than the critical, i.e., nose stalling is not initiated by a breakdown in the momentum transfer mechanism of the laminar separation bubble. The turbulence generated in the vortex sheet is diffused into the adjacent attached layer and hence must produce a thickening of the turbulent layer as it approaches the chordwise region critical to turbulence separation. This feature will induce separation, at a given spanwise station, at a lower incidence than would be the case in the absence of such a vortex; the experimental evidence supports such a hypothesis.

The effect of the vortex layer on the adjacent boundary layer will depend greatly on the manner in which the leading-edge vortex sheet rolls up. If the sphere of influence of the vortex at the origin can be restricted by inducing the vortex to roll up in an efficient manner, then the origin might be expected to be further outboard than it would be otherwise.

Since the local air flow in the vortex passes outboard in the general direction of the vortex axis, conditions near the origin and further outboard must be interrelated. An inefficient rolling up of the sheet at the origin will, for obvious reasons, be felt in the outboard regions whilst irregular motions in these outer regions will increase the mixing losses and reduce the spanwise pressure gradients tending to induce an orderly vortex flow near the origin.

Experiments using spanwise blowing from the tip of a swept wing (Ref. 8) demonstrate an entrainment of the leading-edge vortex by the tip jet sheet. As a consequence, the rolled up vortex lies closer to the leading edge and the origin is further outboard at a given incidence.

General mixing in the separated boundary-layer vortex sheet must be interrelated with the re-establishment of boundary-layer flow downstream of the vortex. An improvement in the mixing mechanism, e.g. by means of some device, should result in a reduction of the spanwise extent of the vortex.

The increasing degree of outflow in the leading-edge separated flow as sweep is increased is due to the spanwise pressure gradient; the greater the gradient the more orderly can one expect the vortex motion to be. It is obvious therefore that the spanwise and chordwise pressure gradients of the attached flow in the vicinity of the origin are vital factors.

It would follow from such a statement that, for wings of equal leading-edge sweep, the thinner wing with the more intense gradients would possess the more orderly vortex. Some experimental results which tend to confirm this feature can be obtained from Refs. 2 and 9; in each case the leading-edge sweep was 50 deg but the thinner wing of Ref. 2 had the more orderly separated flow.

In concluding this discussion for wings at Reynolds numbers above the critical, attention is drawn to the fact that a complex interaction must exist between the pressure and inertia forces in both the attached and separated flows, particularly near the origin.

For Reynolds numbers below the critical, the rate at which the origin moves inboard with increasing incidence is very rapid. This can be illustrated from the present series of tests where, for the plain original wing, an increase of 0·5 deg in incidence was sufficient to move the origin from station A to station C at 80 f.p.s. as against 1·75 deg for 180 f.p.s. This touchiness of the flow can possibly be attributed to ultra critical conditions in the laminar separation bubble, whereas at 180 f.p.s. normal boundary-layer mixing processes tend to retard the development of the stall.

In the critical Reynolds number region (*see* Fig. 5), intermittency is experienced with the origin continually on the move leading-edgewise at a fixed incidence. This effect was also encountered in the tests of Ref. 2. It can be inferred immediately that conditions at the origin are not conducive to flow equilibrium. No precise explanation can be offered but an important factor is the leading-edge boundary-layer

Reynolds number which suffers a large reduction in magnitude when nose separation occurs on thin wings. Since relatively smaller changes are required to change the nature of the nose stall, as defined in Section 4, it is not altogether surprising that the flow in the vicinity of the origin will tend to hunt from a low to a high Reynolds number type of nose separation.

The deductions which might be drawn from the foregoing discussion are as follows: the vortex origin on a given wing will move outboard if,

(*a*) the laminar separation bubble is suppressed,

(*b*) suitable turbulent boundary-layer control is applied,

(*c*) the entire separated flow vortex sheet is induced to roll up in an orderly manner by means of some device, e.g. *see* Ref. 8.

The origin in the case of nose droop is located further from the leading-edge. The shear layer separating from the leading edge progressively affects the attached inboard flow until the region critical to turbulent separation is passed. A similar flow condition is present on the Avro 707 delta with the modified droop leading edge (Ref. 10). Since the whole problem of flow hysteresis is closely related to flow phenomena at the origin this aspect will now be considered in some detail.

6.1.4. *Hysteresis*

It will be seen from Figs. 5 and 6 that the question of hysteresis is a very important one; difficulty in re-establishing flow over an aircraft wing could well be serious.

Hysteresis is always present, in varying degrees, when a region critical to flow separation develops inboard from the tip extremity and/or upstream of the trailing edge. It is rarely present, however, when separation sets in at an early incidence at the tip of a swept wing or moves forward slowly with incidence on a rear stalling type of wing.

An attempt will now be made to discuss some of the factors involved in the phenomenon. Hysteresis means that at a given incidence two alternative types of flow can be present. It would therefore be instructive to study the main features of such flows in the region where the flow leaves the surface. The example chosen is a two-dimensional nose stalling type of aerofoil at high Reynolds numbers, i.e., *nose separation is the result of turbulent separation from a region just downstream of the leading-edge.*

(*a*) *Attached flow*

The turbulent boundary layer will, at incidence, suffer deterioration as it moves downchord into the critical region. Downstream of the critical region, however, the boundary layer is re-energised as momentum transfer once again becomes adequate.

In avoiding separation the boundary layer is able to transfer sufficient momentum to deal with the demands of skin friction and an increase in static pressure.

(*b*) *Separated flow*

It will be assumed initially that the separation point does not move forward to the laminar separation bubble. As the turbulent layer approaches the separation point, or more correctly the separation region, it has to deal with another factor in addition to skin friction and pressure rise. This factor is associated with the mixing which takes place in the separated flow; in the region where the flow leaves the surface one cannot ignore the interaction between the attached and separated flows. In its simplest concept one can consider the backflow along the surface into the region of separation. This reverse flow is halted by the momentum of the attached part of the flow. In actual fact the behaviour of the separated flow in this region of interaction is a very complex one but enough has been said to indicate its importance.

Hence before the boundary-layer flow can re-attach to the surface it has to deal successfully with this additional factor. The demands which the pressure rise makes on the layer must therefore be decreased by incidence reduction if re-attachment is to be achieved.

There are two interesting points which arise out of the above explanation. Firstly, it follows that once general separation occurs downstream of the leading edge it will move forward in order that equilibrium may be achieved at the separation point for a given incidence. This, on a thin symmetrical aerofoil, usually results in nose separation from the upstream edge of the earlier laminar separation bubble.

Secondly, when separation moves forward from the trailing edge of a rear stalling aerofoil it can be postulated that the separated flow exerts a first order influence on the position of separation, or in other words, calculations of skin friction and pressure gradient are not sufficient to permit an estimate of the separation point. Assume for argument that separation has moved forward to the 30 per cent chord position. Suppose boundary-layer control is applied at 60 per cent chord and the aerofoil incidence increased to the same value as before; if the foregoing argument is true, separation need not move forward to the 30 per cent chord position despite the fact that pressure gradients and skin friction at 30 per cent would be higher in the second case, where separation has been delayed, than in the first. Experiments which the author has conducted verify the result if not the reasoning.

In three dimensions the same phenomena are present. The appearance of the vortex origin (*see* preceding sub-section) in a region known to have boundary-layer stability in the absence of separation, is a case in point. It is therefore clear that hysteresis can only be fully understood when a detailed study is made of the interaction of separated and attached flows.

A study of the separation and re-attachment curves, Fig. 5 and 6, for the plain wing are of interest. At the higher Reynolds number, where hysteresis is relatively large, nose separation is initiated by a turbulent separation just downstream of the leading edge [*see* Fig. 13 (18·75 deg)]; the separation line in the critical region inboard of station B then moves forward to the laminar separation line, Fig. 13 (19 deg). The large hysteresis is therefore probably due to the poor momentum transfer properties of a separating laminar layer. Lower surface air jets or vortex generators, which were used to precipitate transition, produced a substantial improvement, Figs. 5 to 7.

A similar transition trend will accompany increasing Reynolds number. At a sufficiently high value the degree of hysteresis present should reduce to a minimum. The prediction of the minimum Reynolds number for this condition presents a major difficulty. As indicated in Section 4, free stream turbulence and surface roughness play important roles in the transition phenomenon. In this connection wind tunnel turbulance is of an appropriate scale to aid the transition process whereas atmospheric turbulence is normally on too large a scale. It is not surprising therefore that the phenomena observed in the wind tunnel are not present on actual aircraft until appreciably higher Reynolds numbers have been reached. From evidence available to the author it appears likely that most aircraft, near the stalling speed, operate below the Reynolds number applicable to negligible hysteresis, in the above context. For example, a hysteresis phenomenon occurred on the Avro 707A aircraft (Ref. 11) at a flight Reynolds number of approximately 12×10^6. After considerable difficulty the phenomenon was re-produced in wind tunnel tests (Ref. 10) over a limited Reynolds number range in the vicinity of $Re = 2 \times 10^6$. Wind tunnel and flight tests, (Ref. 12), on a Vampire fighter aircraft also highlighted the hysteresis problem in relation to aircraft control problems at the stall. It should be emphasised, however, that not all aircraft have a stall-out pattern which lends itself to hysteresis. The possibility must, nevertheless, be kept in mind during the wind tunnel and flight development of a new aircraft. A sudden and momentary change in incidence due to air gusts could have serious consequences if the aircraft is flying near its minimum speed.

The flow returning along the surface of the leading-edge in the vicinity of the vortex origin will influence the behaviour of the separating laminar layer in the plain wing cases. Hence the detailed flow differences introduced by droop at the origin might be expected to have an effect on hysteresis. The data available does not, however, permit any serious speculation on this question.

For low Reynolds numbers, the hysteresis for the plain wing cases is very small. It will be remembered that nose separation at these Reynolds numbers is assumed to arise out of a breakdown in the momentum transfer mechanism at the downstream edge of the laminar separation bubble. The initial boundary-layer conditions for both separation and re-attachment is therefore the same, namely, a laminar separation; however, due to a collapse of the suction peak in the latter case, the boundary-layer Raynolds number will be somewhat less. Further analysis is, however, unwise in view of the relatively unknown nature of the downstream mixing which occurs in either case.

The foregoing arguments regarding hysteresis have been suggested by the wind tunnel data which are available. It is not intended that these ideas should be accepted without qualification; the purpose in presenting this discussion is to arouse interest in this important fundamental problem.

6.1.5. *Leading-edge droop*

The large improvements due to droop can be attributed to the factors listed below:

(*a*) For a given C_L or α, the suction peak is greatly reduced, Fig. 36.

(*b*) At a given $C_{p\min}$, the total pressure recovery in the nose region is reduced by the introduction of droop, Fig. 32.

(*c*) Due to (*b*), the turbulent separation which initiates general nose separation is delayed to a greater $C_{p\min}$.

(*d*) The higher local velocity i.e. Reynolds number associated with this increased suction peak tends to restrict the size of the laminar separation bubble and hence minimises boundary-layer thickening due to such.

These improvements have, of course, been augmented to some extent by the increase in nose radius.

The introduction of droop has modified the problems associated with flow separation but has not altered the basic features. On the plain wing at the higher Reynolds numbers droop has shifted the region critical to separation downchord by at least 10 per cent. This has made the task of the upper surface air jets a little easier as greater time is now available for the establishment of a strong mixing action.

The above results focus attention on the problem of re-energising the boundary-layer flow over the rear of the wing. The adverse pressure gradients in this region have, due to the large incidence, increased to values approaching those found on thick rear stalling wings. In order to capitalise fully on the nose flow stabilising properties of the upper surface jets used, consideration must be paid to this additional problem.

6.1.6. *Trailing-edge flaps*

The main purpose of the tests with trailing-edge split flaps is to determine the probable influence of such flaps on the manner in which nose separation is initiated. Since trailing-edge flaps in practice usually terminate well short of the wing tips, the part-span configuration is the one with most interest. It is believed that these split flaps will have a less favourable effect on general nose separation than the modified Fowler type fitted to the Victor.

A few comments will now be made on the qualitative aspects of the nose separation and lifting characteristics of the part-span flap configuration. When compared with the unflapped case, the flow around the flapped part of the wing modifies that around the outboard portion in such a manner as to increase the effective incidence, thereby increasing the local lift for the incidence in question. $C_{p\min}$ is also increased, but the net result is favourable as the action of the flap is to reduce $C_{p\min}$ for a given C_{LL}.

Although the lift increase over the flapped portion of the wing is not so great as in the case of the full-span flap this is compensated for by the increase in lift over the outer part of the wing. This is a favourable trend from a longitudinal stability point of view.

The manner in which nose separation occurs and develops on the wing appears to be relatively independent of the flap arrangement. This supports the general belief that flap application does not necessarily introduce stability difficulties arising from nose stalling. With highly efficient slotted flap arrangements, the $C_{p\min}$ for a given local lift coefficient will be significantly less than in the present split flap cases.

6.1.7. *Spanwise control of separation*

The onset of general nose separation on the wing in question produces a relatively unsatisfactory type of stall insofar as the tip flow either initiates the separation or is incapable of maintaining an attached condition in the face of inboard separation. The reducing thickness chord ratio of the wing towards the tip contributes to this situation. However, the selective use of air jets or undersurface vortex generators, near the tips, is of interest from a flow control point of view.

From the normal force data of Figs. 26 to 29 for the second droop nose model it will be seen that (with spoiler) the vane type generators were a little more effective than the air jets in maintaining lift in the region of the tip. For the former a $C_{p\min}$ of —14 was recorded at station B just prior to a sudden collapse of the leading-edge flow at 19·5 deg of incidence. In the air jet case the largest suction recorded was at station C for $\alpha = 19{\cdot}5$ deg when $C_{p\min}$ reached $-12{\cdot}5$; at 20 deg of incidence a complete collapse of the nose flow had not occurred as $C_{p\min}$ at station B was still —7.

Some doubt exists concerning the validity of the spoiler results for the wing without jets or vanes but a general comment is in order. It would appear that a suction peak represented by $C_{p\min}$ of the order —10 can be attained over the outer part of the wing before the nose flow collapses at approximately 17·5 deg, due to the effects of the inboard spoiler.

An additional set of experiments concerns the use of a leading-edge boundary-layer fence on the second droop nose model. The fence, which was located at station C and extended to 60 per cent chord, yielded the results of Table 7.

Separation was evident in the leading-edge region inboard of the fence at an incidence of 12 deg.

Although there was a gain in $\alpha_{N.S.}$ for the air jet case, it is rather doubtful whether the lift at $\alpha_{N.S.}$ has been increased; no results are available.

An effective wing fence is normally associated with three flow features, namely,

(i) an early initiation of separation at the leading-edge on the inboard side of the fence,

(ii) increased boundary-layer stability on the nose just outboard of the fence, and

(iii) a delay in the process by which the inboard flow separation contaminates the outer wing flow.

In the present instance, nose droop introduces a large measure of leading-edge boundary-layer stability. In addition, tunnel wall image effects and the increasing thickness/chord ratio of the wing as the root is approached tend to minimise any possible improvement due to a fence on this model.

Finally, the sweep angle is only moderate and hence the spanwise flow of disturbed air is restricted. In the absence of any significant effect on the onset and development of general nose separation, exercised by the fence, it can be concluded that such a device in the present instance is inappropriate.

6.1.8. *On flow separation*

In concluding this sub-section of flow features it is relevant to draw attention to the problem of defining flow separation on swept wings. On the present wing there are six different conditions which could be referred to as separated flows, namely,

(i) Laminar separation bubble.

(ii) Flow separation at tip extremity which gives tip vortex [(*see* Fig. 15 (18 deg)].

(iii) Turbulent separation from critical region just downstream of leading-edge [(*see* Fig. 13 (18·75 deg)].

(iv) Turbulent separation moving forward from trailing-edge [(*see* Figs. 15 (20·25 deg) and 16 (21·25 deg)].

(v) Turbulent separation from the nose with which is associated buffet and a large scale vortex flow [(*see* Figs. 13 (19 deg), 14 (19 deg), 15 (20·5 deg), 16 (20·75 deg)].

(vi) Nose separation on lower surface at small incidences.

The first two have been dealt with in Sections 4 and 6.1.2. The third and fourth have a number of features in common. When air particles near the surface are grossly retarded due to inadequate momentum transfer the particles tend to develop increasing degrees of outflow as pressure forces dominate their flow direction. Since the flow at the edge of the boundary-layer is streamwise there is a large gradient and hence considerable vorticity is present in this three-dimensional 'vortex sheet'. In Fig. 13 (18·75 deg) the sheet which exists in the vicinity of 15 per cent chord and station B has been eliminated by the time the flow reaches the 30 per cent chord region; this is due to improved boundary-layer momentum transfer. In many instances, however, a recovery of this nature is impossible; with increasing outflow a condition is often reached where the sheet is no longer stable. A rolling-up process then occurs which results in a discrete vortex whose axis is approximately in the stream direction. This may occur on the wing, (Ref. 2), or downstream of it.

A study of the surface patterns of Fig. 13 (18·75 deg) illustrates the difficulty associated with locating the point at which turbulent separation occurs. Even although the pattern preserves some degree of regularity just outboard of station B it is fairly obvious that the particles have lost virtually all their dynamic head. Such a condition in two-dimensional flow would definitely constitute separated flow.

When the surface outflows increase towards the trailing edge there is a similar state of affairs. A comparison of Fig. 16 (20·75 deg and 21·25 deg) shows similar oil flow patterns over the rear of the wing despite the large change in the overall flow. For the case illustrated in Fig. 16 (20·75 deg) the flow is steady and surface tufts indicate flow directions in agreement with the oil pattern. When nose separation has occurred, Fig. 16 (21·25 deg), however, the tufts are grossly unsteady and hence the oil is indicating a mean flow drift. It is extremely likely therefore, that in each case the air particles near the surface have lost virtually all dynamic head. However, in the case illustrated by Fig. 16 (20·75 deg) the flow is nominally of an unseparated type.

The phenomenon referred to here as general nose separation has been illustrated in the surface flow patterns of Figs. 13 (19 deg), 14 (19 deg), 15 (20·5 deg) and 16 (20·75 deg) and described in a general manner in the preceding text.

In many swept wing cases there is no clear demarcation line between what one understands in relation to attached or separated flows. As a consequence it is difficult to convey a true picture of a particular flow if such a restricted terminology is used. A description of the type of large scale vortex flow present, however, would convey far more detailed information and avoid any misunderstanding.

6.2. *Application of Test Data to Assessment of Victor Wing Modification*

The preceding results have shown that the addition of modest droop to the leading edge provides a measure of flow control in the forward region which almost converts the wing into a rear-stalling one. With the assistance of air jets or vortex generators, flow separation is no longer initiated in the vicinity of the leading edge. These findings are directly applicable to the full-span Victor wing.

With trailing-edge flaps extended, the C_L of the Victor fitted with hinged leading-edge flaps is approximately 1·4. Since nose separation was known to originate on the 35 deg. swept section of the wing, the arbitrary target set was the attainment of a mean wing plus body lift coefficient of 1·2, flaps-up, before the onset of nose stalling. Lift will nevertheless continue to rise beyond this point and, with the trailing-edge flaps contributing to a $\Delta C_{L_{max}}$ in excess of 0·2, this target is definitely on the generous side. However, the margin is useful from the point of view of providing the possibility of leading-edge design adjustments to give the correct spanwise stall-out behaviour.

The normal coefficient required at the critical station C for a mean wing plus body C_L of 1·2 is 1·4, Fig. 30. For the second droop-nose model this figure is closely approached when employing air jets, Fig. 28. The nose stalling incidences reached on the first droop-nose model, using air jets, suggest that this configuration is also capable of providing the desired lift. For the plain wing in both droop-nose cases, the wing plus body C_L at the onset of nose separation at station C is estimated to be approximately 1·1. In view of the sharp increase in $C_{p\,min}$ with C_L at the higher incidences, large errors in regard to these C_L estimates are not likely.

Flight tests show that the stall for leading-edge flaps down and trailing-edge flaps retracted is initiated at the inboard end of the 35 deg swept wing panel tested in the present work. The separation occurs just downstream of the flap hinge line and spreads gradually to both sides and the trailing edge with increases in incidence. Flow over the outer part of the wing is retained until an aircraft lift coefficient of 1·1 is neared. This feature is responsible for the acceptable pitching moment characteristics of the aircraft at the stall.

In replacing the leading-edge flaps, therefore, a similar stall development must be sought. The present results indicate that it is technically possible to achieve this objective. By spanwise variations of nose droop and/or boundary-layer control, the initial onset of nose separation could be induced to occur at the appropriate inboard position. Adequate control over the outer wing flow, after stall initiation, could be arranged thus ensuring satisfactory longitudinal and lateral stability characteristics. From the test data available the application of trailing-edge flaps is not expected to alter the nature of stall development.

With the appearance of nose separation somewhere between the inboard and outboard extremities of the wing, the possibility of hysteresis should not be overlooked. Due to the relative ease with which vortex generators can be fitted to the Victor, their use on the outer wing regions of the prototype aircraft has been recommended as a precautionary measure. An experimental assessment of the device on the aircraft would also serve a valuable purpose.

(Subsequent to the work described herein, wind tunnel tests were carried out by the R.A.E. on a half model with a new 3 per cent chord extension drooped leading edge. Best results were obtained when the modified nose was terminated abruptly and without fairing at the inboard end of the 35 deg swept wing panel. This discontinuity apparently initiated the onset of separation in an appropriate locality.)

6.3. *Design Criteria*

The experimental data obtained are useful in relation to the design development of new wings. Normal design techniques can be applied in determining the distributions of thickness, chord, twist and basic camber. In the absence of movable leading-edge devices or with the necessity to demonstrate satisfactory stall characteristics on the clean wing, the wing leading edge must be designed to stall out in an appropriate manner at the desired lift coefficient. With turbulent separation just downstream of the leading edge initiating the stall (provided the flight Reynolds number is high enough) the most important variables are the magnitude and gradient of the pressure recovery taking place on the aerofoil nose. $C_{p\min}$ is a measure of the former and the latter is fixed by the nose contouring. Separation is imminent when $C_{p\min}$ reaches a value which is sensibly a constant for a given type of section.

In achieving the desired stalling characteristics, the leading-edge region must be the subject of detailed design modifications aimed at ensuring that the most critical leading-edge section is in the desired spanwise position; at the nose stalling incidence, the values of $C_{p\min}$ for outboard wing sections should have sufficient reserve in order to counter any tendency for the separation to engulf these outer regions.

The original calculations of $C_{p\min}$ at various spanwise stations on the Victor wing were shown to be completely unreliable. The experimental results suggested that, to a first order, each spanwise section could be treated as a two-dimensional one for which a unique relation existed between $C_{p\min}$ and C_{LL}. By the time the third and final droop (as tested by the R.A.E.) was designed, Handley Page Ltd. had developed a three-dimensional theory which was accurate in predicting the $C_{p\min}$ versus C_{LL} relation at any spanwise position.

Although the application of trailing-edge flaps does not appear to alter appreciably the stall-out properties of a wing, there is an obvious need for a method whereby the above vital relationship can be established at any station for any given flap system. However, due to the problem of establishing actual flow conditions in the vicinity of the flaps, there is little likelihood of a practical solution. Since the main outcome when using trailing edge flaps is the introduction of a bodily displacement of the $C_{p\min}$ versus C_{LL} curve along the lift axis, the magnitude of this displacement for representative flap arrangements would be useful design data; such data could, of course, be established from a series of carefully planned wind tunnel experiments. The present results do little more than illustrate the main features of the problem. As a guide to the values of $C_{p\min}$ for nose stalling, applicable to aerofoil sections of the type studied, the data of Table 8 are presented.

The above data relate to flow Reynolds numbers above the critical. Since aircraft wings normally stall at an incidence approximately 4 deg greater than that experienced in the normal type of low Reynolds number model testing, these data are the more relevant for design purposes. When the wing is highly tapered or the aircraft is relatively small, the Reynolds numbers will, for low speed flight, be in or below the critical range over part or all of the wing surface. Wherever possible, design steps should be taken to influence the leading edge flow for the purpose of establishing flows of an above-critical type.

The important changes in stall and hysteresis behaviour associated with the critical Reynolds number range, and the difficulty of correlating wind tunnel results and flight experience in this regard, provide a strong case for systematic wind tunnel and flight studies of the general problem. These would provide data which, in conjunction with the leading-edge design information presented above, would permit a more informed approach to the wing-stall design problem.

Once separation has occurred at the desired spanwise position, the subsequent development is of interest. Firstly, the inboard separation will, on the outer attached flow sections of the wing, reduce lift and hence $C_{p\,\min}$. Secondly, the outboard flow will remain attached only if the resulting $C_{p\,\min}$ in the area is less than a limiting value, which will obviously be a function of detailed wing design features. With the spoiler on the second droop nose model, the following values of $C_{p\,\min}$ were recorded just prior to complete leading-edge separation:

Plain wing	—10
Wing with L.S. and U.S. air jets	—12·5
Wing with vane type vortex generators	—14

When leading edge flow conditions are non-conducive to providing a measure of control over the outward spread of separation, the boundary-layer fence is an extremely useful device. The normal cut-and-try design method should, however, be replaced by one in which the type and location of the fence(s) is integrated into the detailed leading-edge design problem. A sudden change of nose section in the locality of the fence, to achieve the desired effect, could result from such a design procedure.

In concluding this Section on design criteria it is suggested that more attention should be paid to the forward turbulent separation and hysteresis problems since these provide the key to a satisfactory wing stall. Experimental work of an appropriate nature would soon build up an adequate fund of design information relevant to various wing configurations and requirements. The present data are intended mainly as a guide to the order and importance of these criteria.

6.4. *Usefulness of Air Jets*

The present preliminary investigation on air jets has indicated their usefulness in the following cases:

(i) The delay of nose separation.

(ii) Hysteresis reduction.

(iii) The complete stabilisation of the boundary-layer flow on the nose at the test incidences.

(iv) Delay of separation moving from the rear.

(v) Regulation of the spanwise onset of separation and the ability to hold the tip flow over a worthwhile incidence range.

It should be remembered when assessing the lift increments obtained with air jets that large amounts of boundary-layer control have to be achieved in order to increase the nose separation lift coefficient by 0·1 or 0·2. This is due to the steepness of the $C_{p\,\min}$ versus C_{LL} curves. Hence leading-edge boundary-layer control devices are not an alternative to trailing-edge ones when attempting to increase the lift by a large amount. It will be noted from the above list, however, that the leading edge control achieved can greatly improve the handling properties of an aircraft and at the same time give useful increments in lift for a reasonable outlay in power.

With air jets, peak suction coefficients of the order of —18 have been attained. For further small increases in lift obtained for instance by controlling separation moving forward from the trailing edge, these values will rise rapidly and hence the advisability of attempting greater boundary-layer control is questionable. An answer to the problem is, however, desirable. Local sonic conditions could be reached at present day stalling speeds and, although this may not be a limiting factor, some experimental data relating to the problem would be most welcome. (When jet aircraft fly near their maximum ceiling and hence at moderately high lift coefficients, shock-induced separation on the aerofoil nose must become a relevant factor.)

The simplicity of air jet installation and operation combined with the present effectiveness of such jets at both low and high speeds, make the device an attractive one.

Acknowledgment

The author wishes to acknowledge the assistance of Mr. W. S. Walker and other members of the N.P.L. staff when carrying out the above experimental work.

NOTATION

c	Wing chord
$\bar{c}$	Mean wing chord (46·4 in.)
C_N	Local normal force coefficient
C_{LL}	Local lift coefficient
$C_{p\,min}$	Pressure coefficient at point of maximum local velocity
C_Q	Air flow coefficient $\frac{Q}{V\bar{c}}$
Q	Air jet flow; cusecs (at atmospheric pressure) per ft. of aerofoil span
s	Semi-span of complete wing
V	Tunnel speed
y	Distance from centre line of complete wing (measured normal to median plane)
α	Incidence of root chord of model
$\alpha_{N.S.}$	Incidence at which nose separation appears on model

REFERENCES

No.	*Author*	*Title, etc.*
1	R. A. Wallis	... On the proposed use of air jets as a method of boundary-layer control on the Handley Page 'Victor'. N.P.L./Aero/309. June, 1956.
2	R. A. Wallis and ..	.. Experiments with and without air jets on an NACA 64A006 semi-wing having 50 deg sweepback on the leading edge. A.R.L. (Melb.) Aero. Report A.113. July, 1959.
3	R. A. Wallis	... A preliminary note on a modified type of air jet for boundary-layer control. A.R.C. C.P.513 May, 1956.
4	R. A. Wallis	... Boundary-layer transition at the leading edge of thin wings and its effect on general nose separation. *Advances in the Aeronautical Sciences* Vol. 3, 1962. Pergamon Press (2nd I.C.A.S. Congress, Zurich, 1960).
5	R. A. Wallis and N. Ruglen ...	... Note on the breakdown of the laminar separation bubble on the nose of a thin wing. A.R.L. (Melb.) Aero. Note 161 May, 1957.
6	D. G. Hurley and G. F. Ward ...	... Experiments on the effects of air jets and surface roughness on the boundary layer near the nose of a NACA 64A006 aerofoil. A.R.L. (Melb.) Aero. Note 128, September, 1953.
7	R. A. Wallis	... The turbulent boundary layer on the articulated nose of a thin wing provided with air jets. A.R.L. (Melb.) Aero. Note 141, Oct., 1954.
8	R. F. Ayers and M. R. Wilde ...	... Aerodynamic characteristics of a swept wing with spanwise blowing. A.R.C. 19.021. September, 1956.
9	H. C. Garner and D. W. Bryer ..	.. Experimental study of surface flow and part-span vortex layers on a cropped arrowhead wing. A.R.C. R and M 3107. April, 1957.
10	P. B. Atkins and D. G. Hurley	... Wind tunnel investigation of aerodynamic hysteresis on the Avro 707A. A.R.L. (Melb.) Aero. Note 172, March, 1959.
11	P. B. Atkins	... Flight investigation of aerodynamic hysteresis on the Avro 707A. A.R.L. (Melb.) Flight Note 31. November, 1960.
12	A. A. Keeler	... Further flight tests on a Vampire aircraft fitted with turbulence strips. A.R.L. (Melb.) Flight Note 24. September, 1955.

TABLE 1

Description of work	Configuration	Wing without nose droop		Wing with 1st nose droop		Wing with 2nd nose droop	
		Wind Speed (f.p.s.)	R_e	Wind Speed (f.p.s.)	R_e	Wind Speed (f.p.s.)	R_e
Nose stalling tests	Plain wing and wing with air jets	80 to 180	2·0 to $4{\cdot}4 \times 10^6$	60 to 160	1·5 to $3{\cdot}9 \times 10^6$	60 to 160	1·5 to $3{\cdot}9 \times 10^6$
Pressure distribution and flow visualisation	Plain wing	180	$4{\cdot}4 \times 10^6$	160	$3{\cdot}9 \times 10^6$	140	$3{\cdot}4 \times 10^6$
	Wing with L.S. air jets	160	$3{\cdot}9 \times 10^6$	160	$3{\cdot}9 \times 10^6$	140	$3{\cdot}4 \times 10^6$
	Wing with both L.S. and U.S. air jets	160	$3{\cdot}9 \times 10^6$	140	$3{\cdot}4 \times 10^6$	140	$3{\cdot}4 \times 10^6$
	Wing with vane type vortex generators					140	$3{\cdot}4 \times 10^6$
	Wing with T.E. flaps					140	$3{\cdot}4 \times 10^6$

TABLE 2

Wing without nose droop

Configuration	Distance from L.E. (in.)	Pitch (in.)	Diameter (in.)	Angle with stream direction	Angle with crossflow direction	Remarks
L.S. jets	$\frac{5}{16}$ at tip to $\frac{7}{16}$ at root	$\frac{1}{8}$	0·026	90°	90°	
L.S. and U.S. jets	As above and $\frac{3}{4}$	As above and $\frac{1}{2}$	As above and 0·030	As above and 90°	As above and 45°	

TABLE 3

Wing with 1st nose droop

Configuration	Distance from L.E. (in.)	Pitch (in.)	Diameter (in.)	Angle with stream direction	Angle with crossflow direction	Remarks
L.S. jets	$\frac{1}{2}$	$\frac{1}{8}$	0·026	90°	90°	
L.S. jets	$\frac{1}{2}$	$\frac{1}{4}$	0·035	90°	45°	
U.S. jets	$\frac{3}{4}$	$\frac{3}{8}$	0·035	90°	45°	
L.S. jets	$\frac{1}{2}$	$\frac{1}{4}$	0·035	90°	45°	
U.S. jets	$\frac{3}{4}$	$\frac{3}{8}$	0·035	90°	45°	
}	10 per cent chord less $\frac{3}{4}$	$1\frac{1}{2}$	0·066	90°	45°	Most rearward position possible with pressure box

TABLE 4

Wing with 2nd nose droop

Configuration	Distance from L.E. (in.)	Pitch (in.)	Diameter (in.)	Angle with stream direction	Angle with crossflow direction	Remarks
L.S. jets	$\frac{5}{8}$	$\frac{3}{8}$	0·026	90°	45° }	Used together
U.S. jets	$\frac{3}{4}$	$\frac{1}{2}$	0·035	90°	45° }	

TABLE 5

Near-optimum C_Q for 1st droop nose wing with air jets operative

Configuration	C_Q per row of jets	Total C_Q
L.S. jets	0·00007	0·00007
L.S. jets + →	0·00026	
1 row of U.S. jets →	0·0002	0·00046
L.S. jets + →	0·00026	
2 rows of U.S. jets →	0·0002 and 0·00017	0·00063

TABLE 6

Lower surface vane type vortex generators

Chord of vanes (in.)	Pitch of vanes (in.)	Height i.e. span (in.)	Distance around surface from L.E. (in.)
$\frac{1}{4}$	$\frac{1}{4}$	$\frac{3}{32}$	$\frac{3}{4}$
$\frac{3}{8}$	$\frac{3}{8}$	$\frac{9}{64}$	$\frac{3}{4}$

TABLE 7

Second droop nose model with b.l. fence (140 *f.p.s.*)

	$\alpha_{N.S.}$	α re-attachment
Plain wing	19·3°	14·7°
Wing with air jets	21·1°	20·0°

TABLE 8

Values of $C_{p\,min}$ *just prior to nose stalling*

Configuration	$C_{p\,min}$	Remarks
Original wing		
Plain	—7·5	All results adversely affected by tip flow
with L.S. air jets	—11	
with L.S. and U.S. air jets	—13	
First droop nose wing		
Plain	—13·5	
with L.S. air jets	—15	
with L.S. and 1 row U.S. air jets	—16·5	Effectiveness of air jets curtailed by trailing edge type separation
with L.S. and 2 rows U.S. air jets	—17·5	
Second droop nose wing		
Plain	—15	
Wing with full-span T.E. flap	—16	

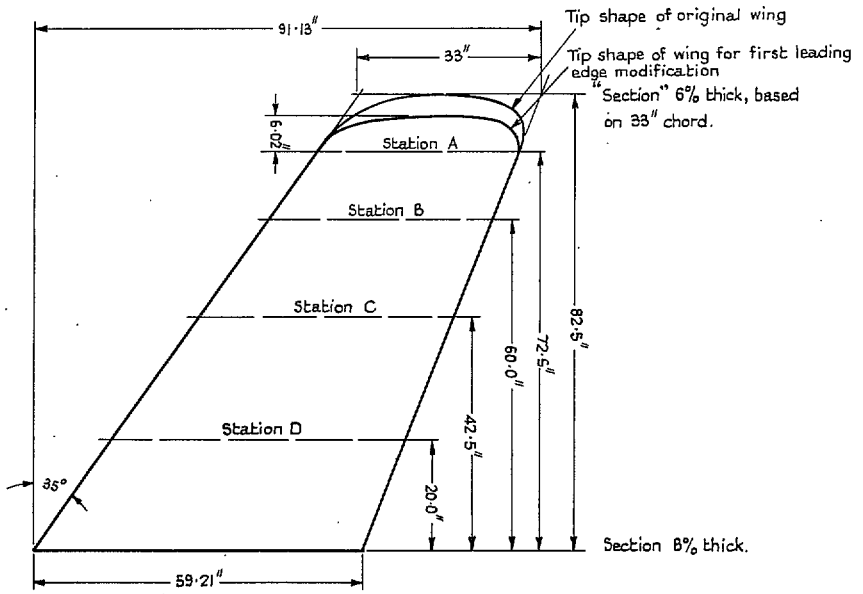

FIG. 1. Planform of wing – without chord extension

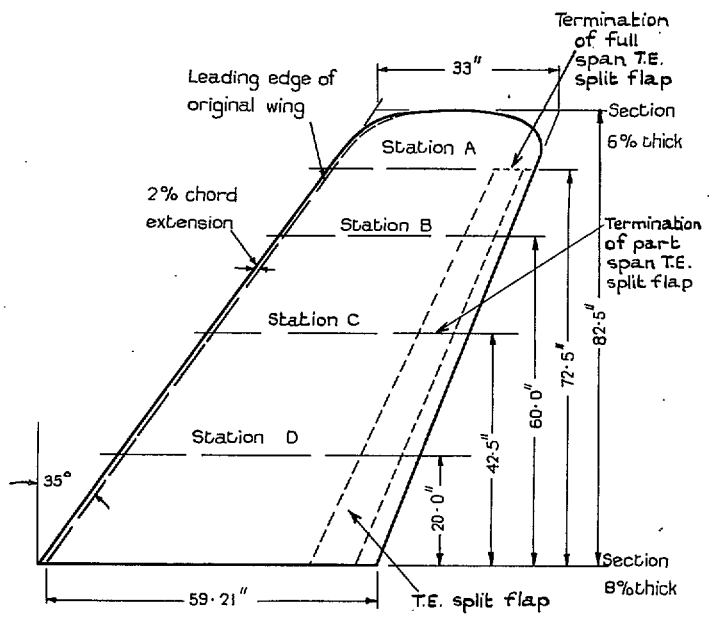

FIG. 2. Planform of wing – with chord extension for second droop nose

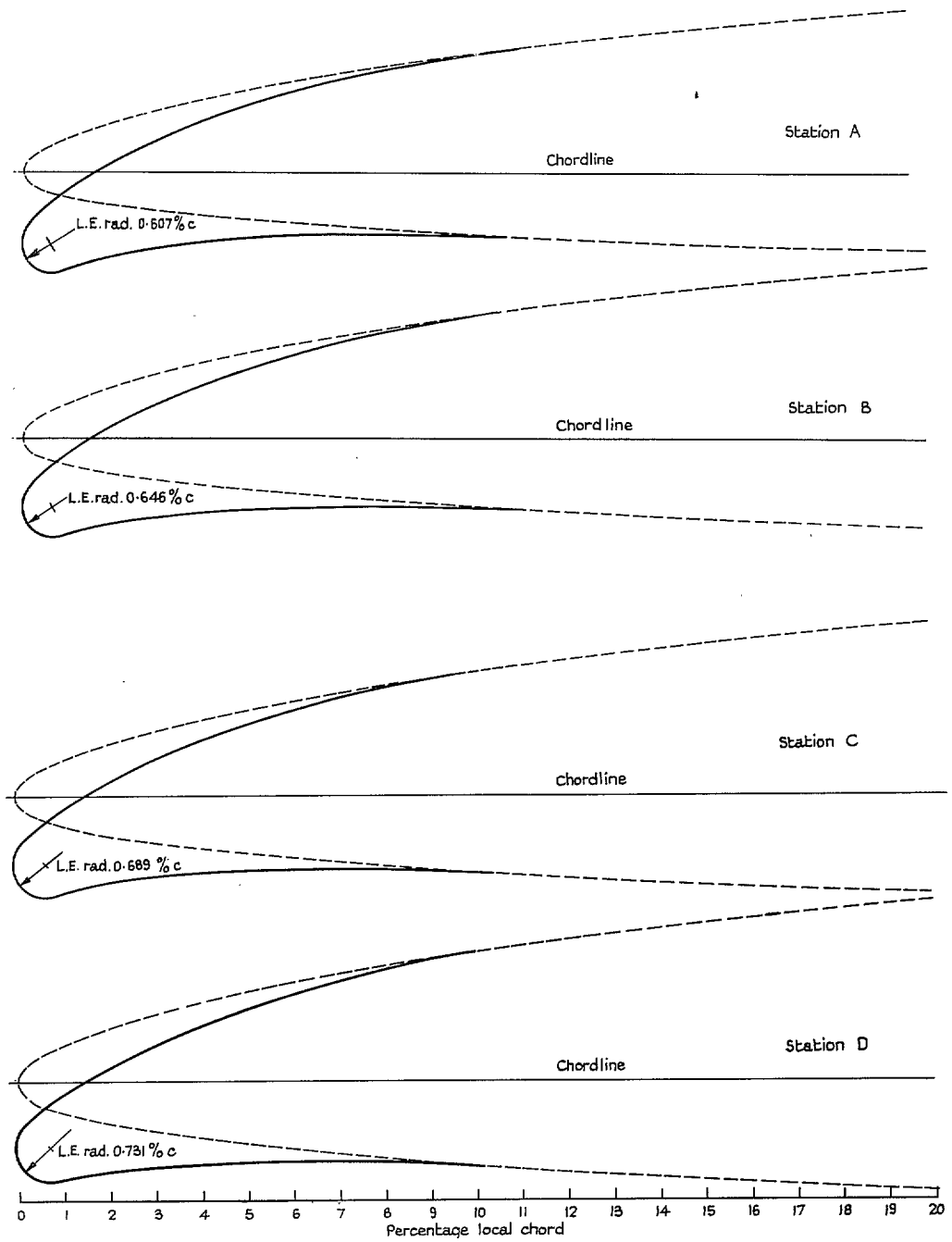

FIG. 3. Comparison of first modification with original nose

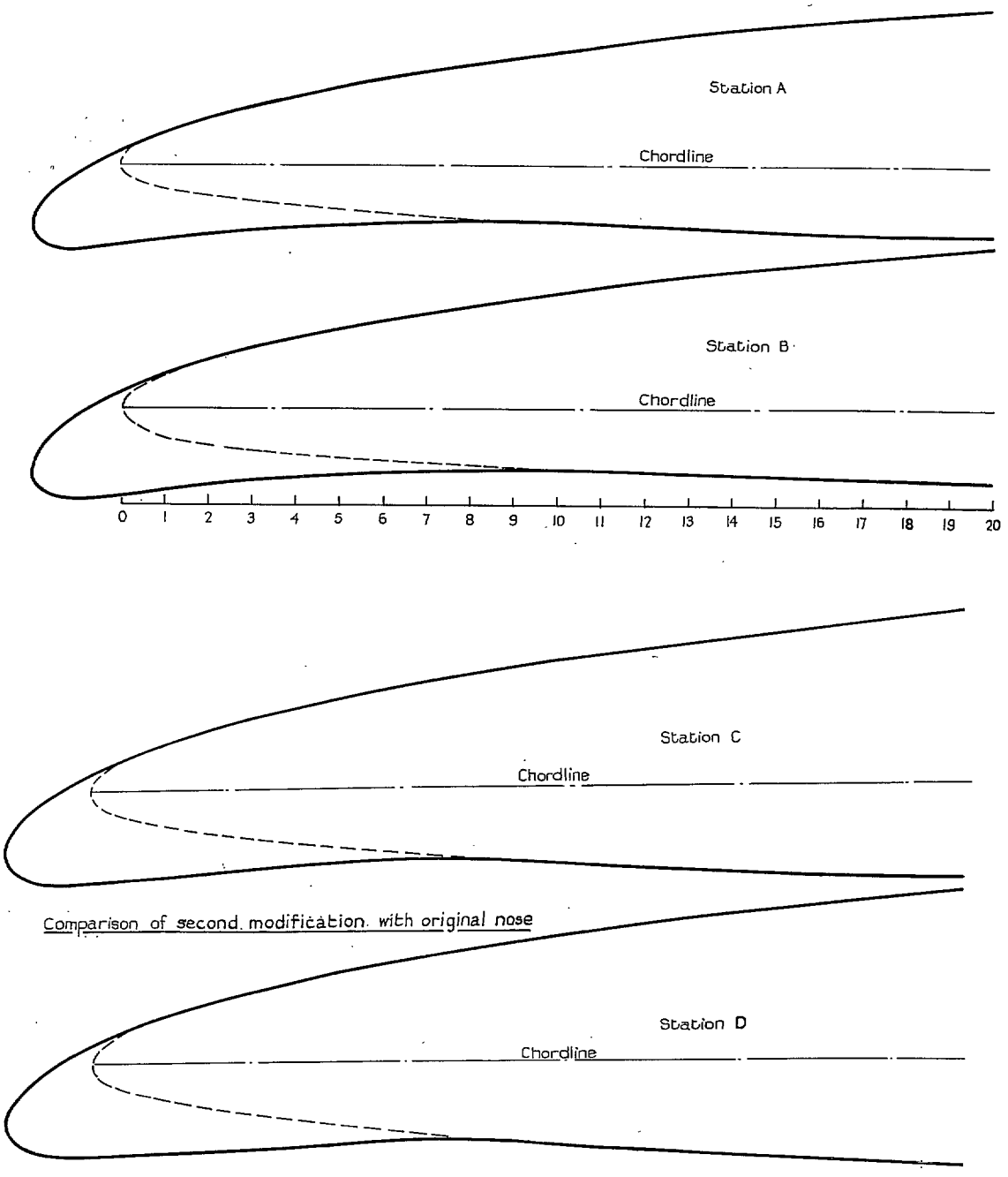

FIG. 4. Comparison of second modification with original nose

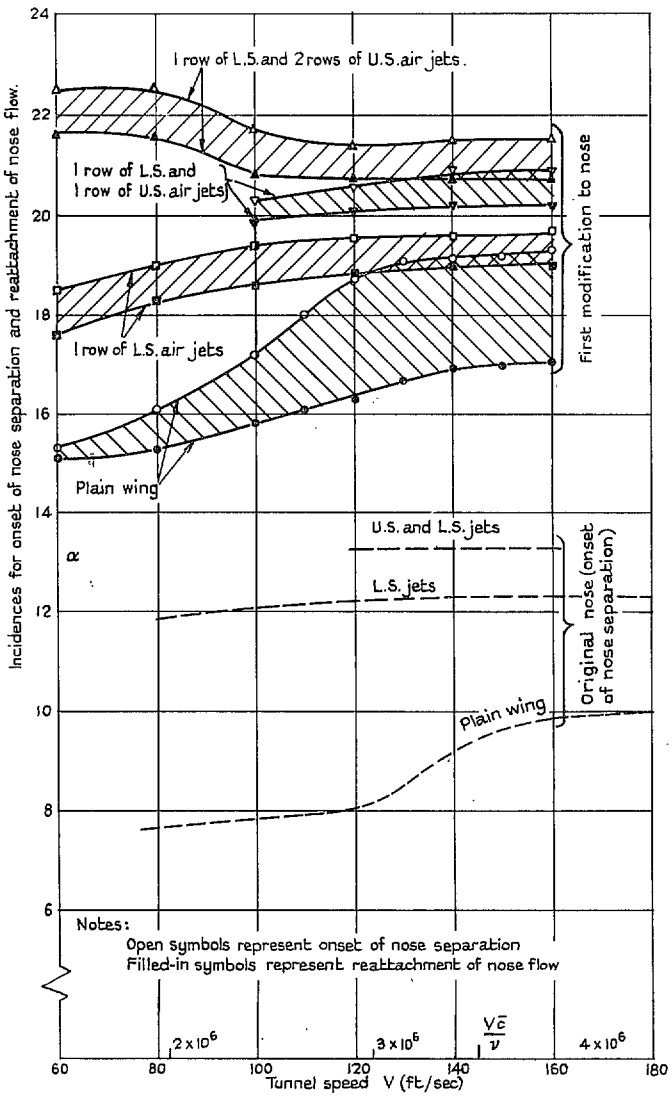

FIG. 5. Effect of Reynolds number – first two series of tests

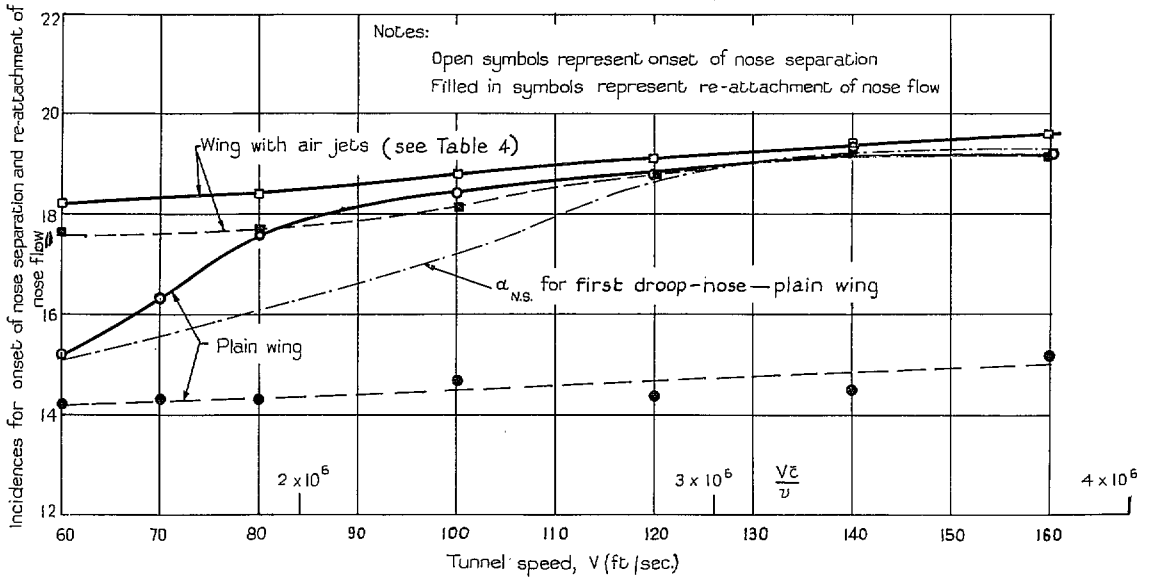

FIG. 6. Effect of Reynolds number – last series of tests

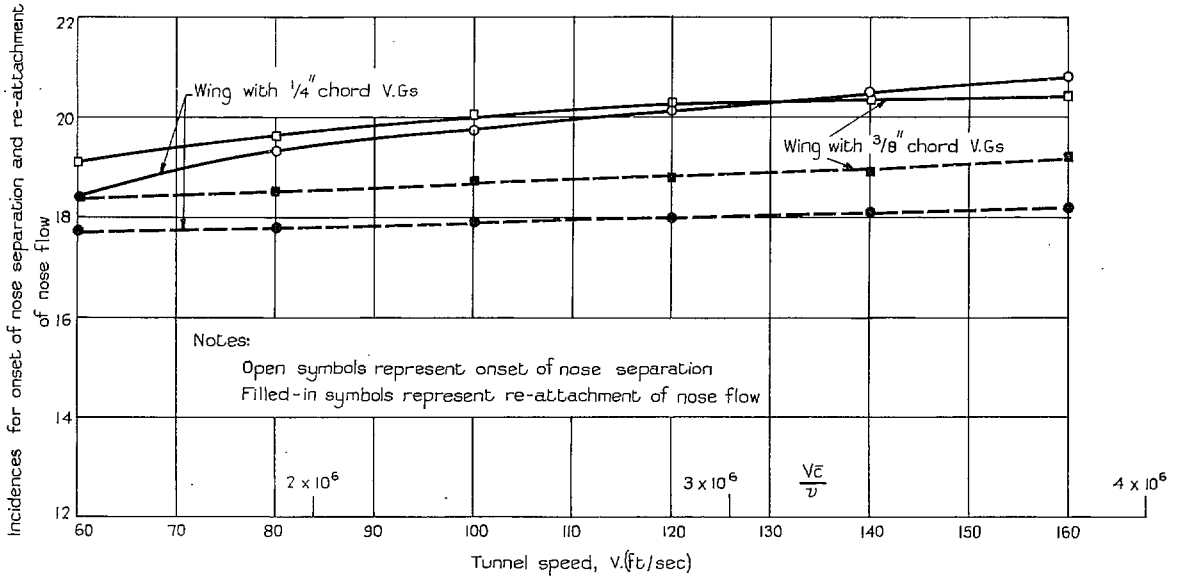

FIG. 7. Effect of Reynolds number – last series of tests – wing with undersurface vane type vortex generators

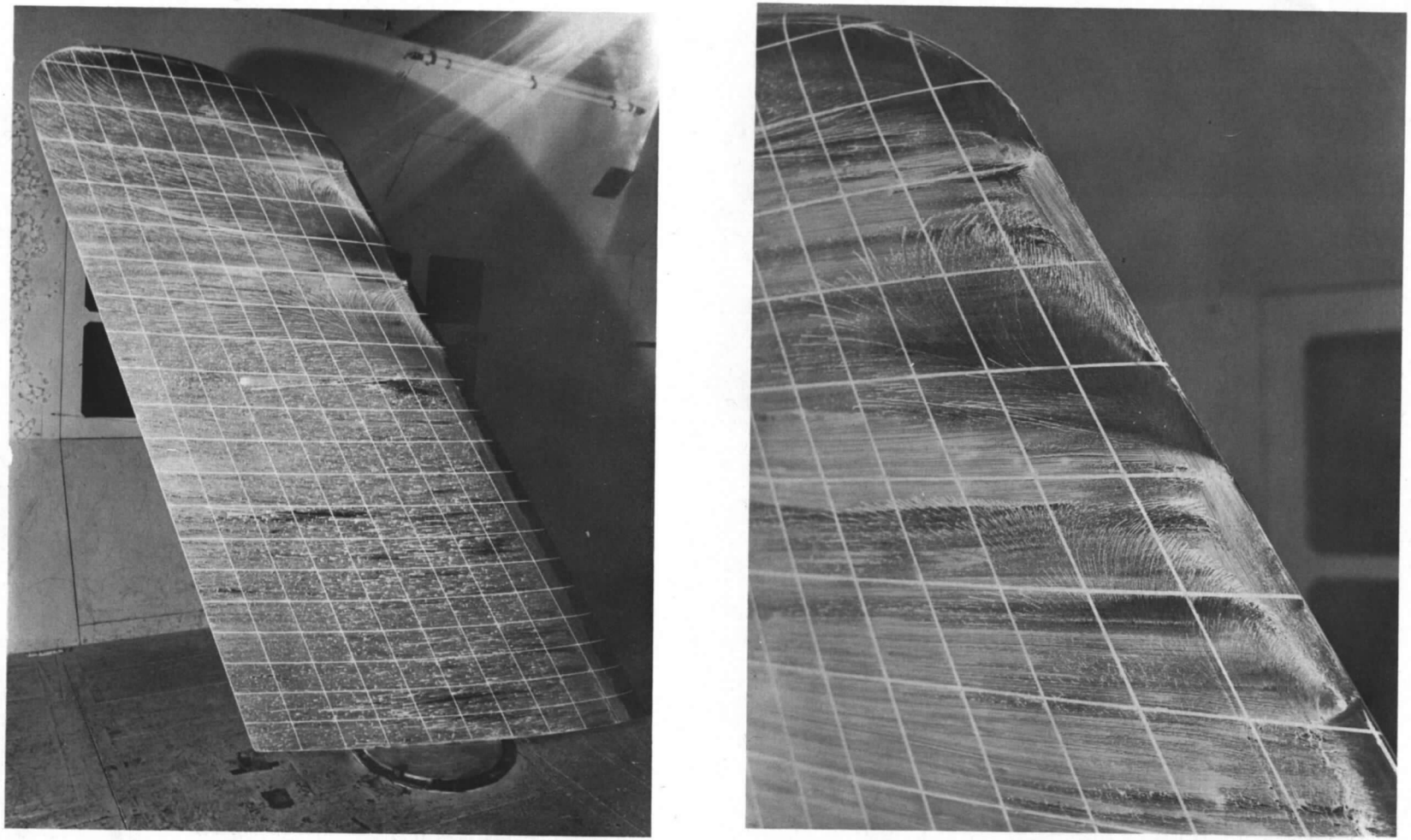

$\alpha = 11°$ $\alpha = 11°$

Fig. 8. Oil flow photographs for plain wing (original), V=180 ft/sec

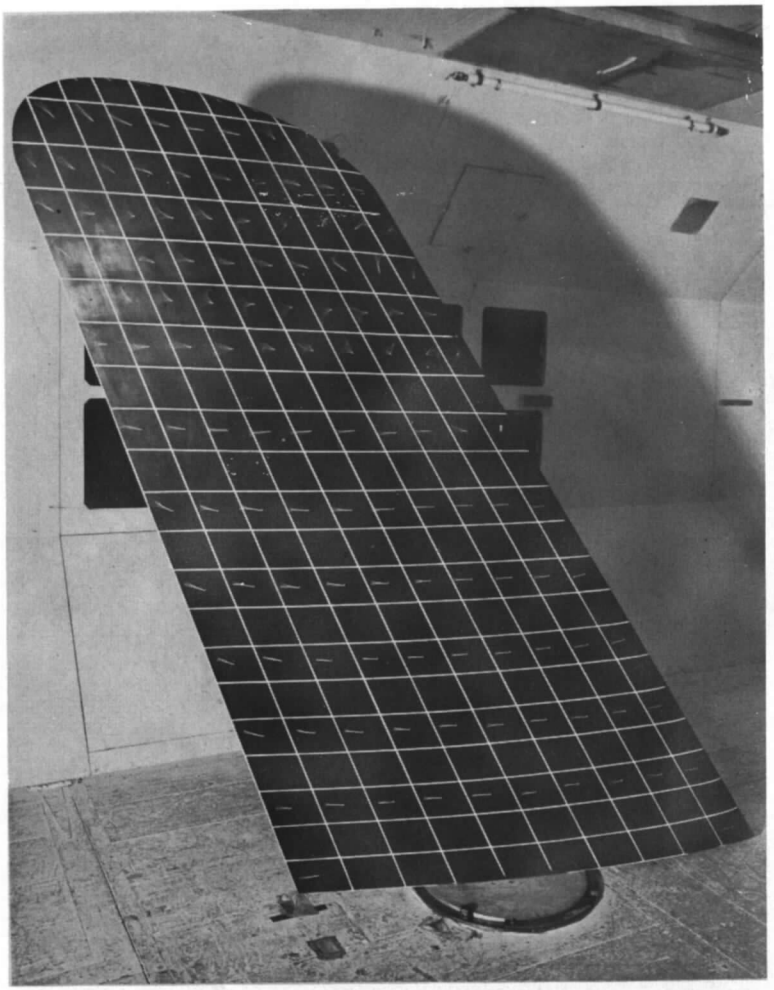

$\alpha = 11°$

FIG. 8 (contd.). Tuft photograph for plain wing (original), V = 180 ft/sec

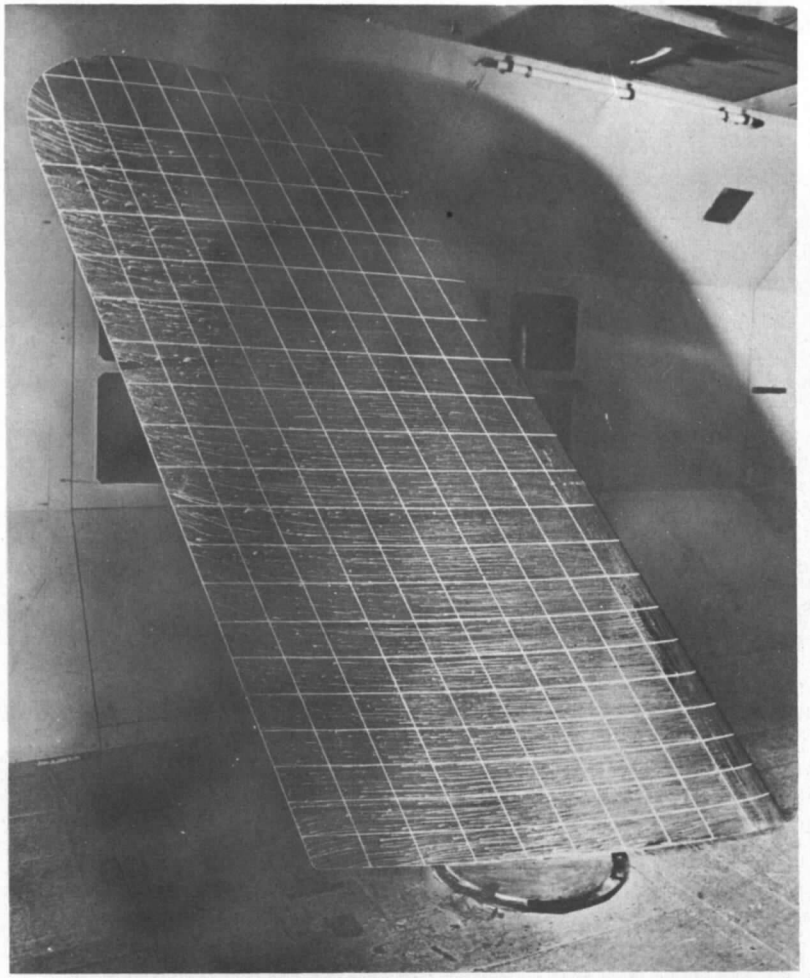

$\alpha = 12°$

FIG. 9. Oil photograph for wing (original) with lower surface air jets, V = 160 ft/sec

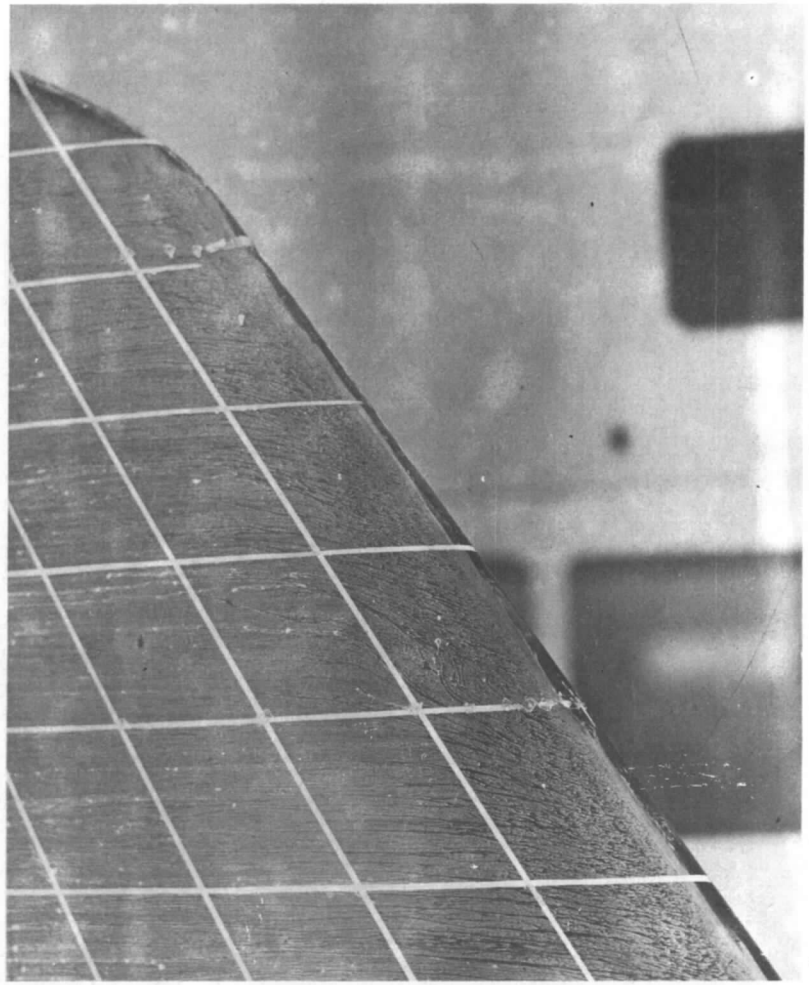

$\alpha = 12°$

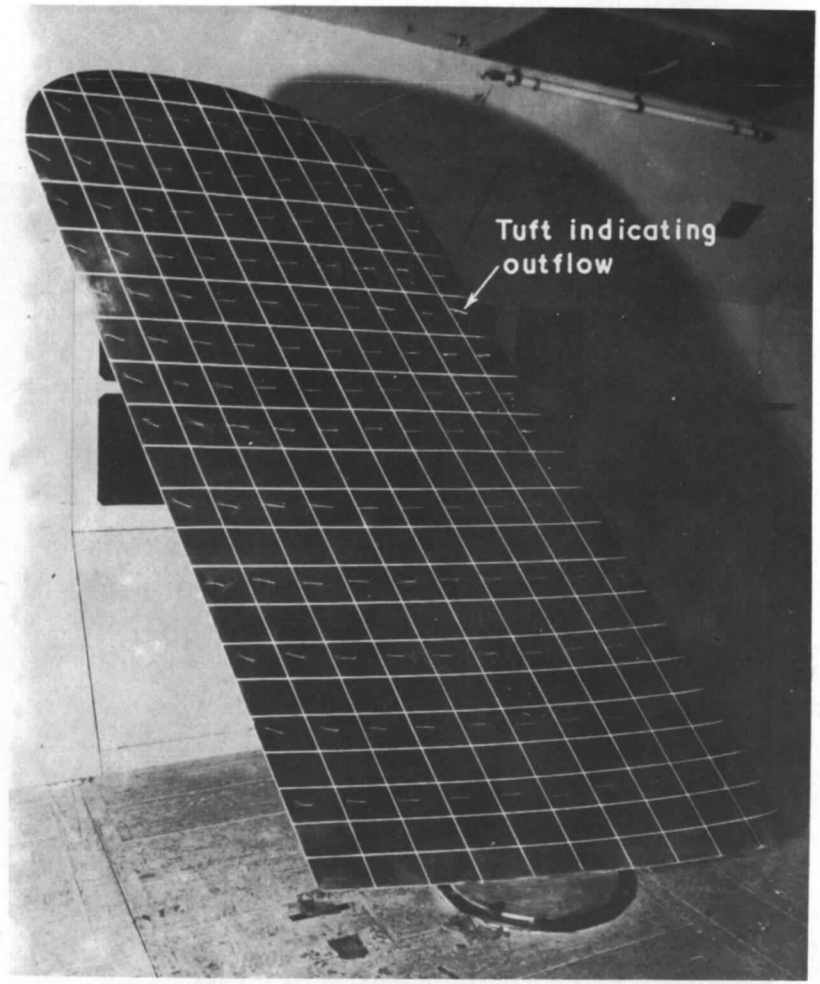

$\alpha = 12°$

FIG. 9 (contd.). Oil flow and tuft photographs for wing (original) with lower surface air jets, V = 160 ft/sec

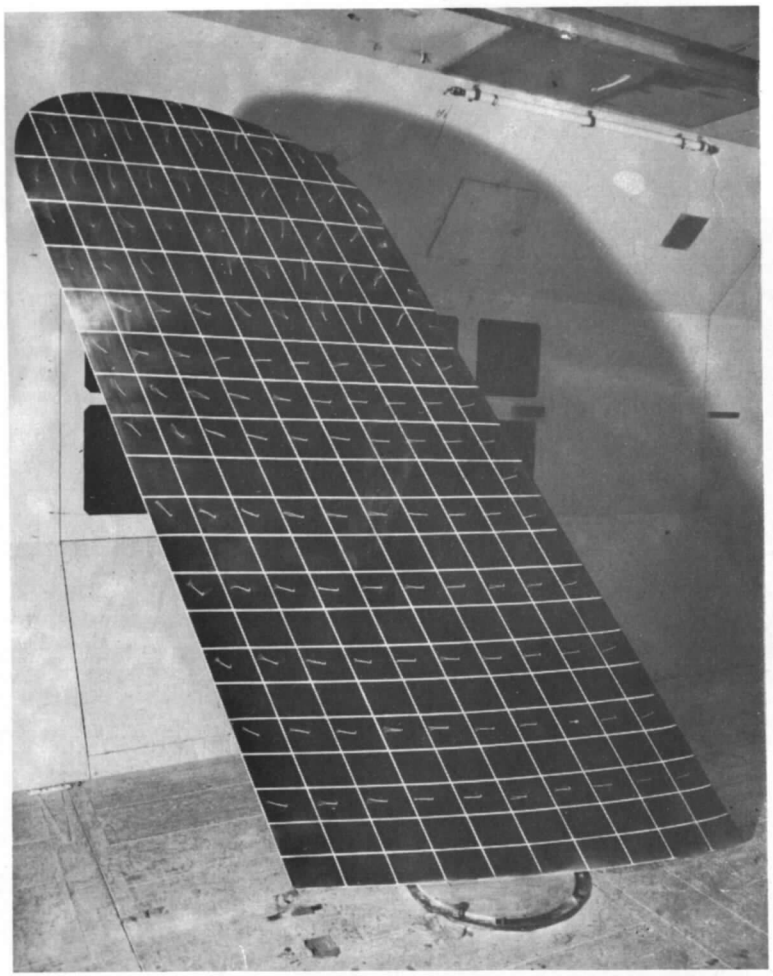

$\alpha = 13{\cdot}5°$

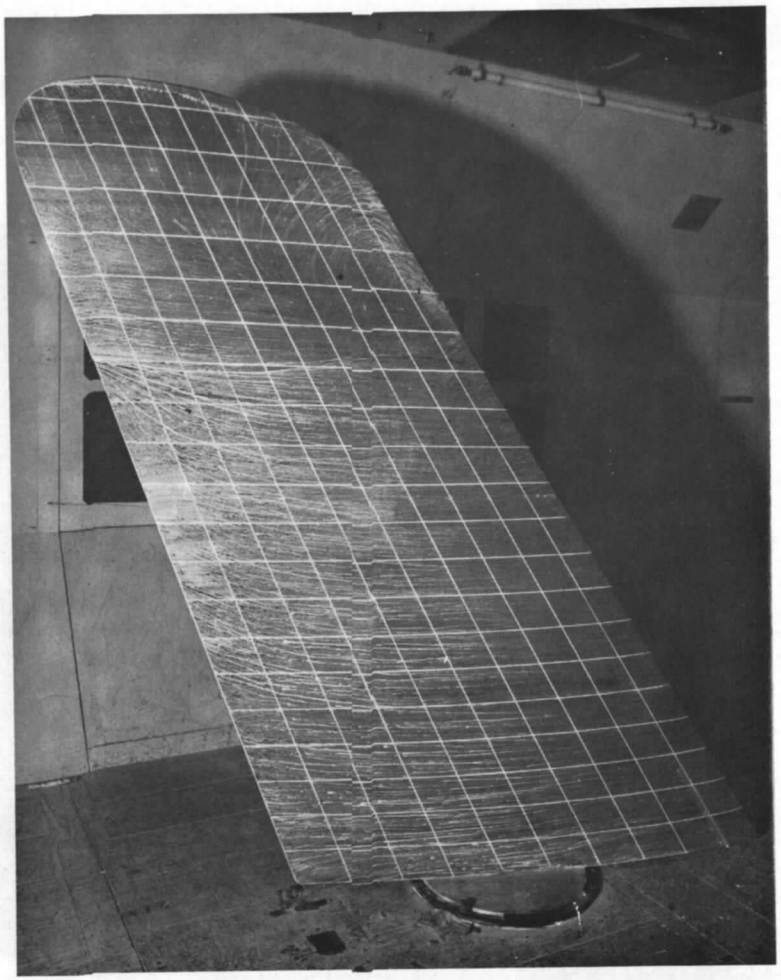

$\alpha = 13{\cdot}5°$ No significant buffeting

FIG. 10. Tuft and oil flow photographs for wing (original) with lower and upper surface air jets, V = 160 ft/sec

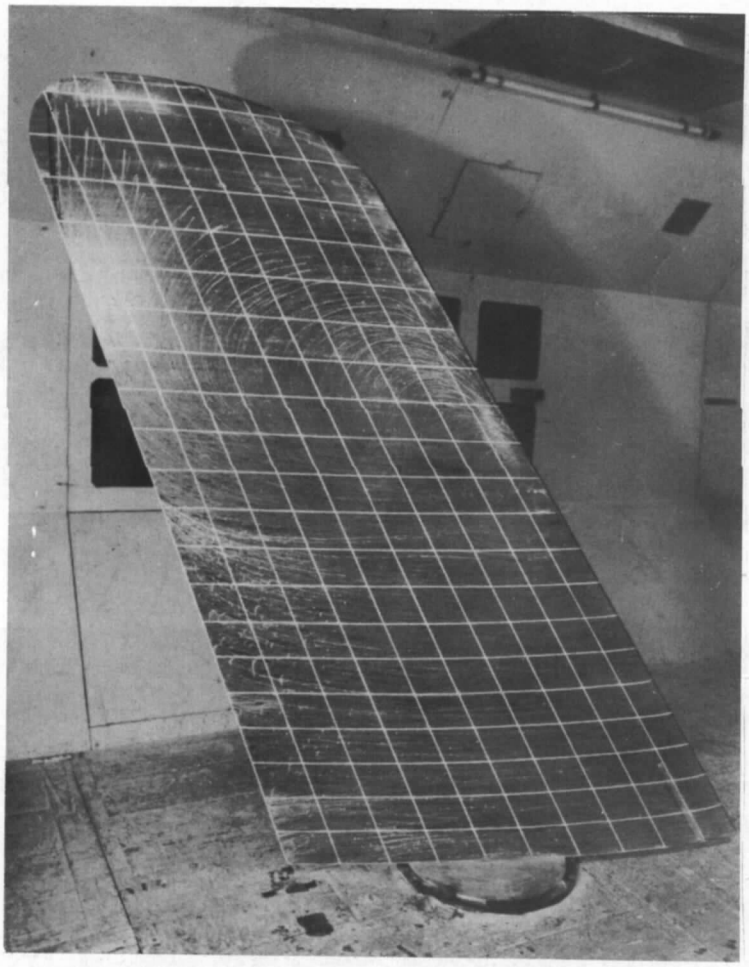

$\alpha = 14°$

FIG. 10 (contd.). Oil flow photograph for wing (original) with lower and upper surface jets, V = 160 ft/sec

Slight buffeting

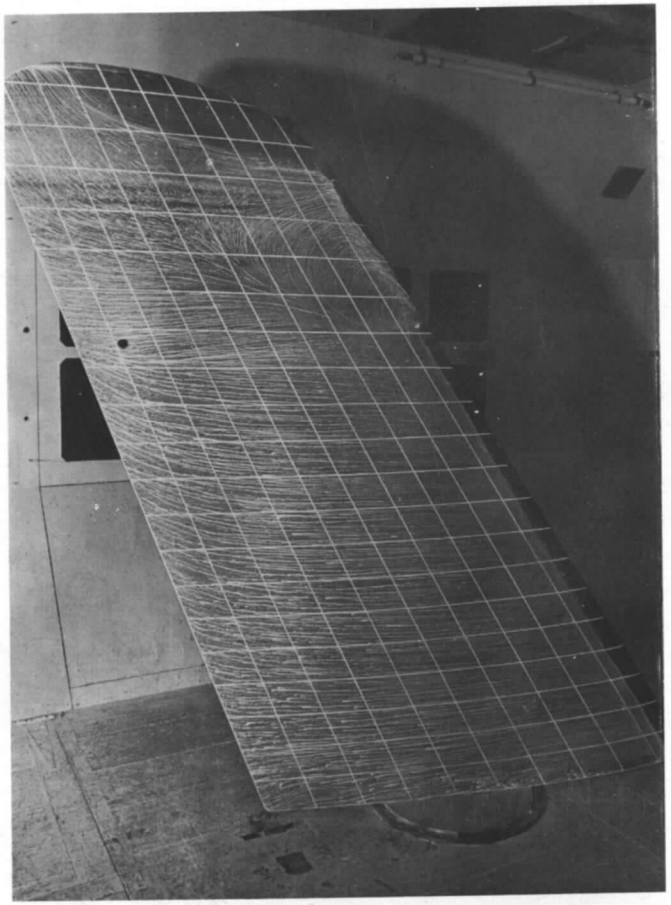

$\alpha = 12{\cdot}5°$

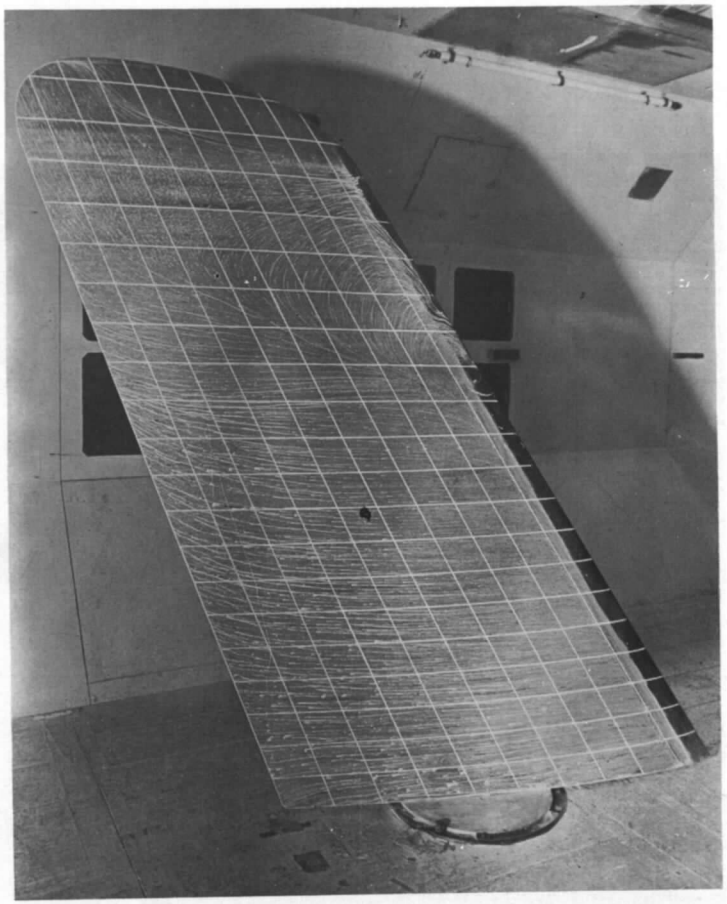

$\alpha = 13°$

FIG. 11. Oil flow photographs for wing (original) with lower surface air jets, V = 160 ft/sec

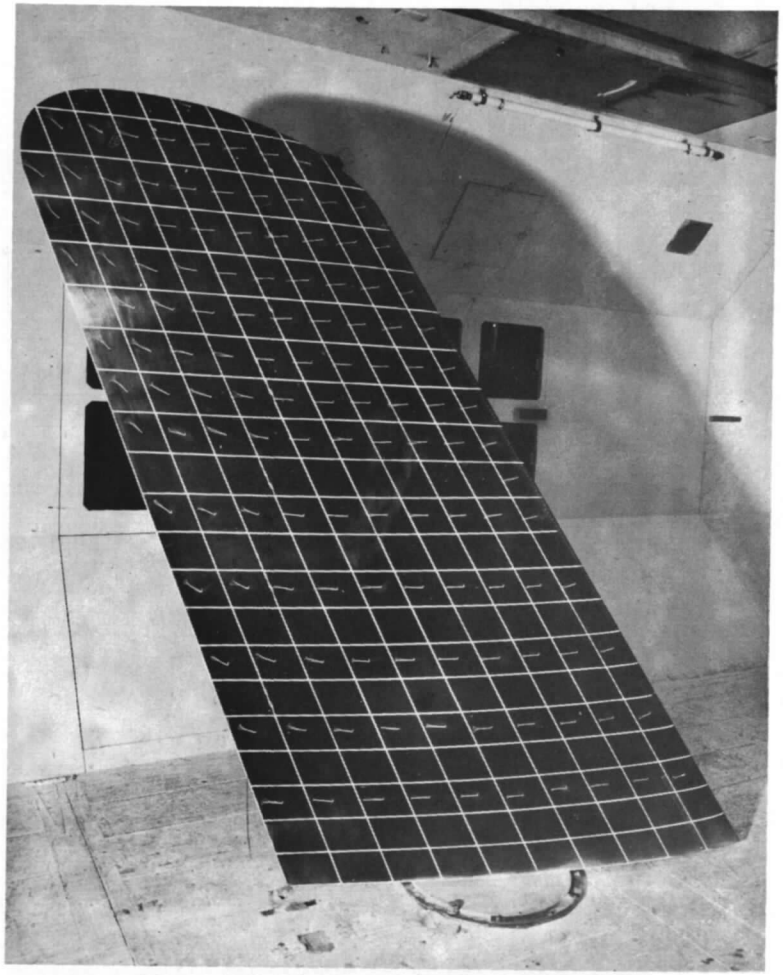

$\alpha = 13°$

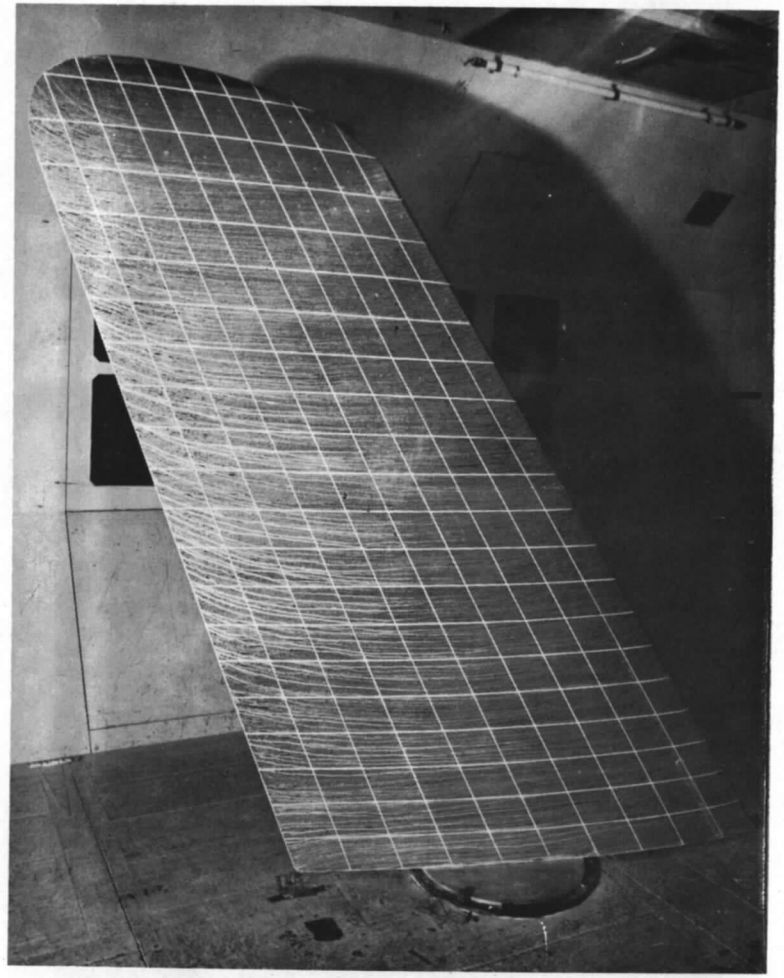

$\alpha = 13°$

FIG. 12. Tuft and oil flow photographs for wing (original) with lower and upper surface air jets, V = 160 ft/sec

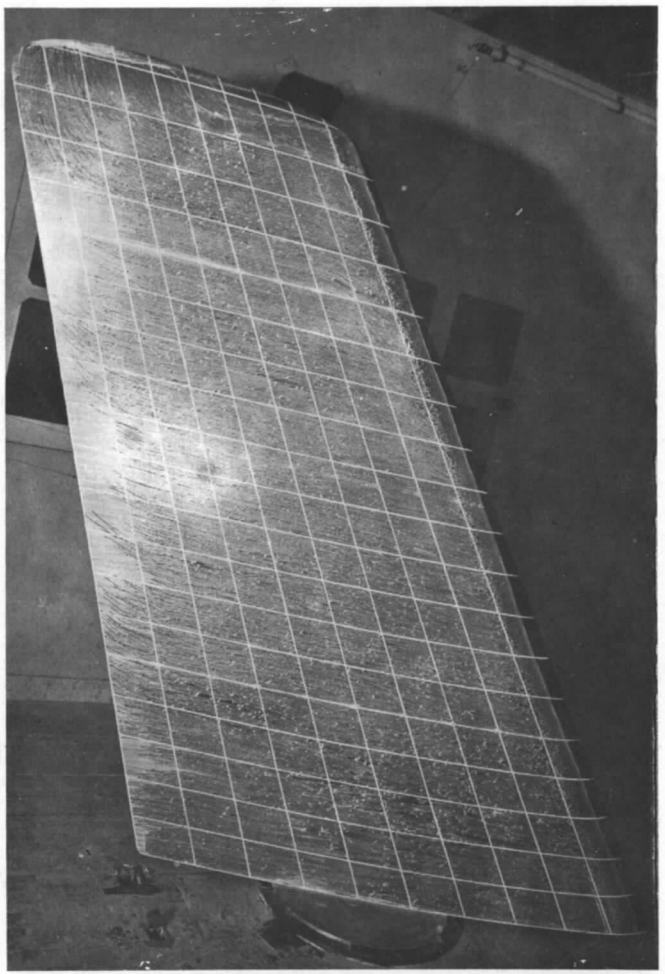

$\alpha = 18°$

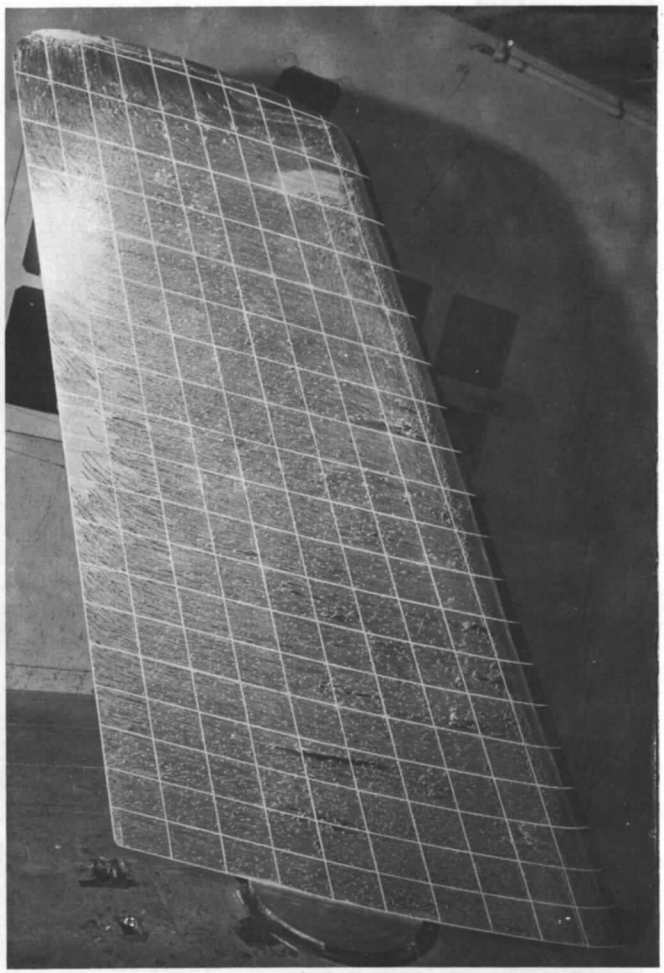

$\alpha = 18{\cdot}75°$

FIG. 13. Oil flow photographs for plain wing (first droop nose), V=160 ft/sec

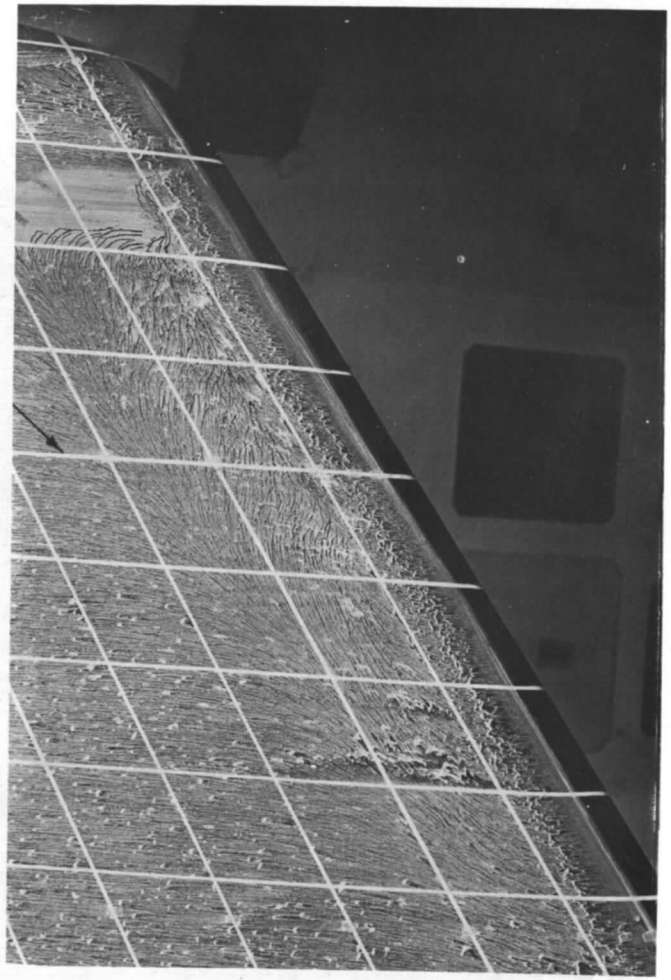

$\alpha = 18{\cdot}75°$

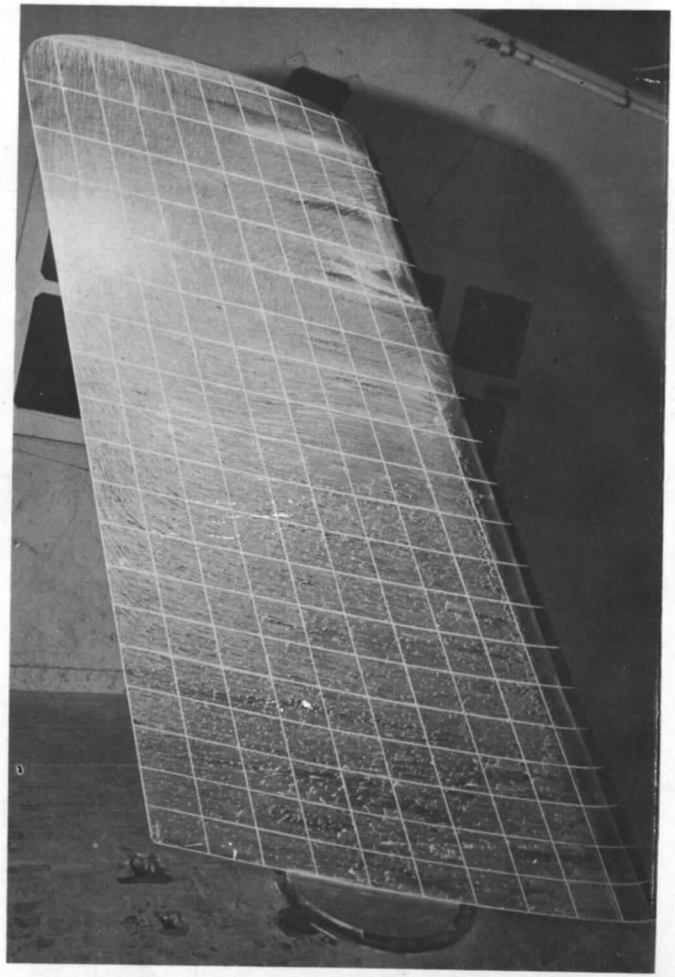

Buffeting

$\alpha = 19°$

FIG. 13 (contd.). Oil flow photographs for plain wing (first droop nose), V = 160 ft/sec

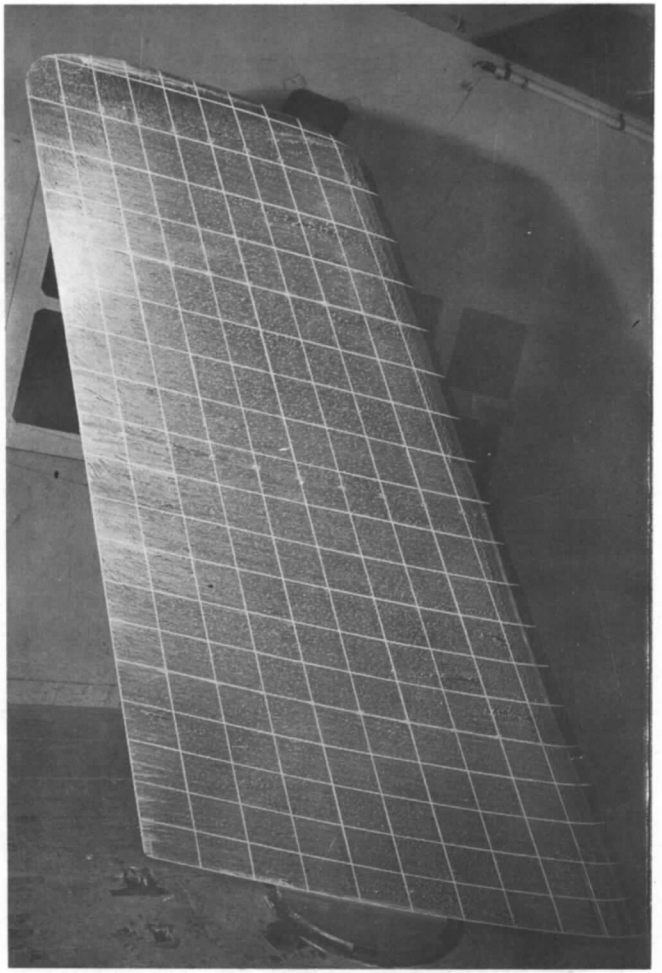

$\alpha = 18°$

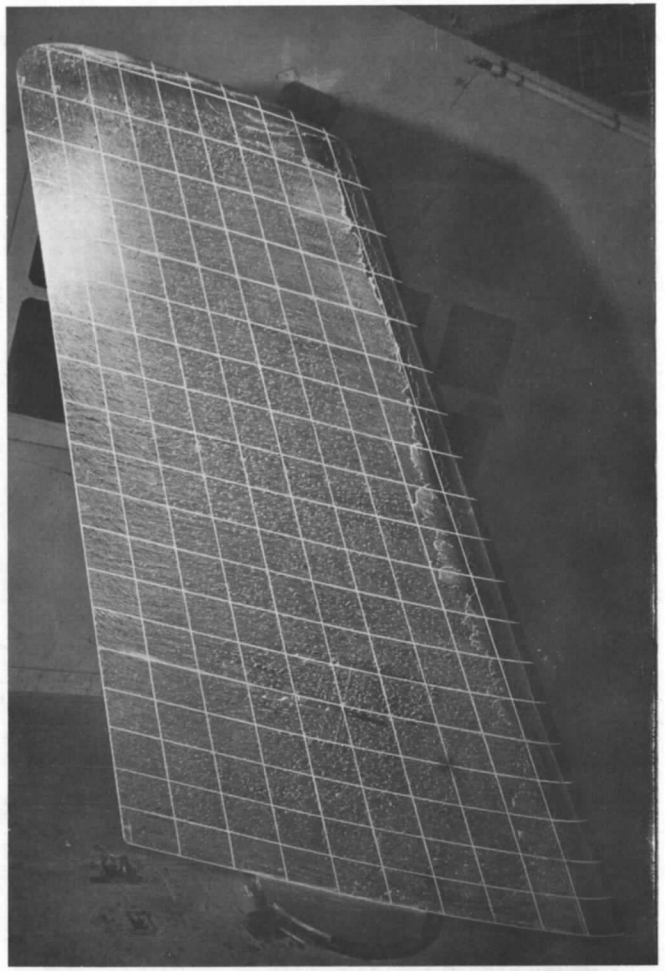

$\alpha = 19{\cdot}25°$

FIG. 14. Oil flow photographs for wing (first droop nose) with lower surface air jets, V = 160 ft/sec

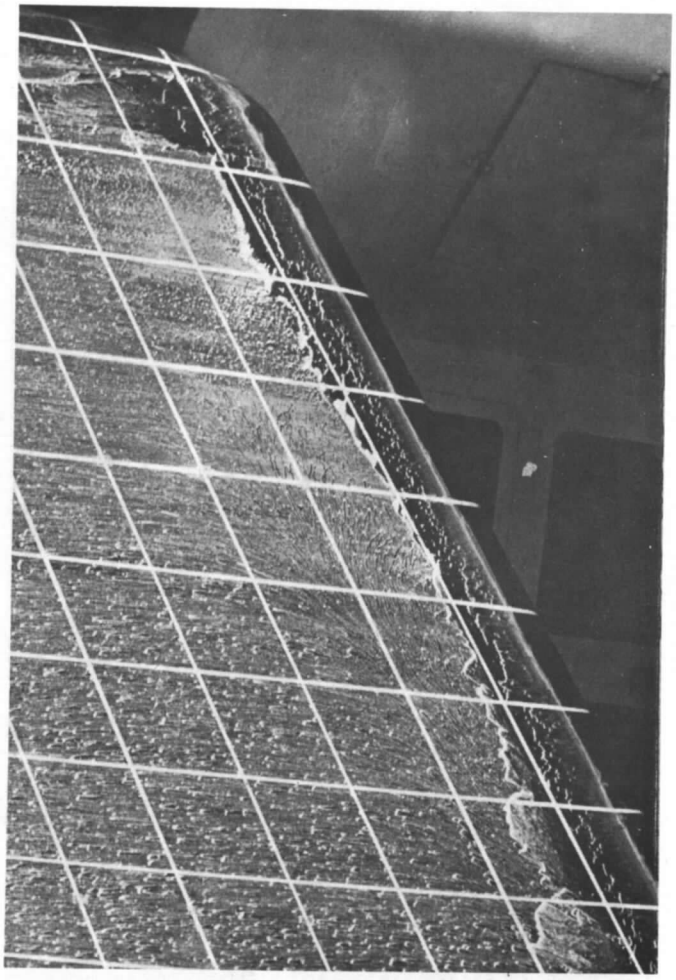

$\alpha = 19{\cdot}25^\circ$

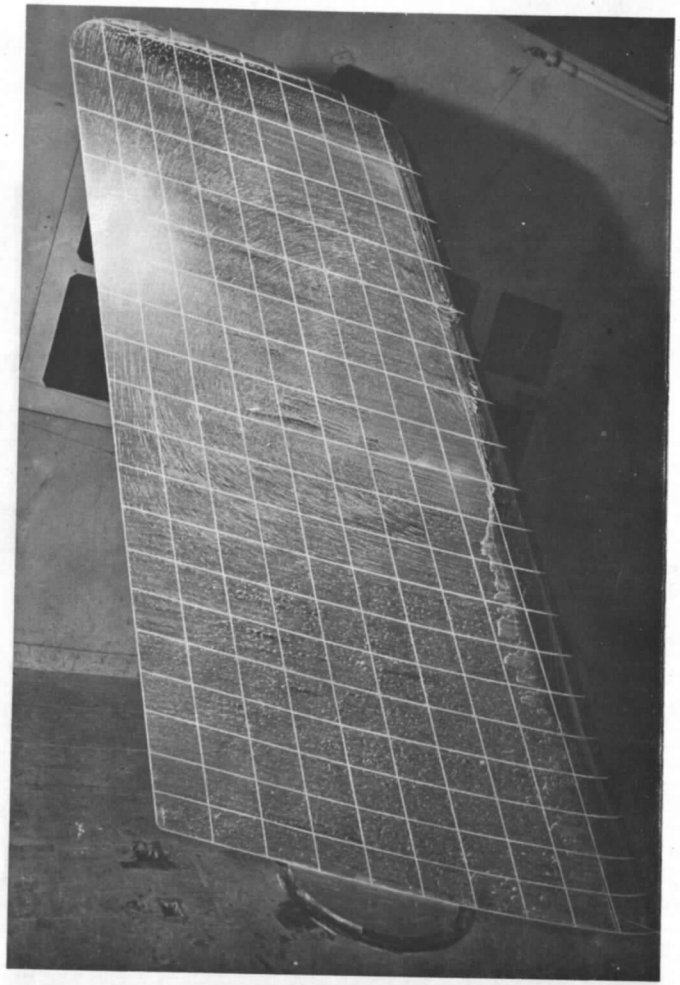

$\alpha = 19^\circ$ (with nose separation)

FIG. 14. (contd.) Oil flow photographs for wing (first drop nose) with lower surface air jets, V = 160 ft/sec

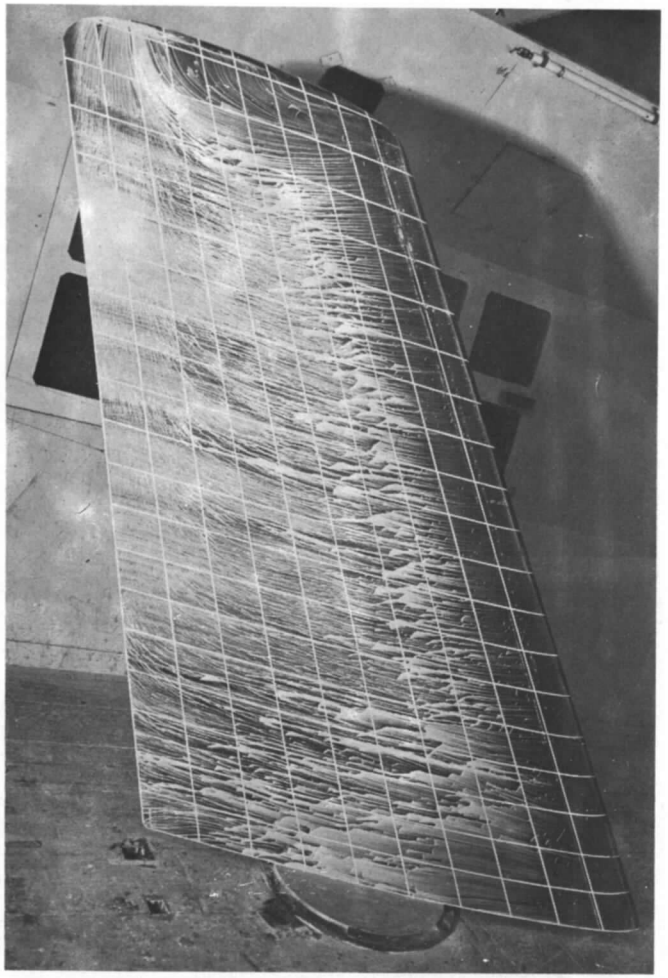

$\alpha = 18°$

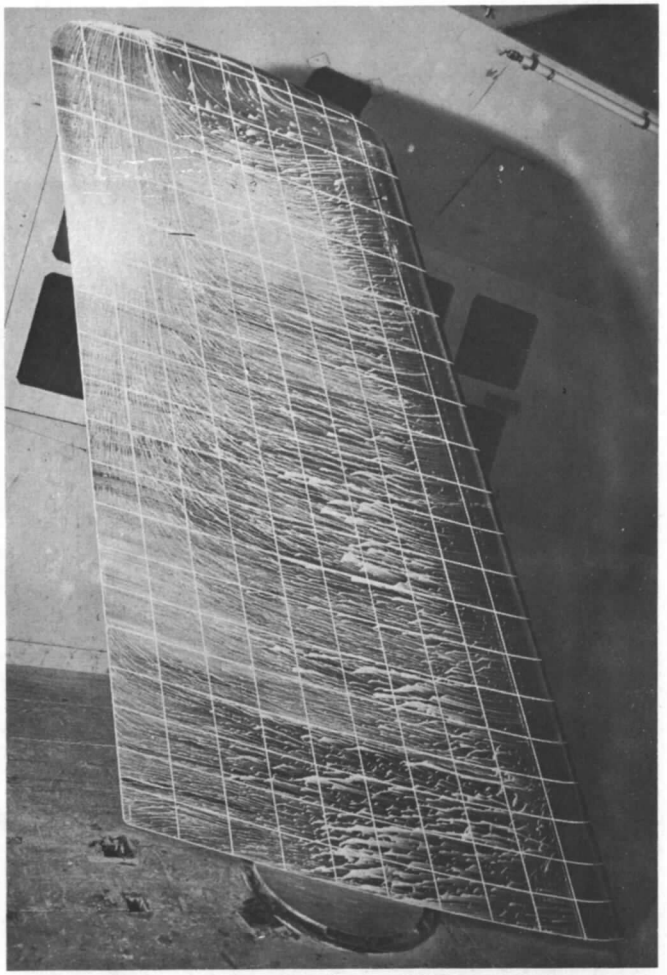

$\alpha = 19$

FIG. 15. Oil flow photographs for wing (first droop nose) with one row of upper surface air jets, V = 140 ft/sec

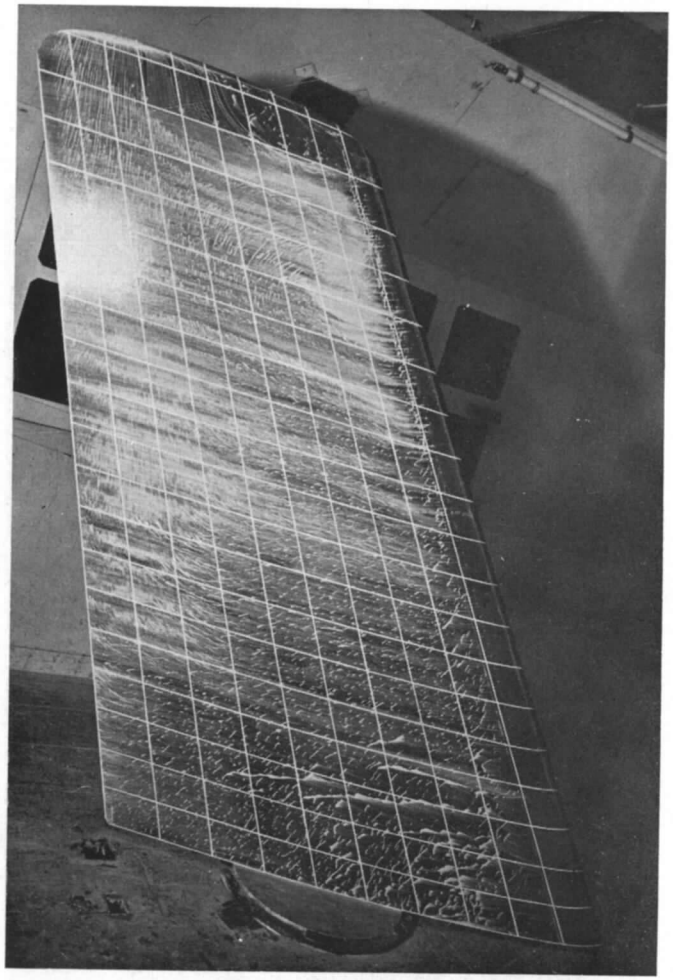

$\alpha = 20{\cdot}25°$

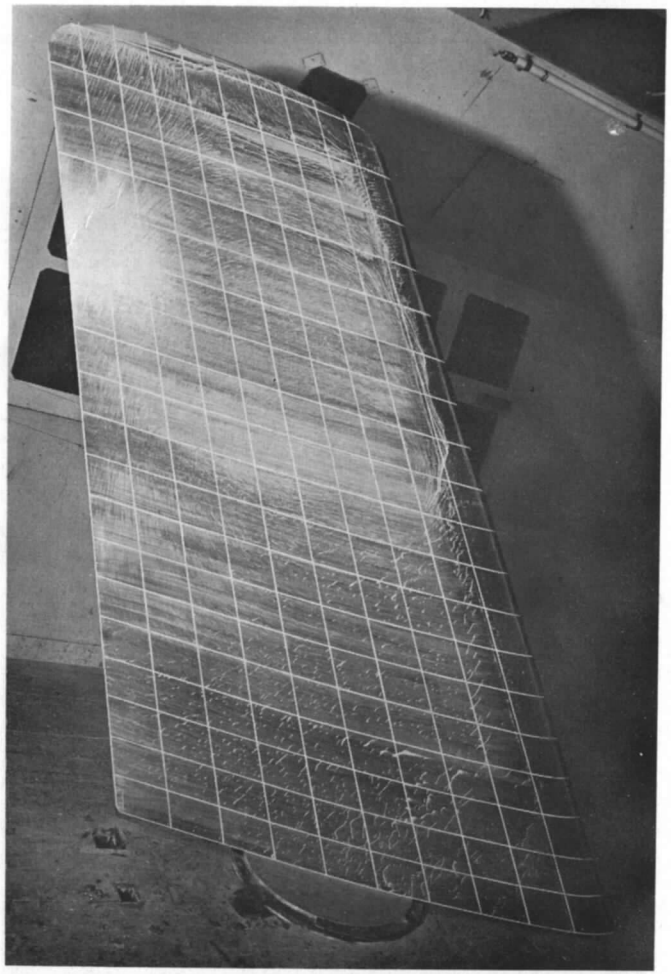

$\alpha = 20{\cdot}5°$

FIG. 15 (contd.) Oil flow photographs for wing (first droop nose) with one row of upper surface air jets, V = 140 ft/sec

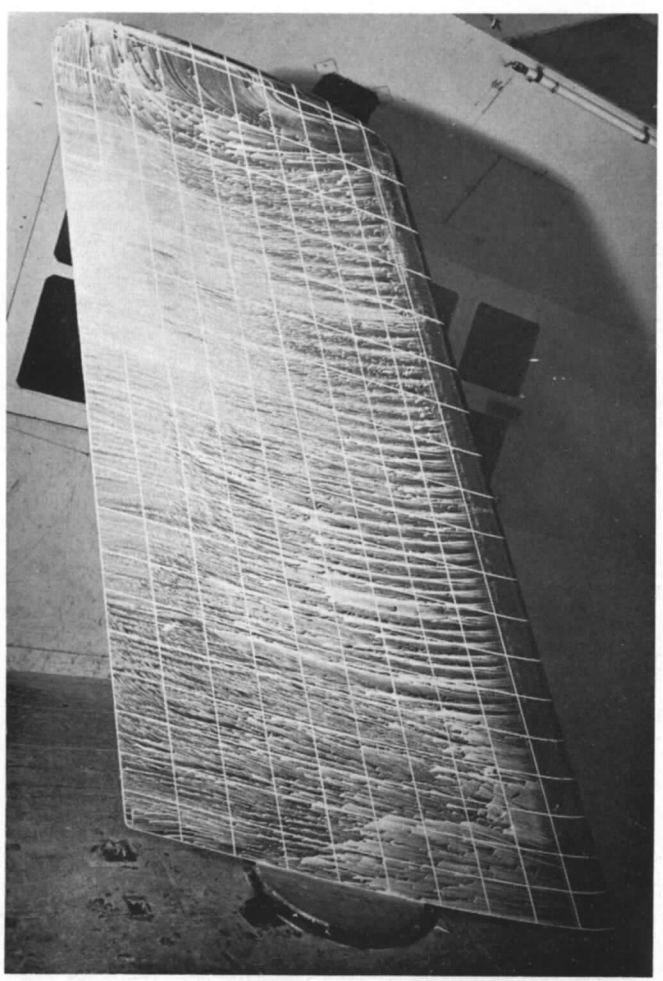

$\alpha = 19°$

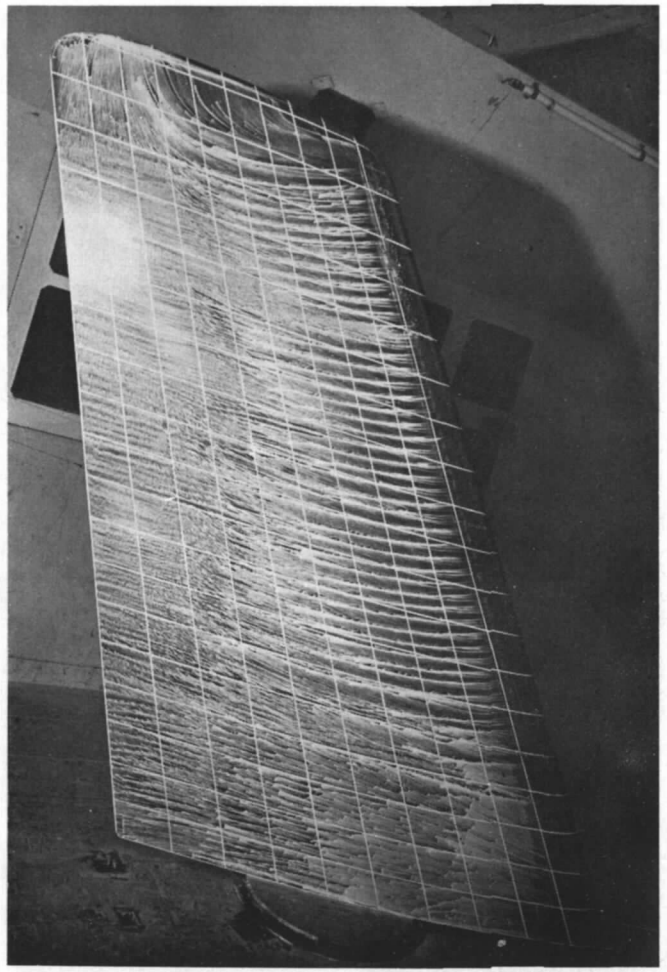

$\alpha = 20°$

FIG. 16. Oil flow photographs for wing (first droop nose) with two rows of upper surface air jets, V = 140 ft/sec

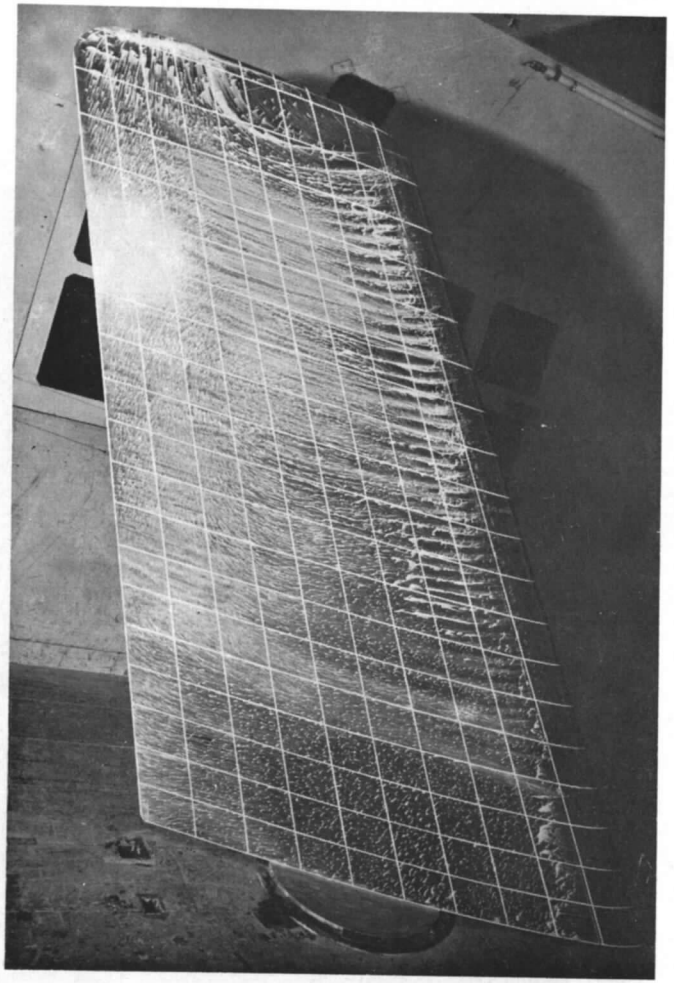

$\alpha = 21{\cdot}25^{\circ}$

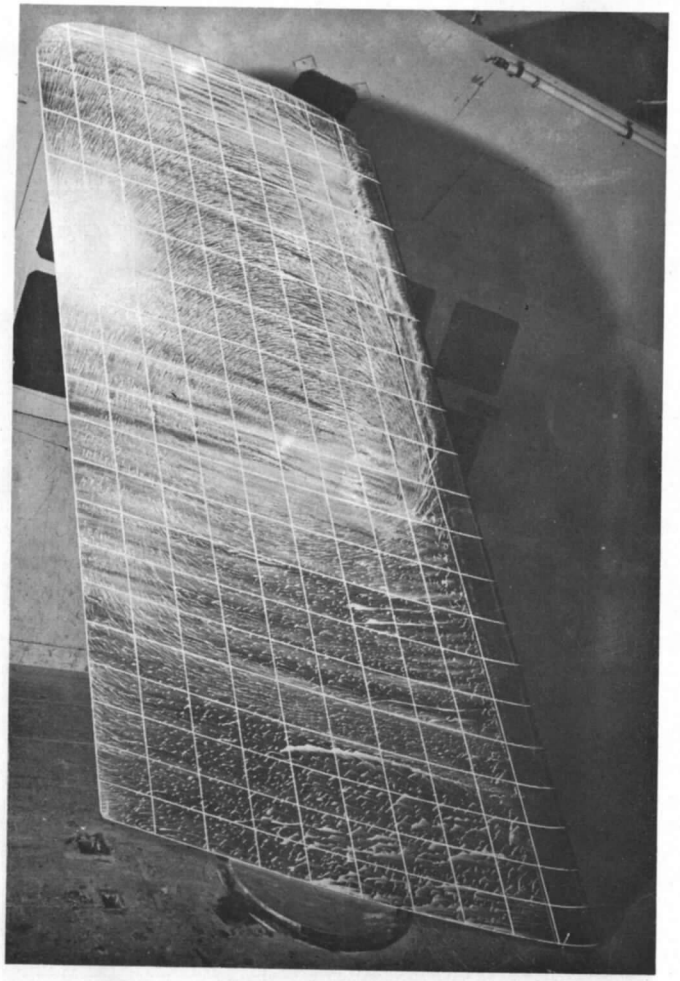

$\alpha = 20{\cdot}75^{\circ}$ (with nose separation)

FIG. 16 (contd.). Oil flow photographs for wing (first droop nose) with two rows of upper surface air jets, V = 140 ft/sec

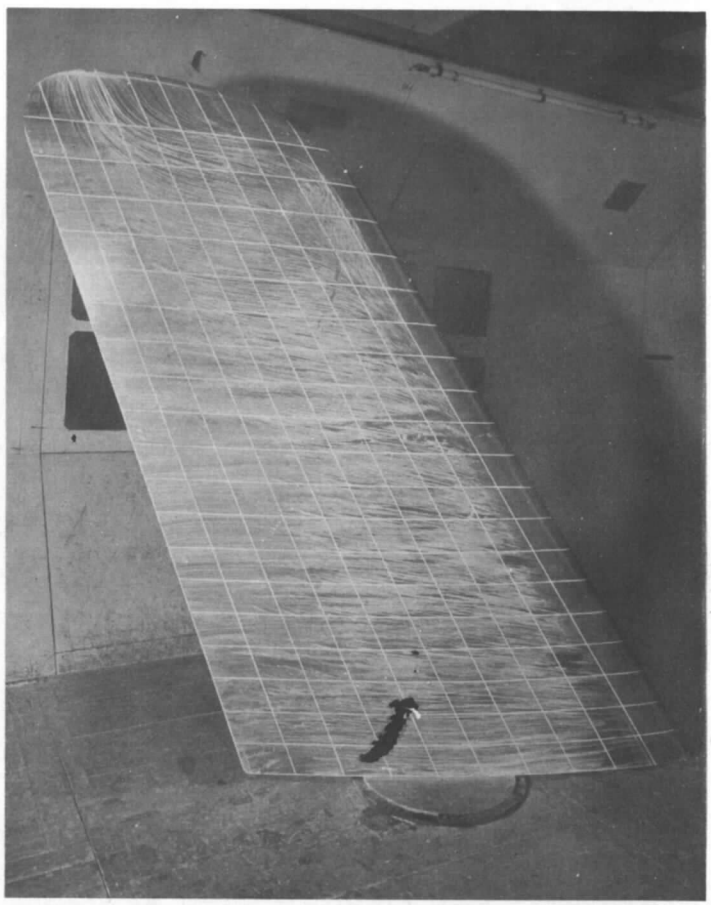

$\alpha = 18{\cdot}5°$

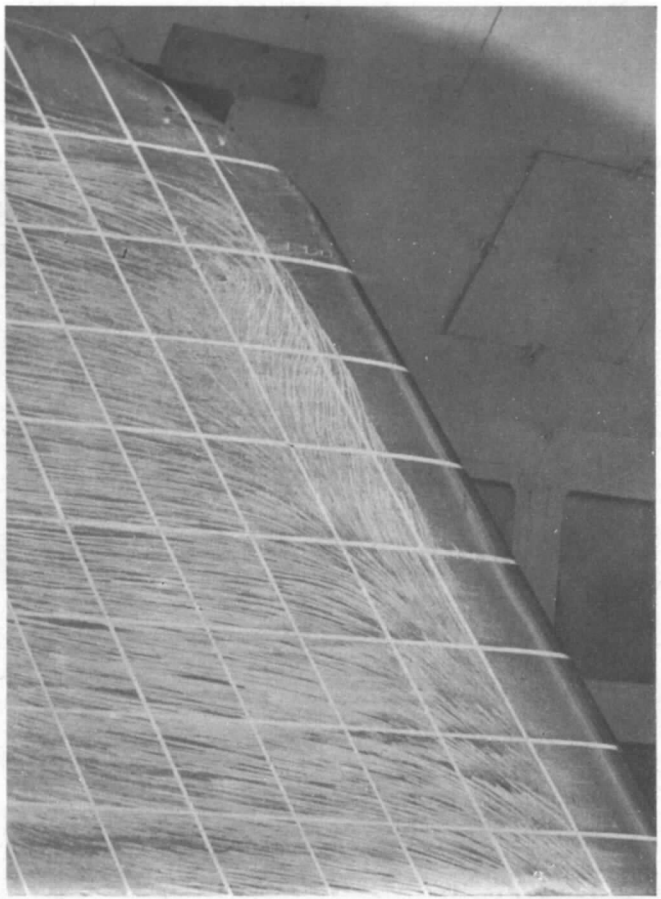

$\alpha = 18{\cdot}5°$

FIG. 17. Oil flow photographs for plain wing (second droop nose) V = 140 ft/sec

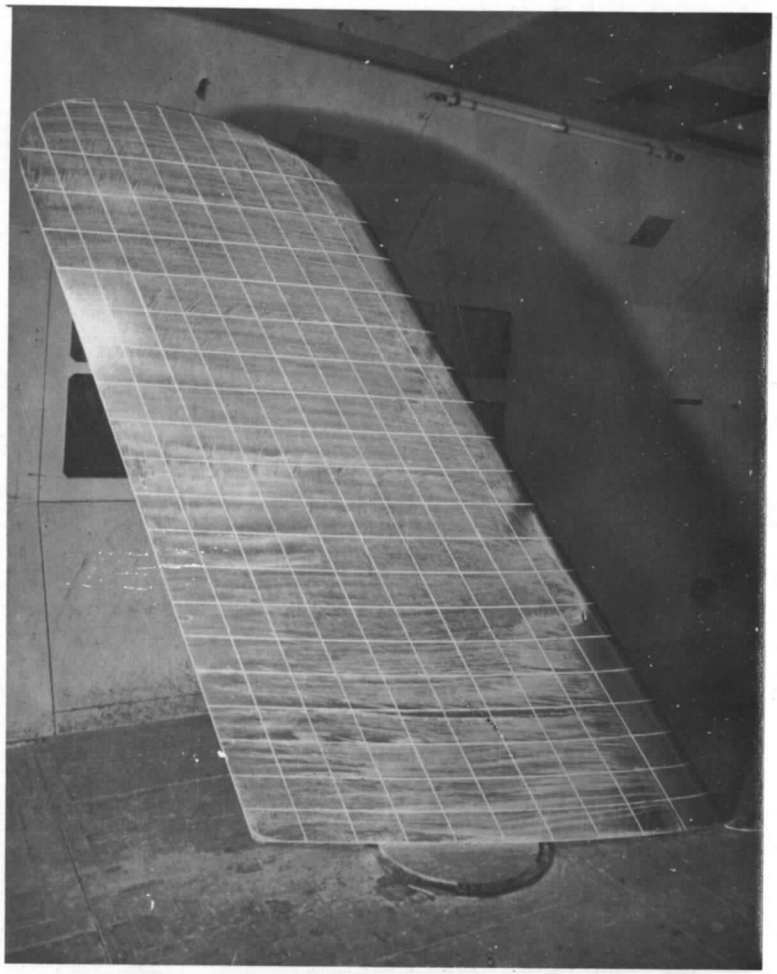

$\alpha = 18{\cdot}5°$ (with nose separation)

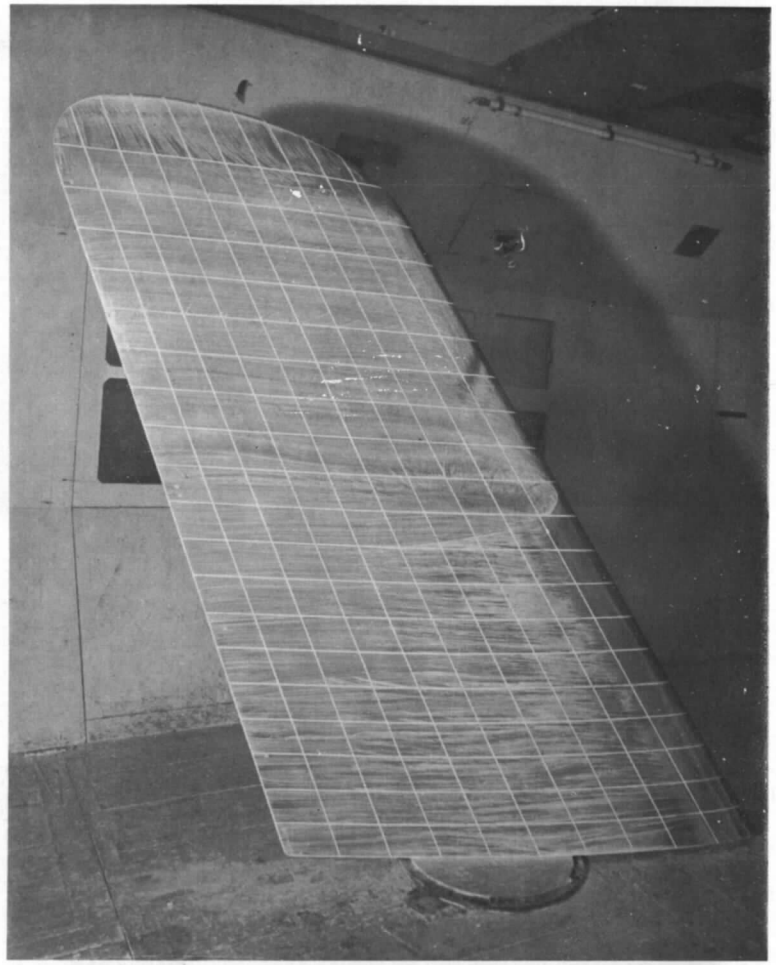

$\alpha = 16°$ (with nose separation)

FIG. 17 (contd.). Oil flow photographs for plain wing (second droop nose), V = 140 ft/sec

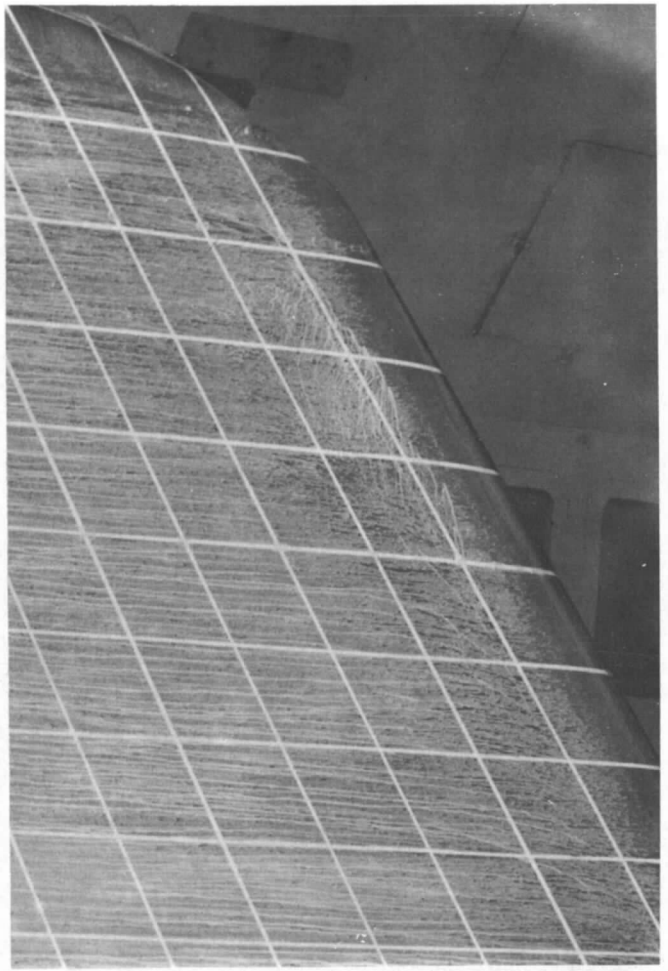

$\alpha = 16{\cdot}5°$

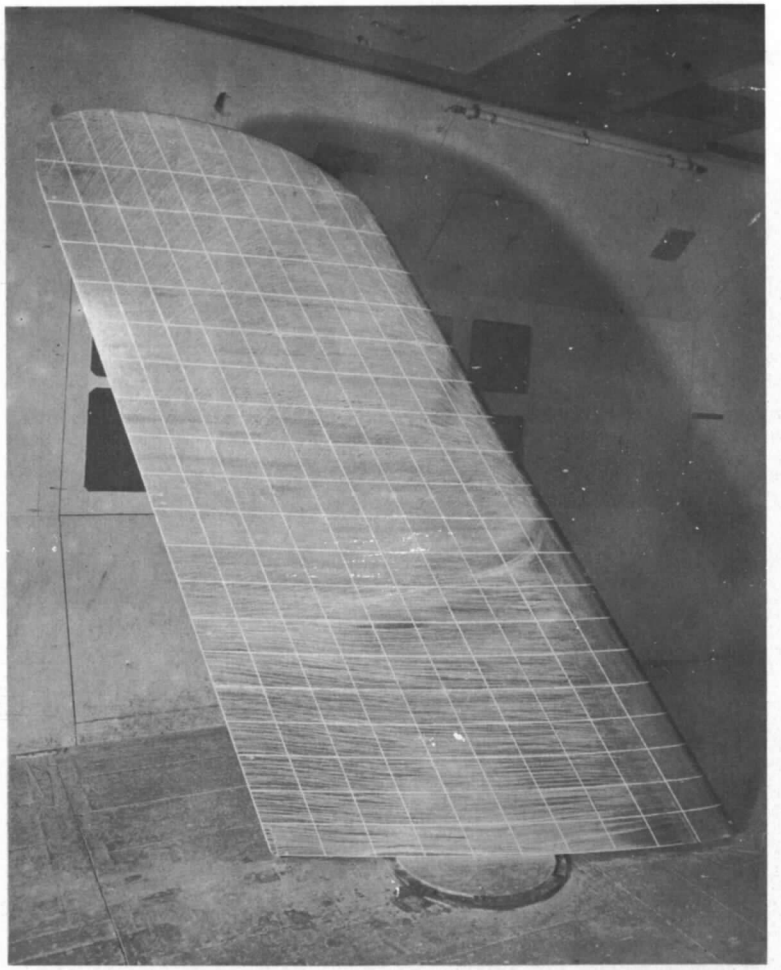

$\alpha = 16{\cdot}5°$ (with nose separation)

FIG. 18. Oil flow photographs for plain wing (second droop nose) with part-span flap.
V = 140 ft/sec

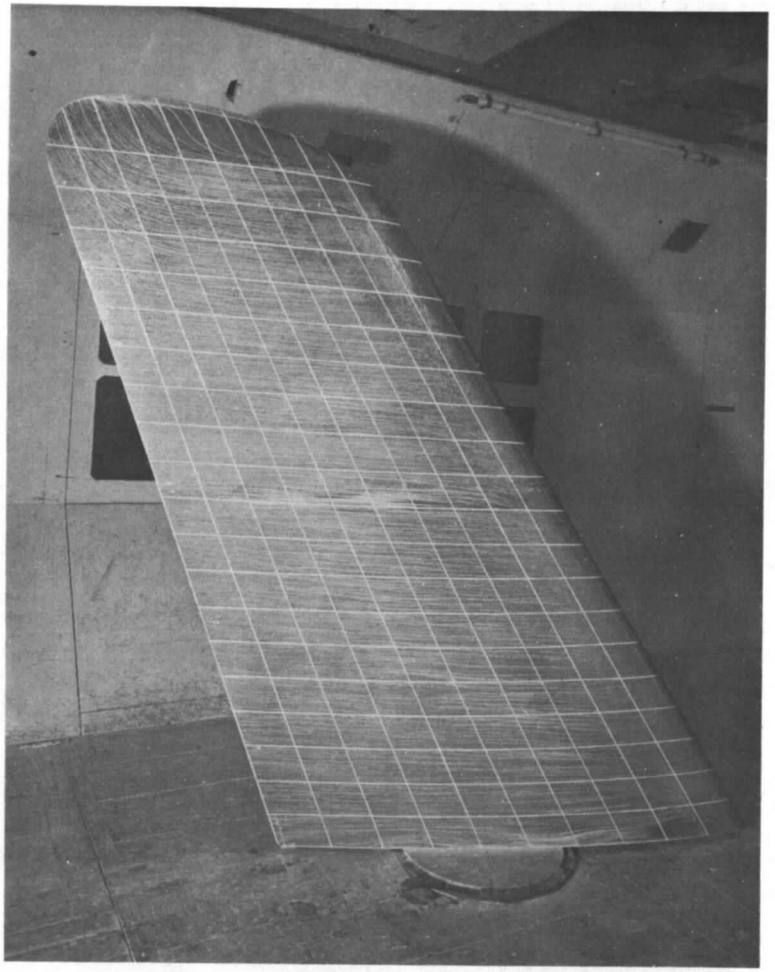

$\alpha = 16{\cdot}5$

FIG. 18. (contd.) Oil flow photograph for plain wing (second droop nose) with part-span flap, V=140 ft/sec

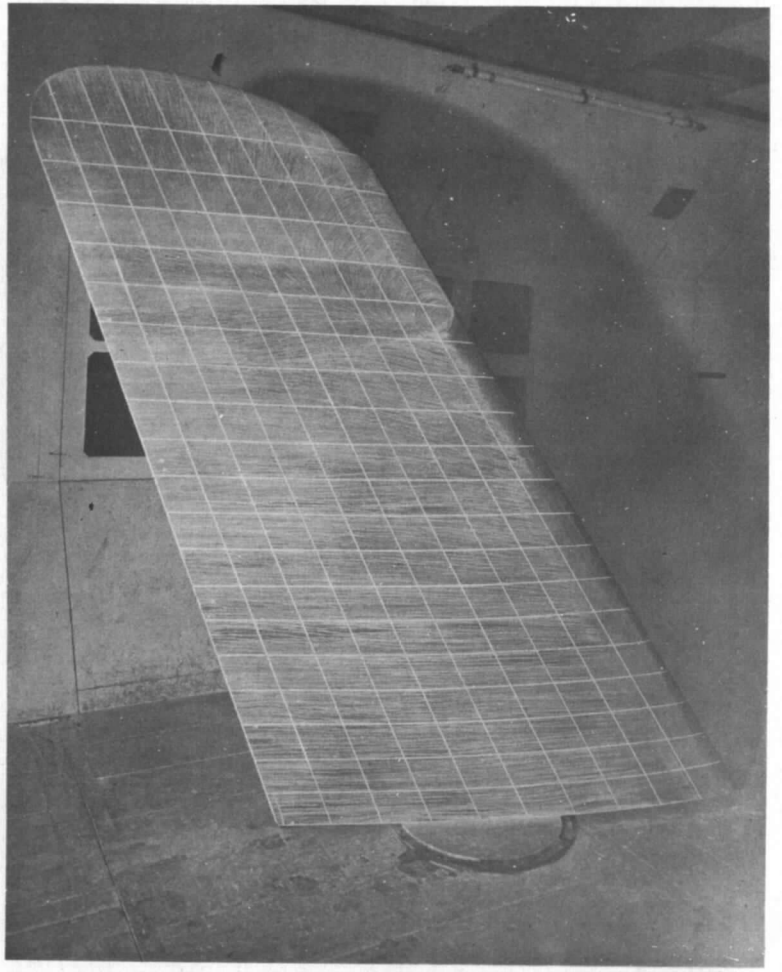

$\alpha = 14°$ (with nose separation)

FIG. 19. Oil flow photograph for plain wing (second droop nose) with full-span flap, V = 140 ft/sec

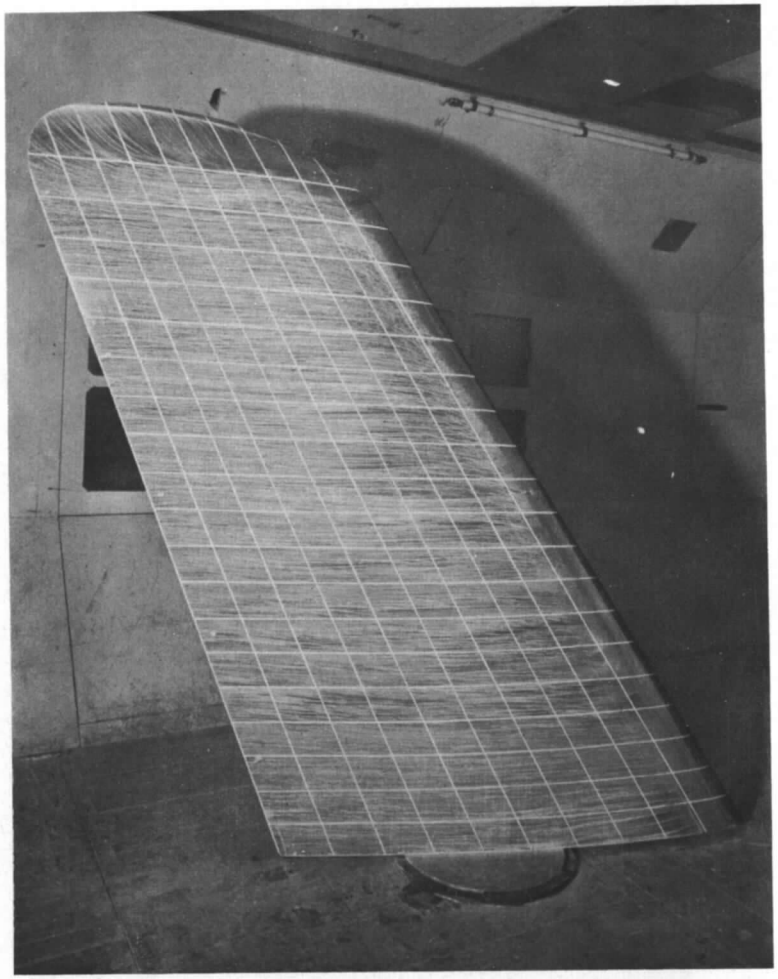

$\alpha = 15°$

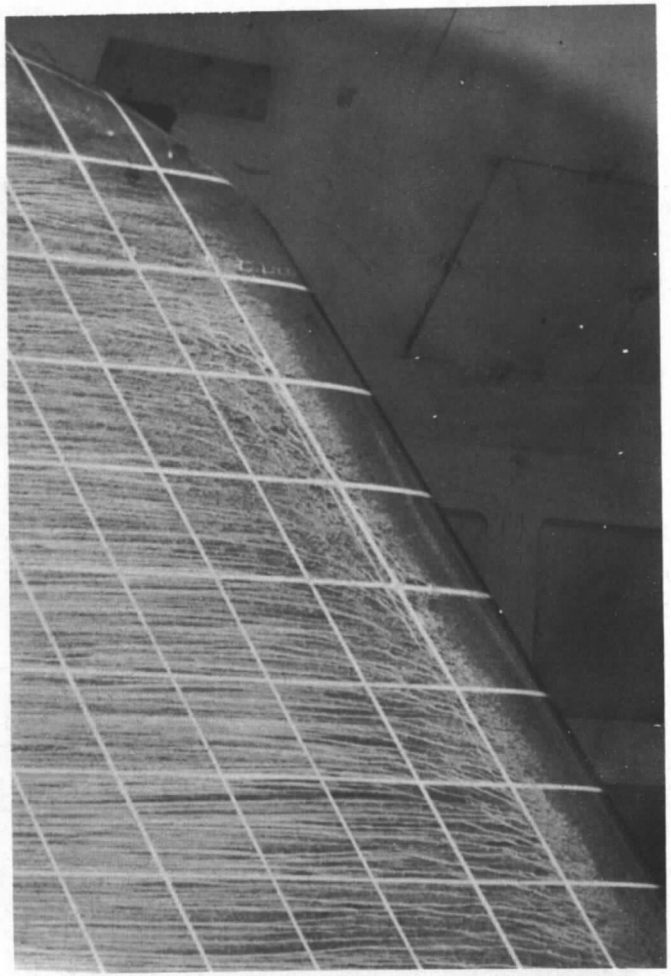

$\alpha = 15°$

FIG. 19 (contd.) Oil flow photographs for plain wing (second droop nose) with full-span flap, V = 140 ft/sec

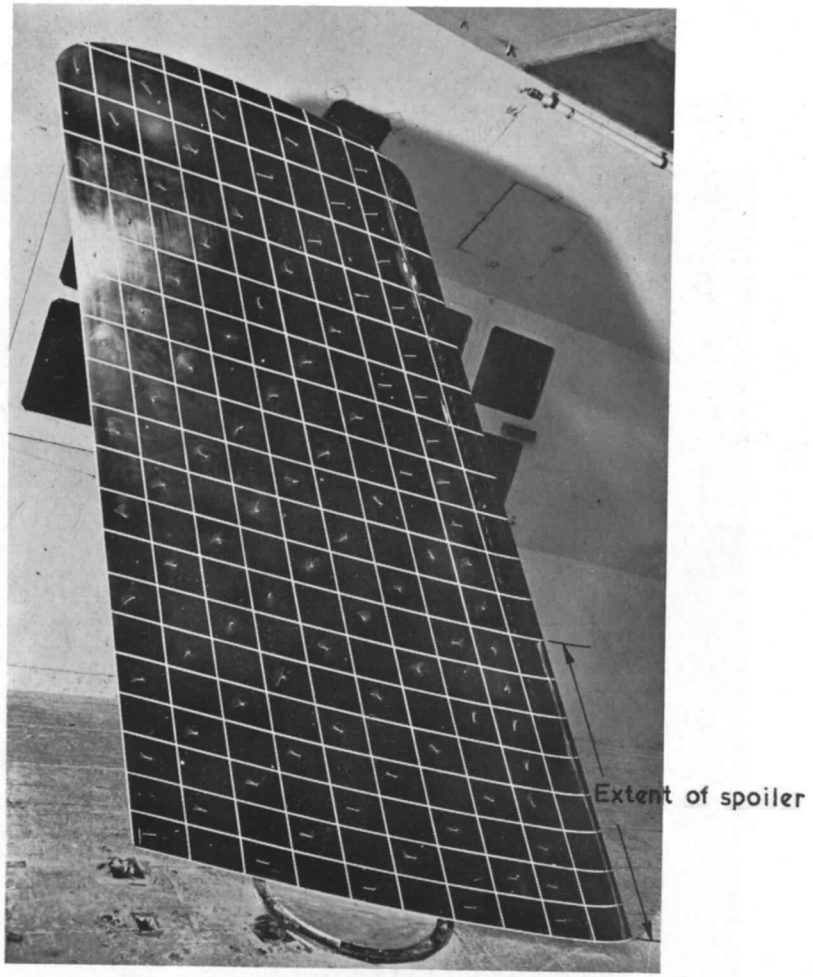

$\alpha = 18°$

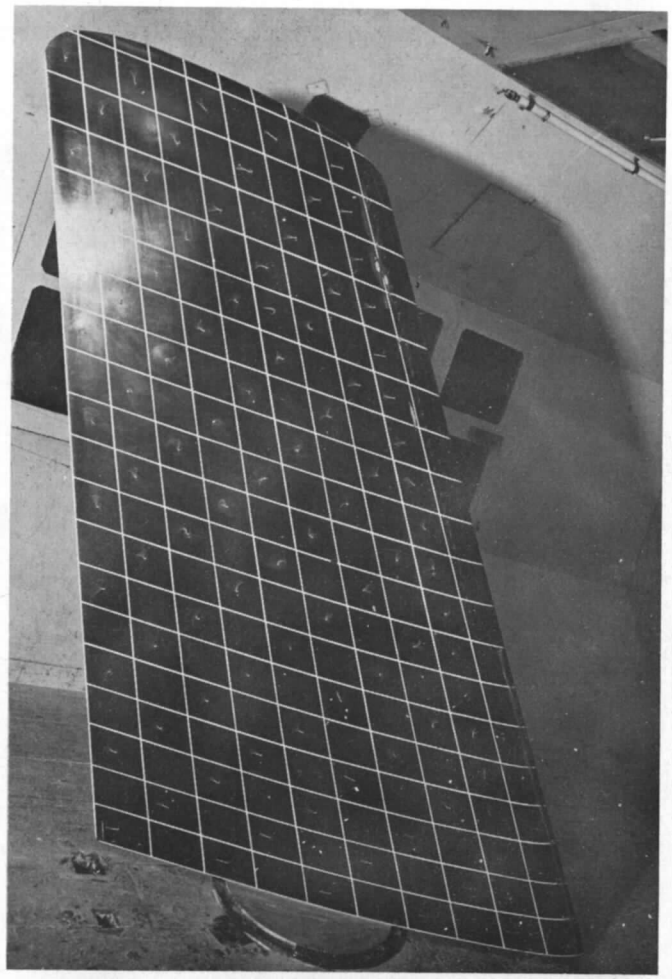

$\alpha = 19°$

FIG. 20. Tuft photographs for wing (first droop nose) with inboard flow spoiler and L.S. and U.S. (two rows) jets, V = 140 ft/sec

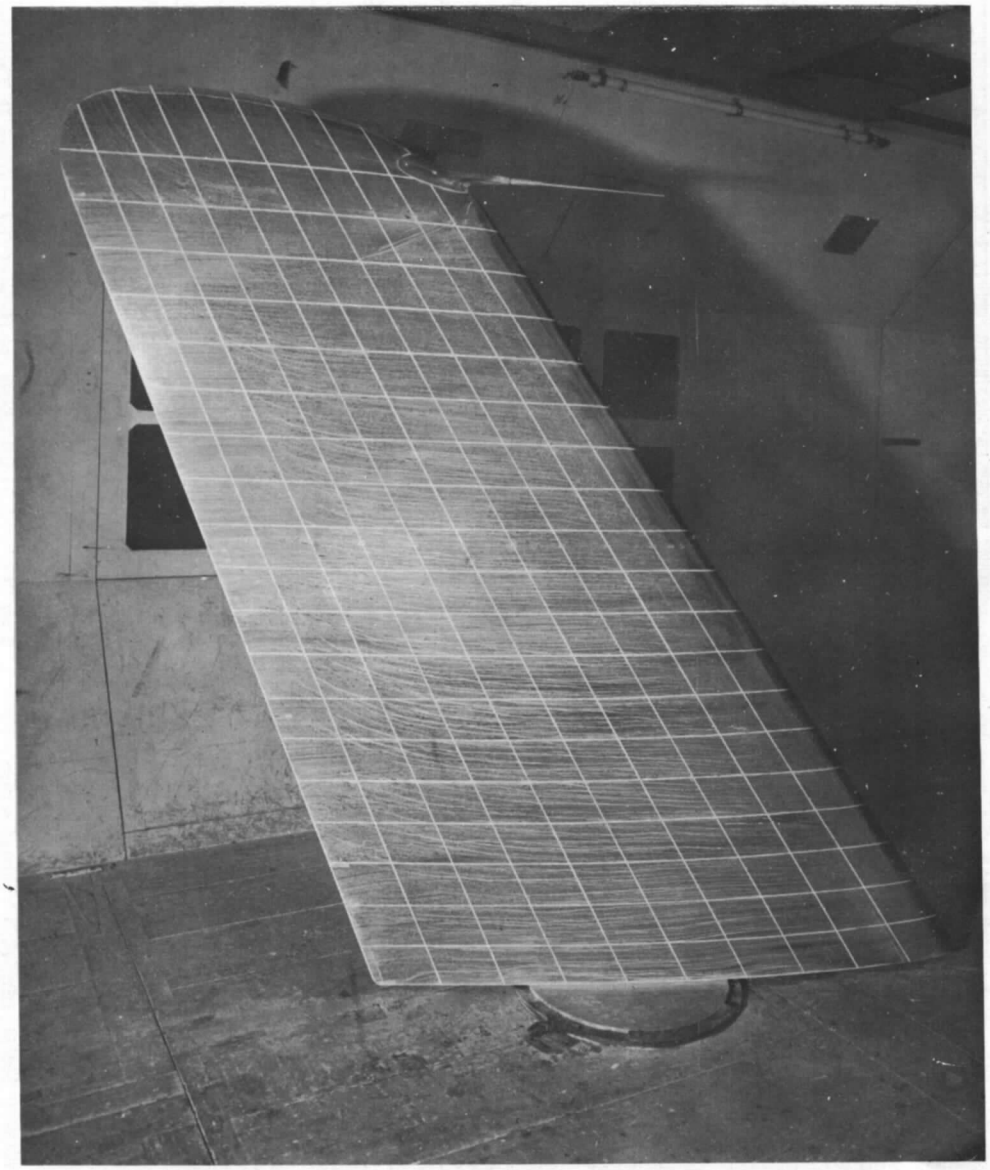

$\alpha = 17{\cdot}5$

FIG. 21. Oil flow photograph for plain wing (second droop nose) with pitot probe. V = 140 ft/sec

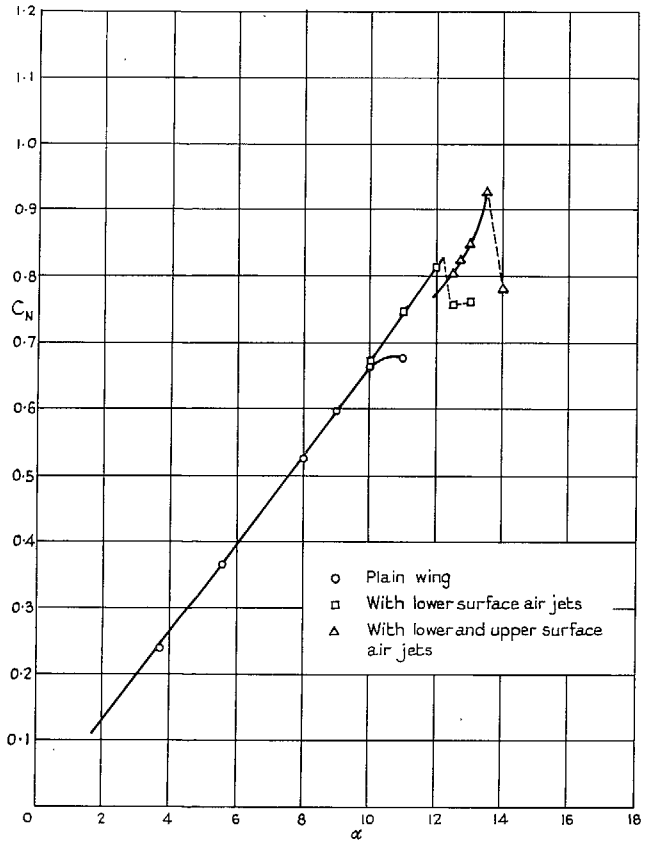

FIG. 22. Normal force coefficient for station A. Original wing

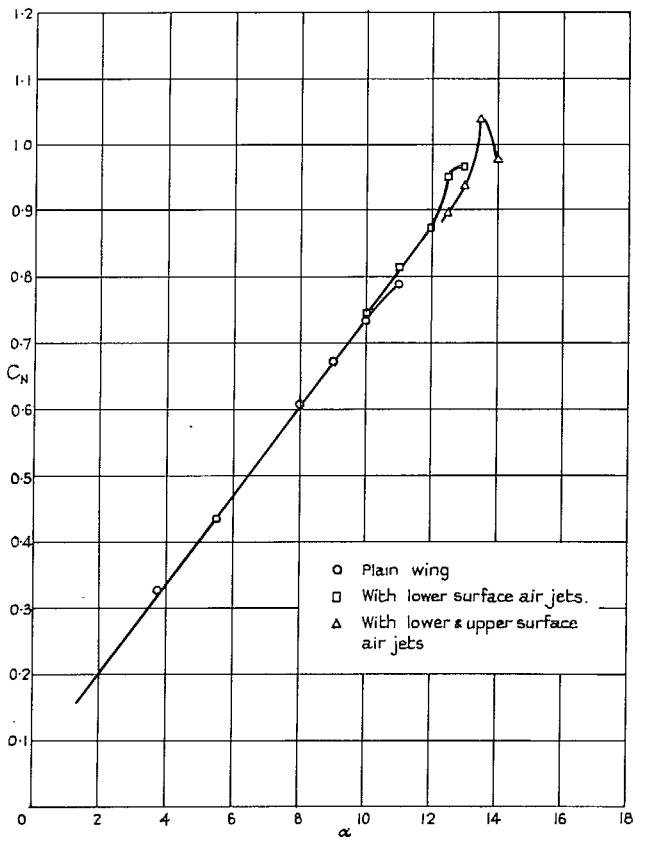

FIG. 23. Normal force coefficient for station B. Original wing

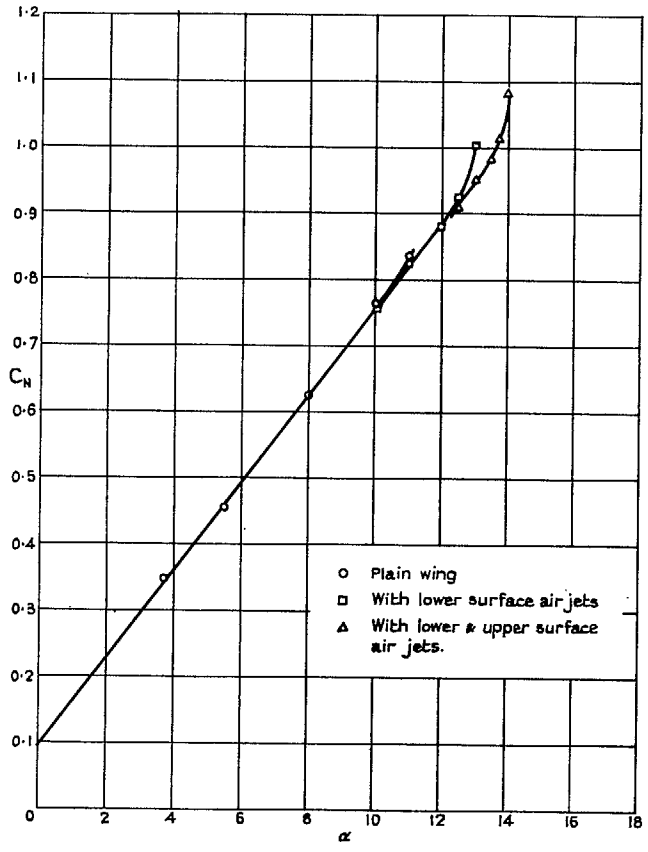

FIG. 24. Normal force coefficient for station C. Original wing.

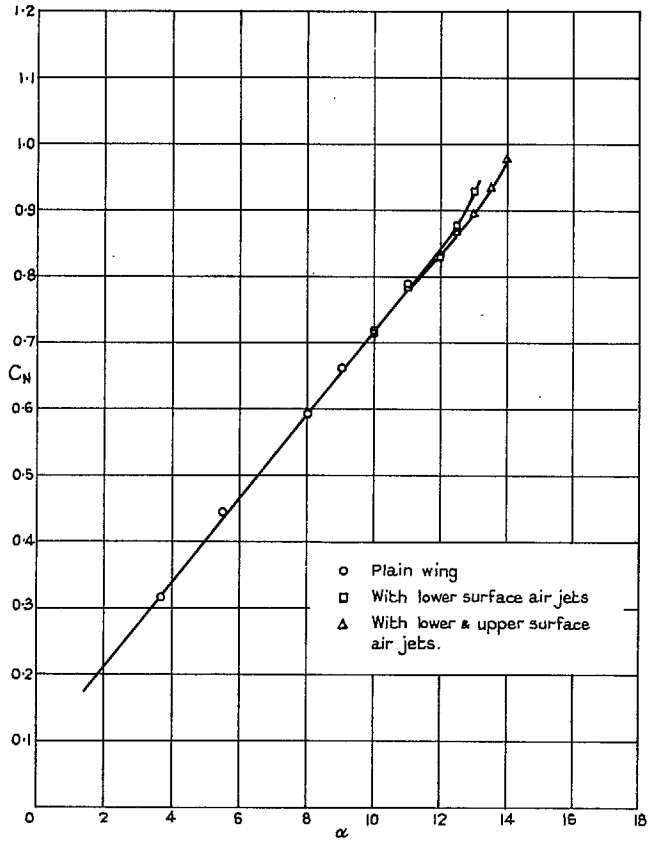

FIG. 25. Normal force coefficient for station D. Original wing.

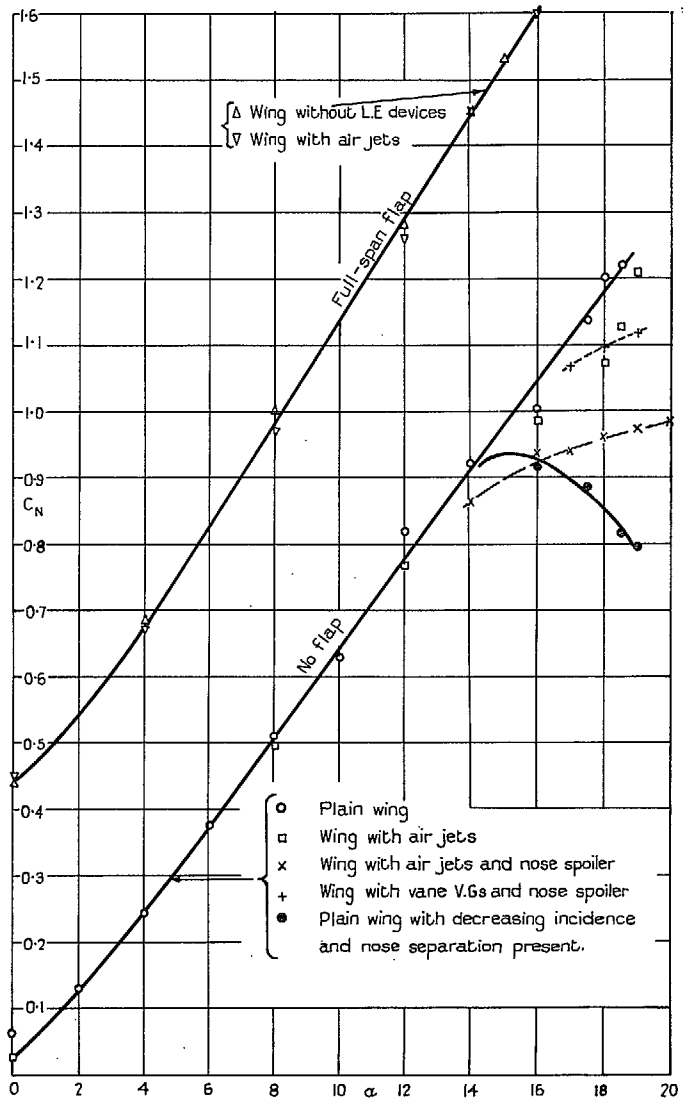

FIG. 26. Normal force coefficient for station A. Second droop nose.

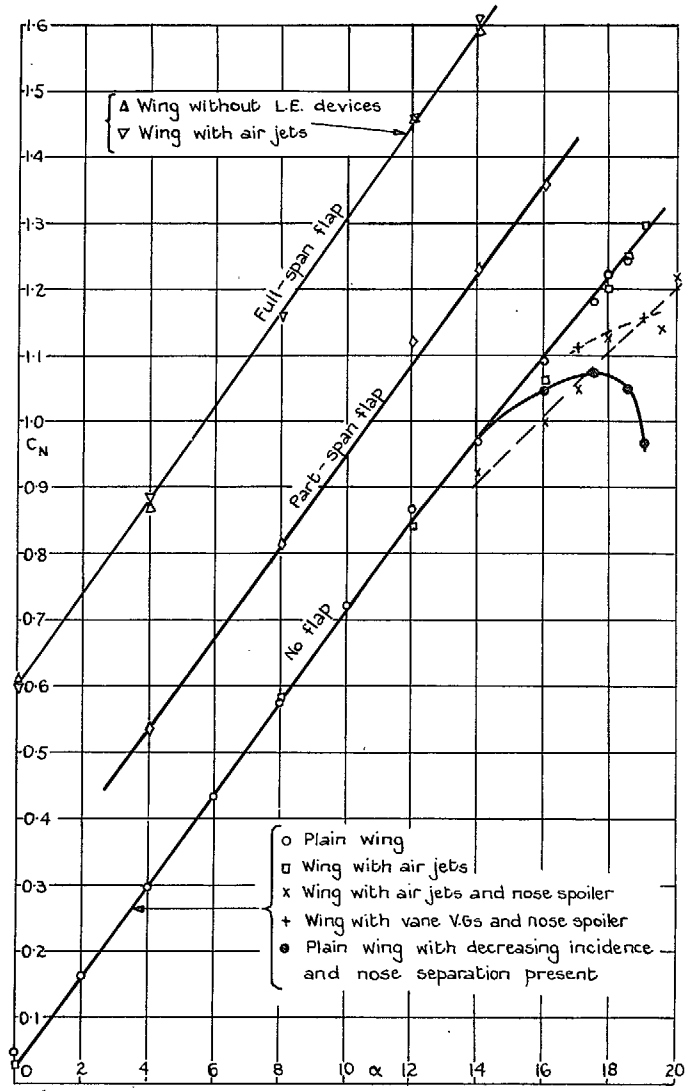

FIG. 27. Normal force coefficient for station B. Second droop nose.

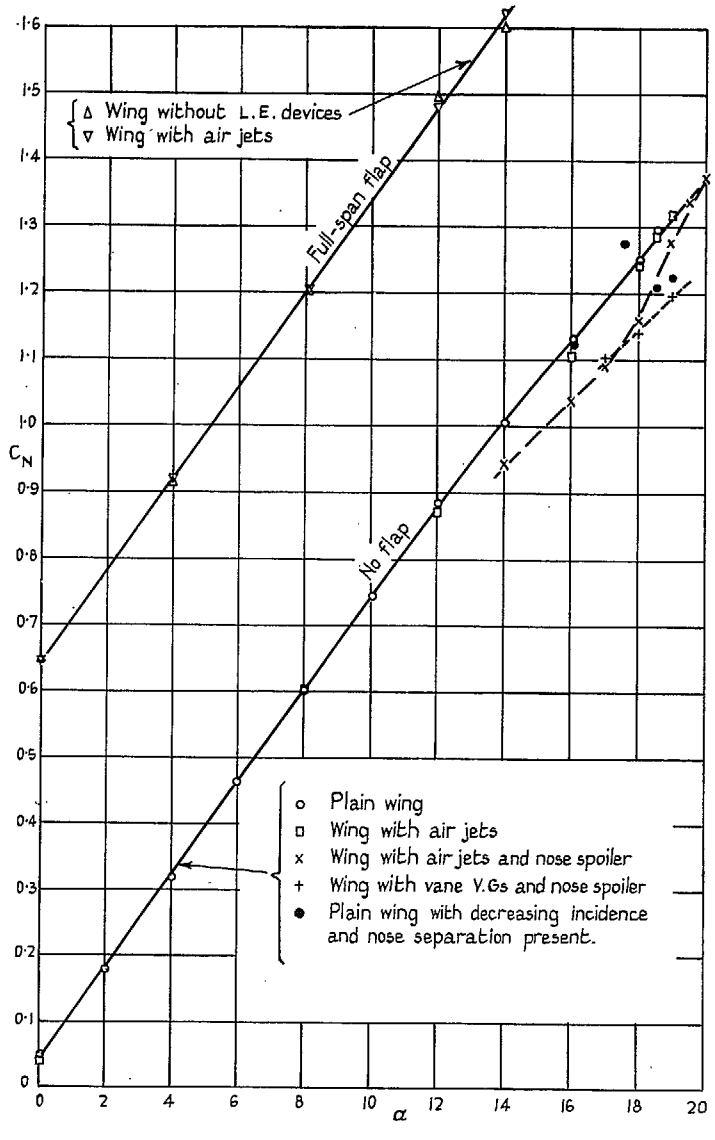

FIG. 28. Normal force coefficient for station C. Second droop nose.

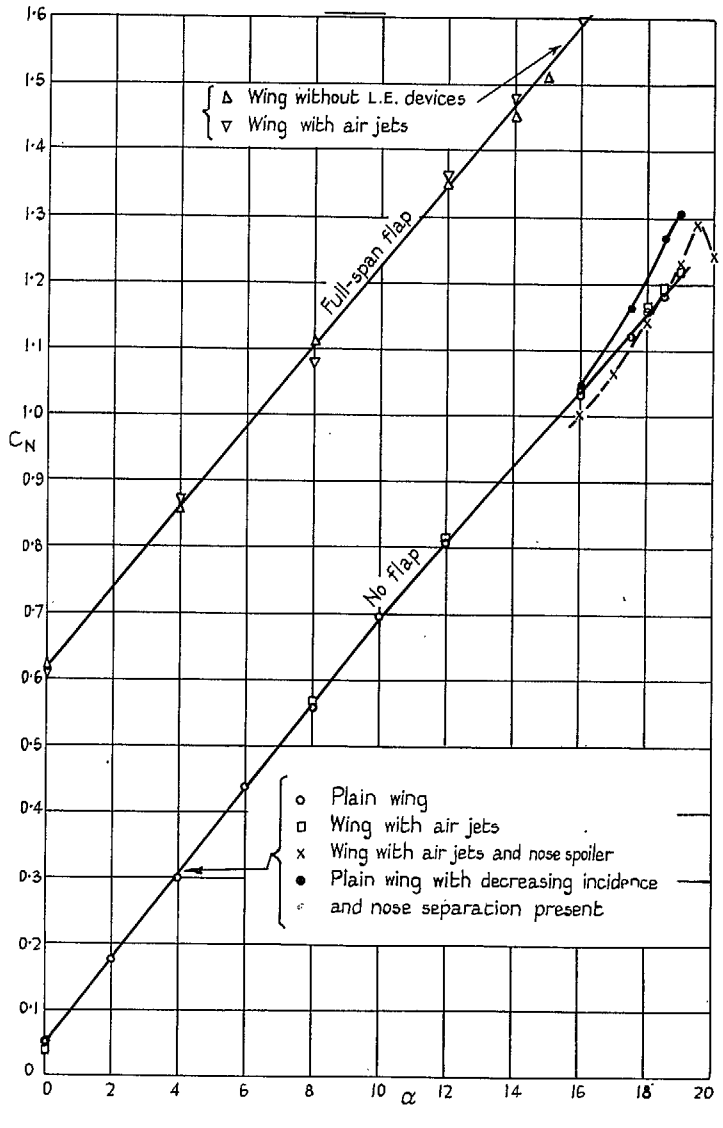

FIG. 29. Normal force coefficient for station D. Second droop nose.

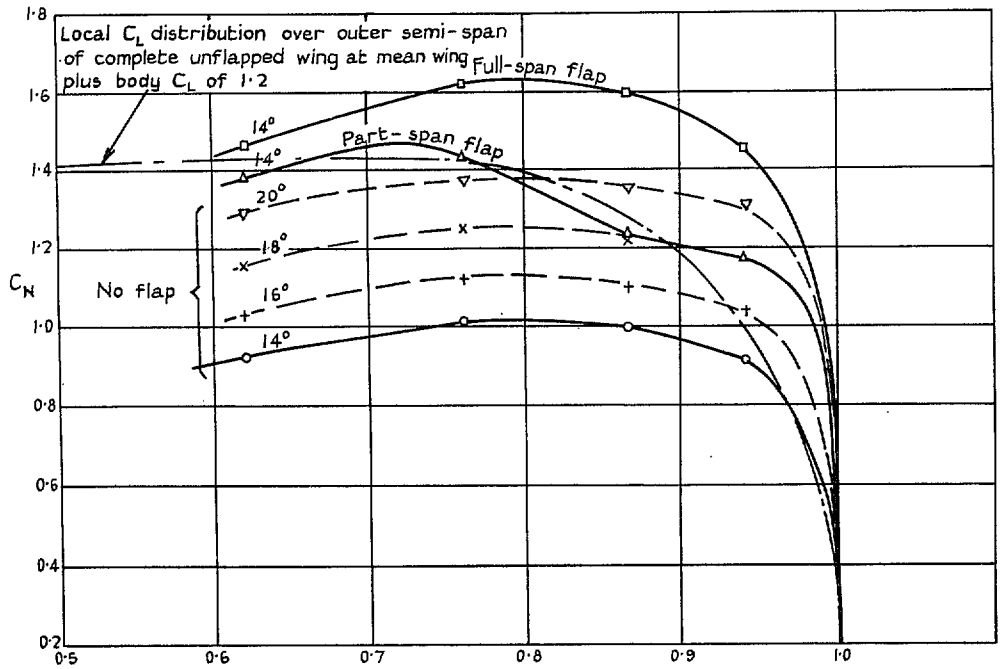

FIG. 30. Spanwise distribution of normal force for different flap conditions and various incidences. Second droop nose

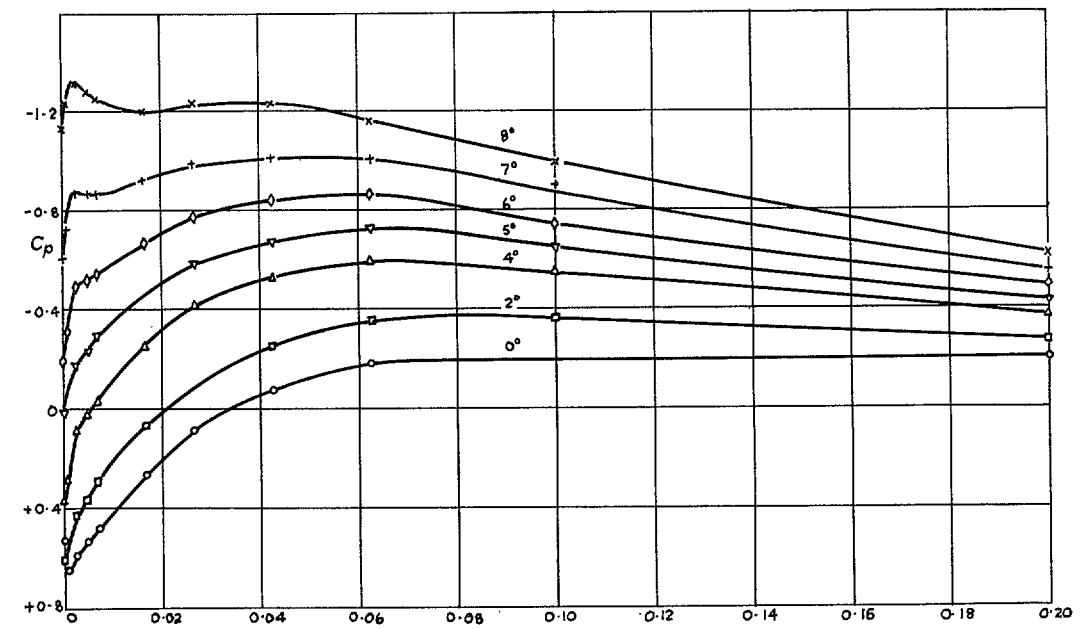

FIG. 31. Development of leading edge suction peak on upper surface. Station C. First droop nose.

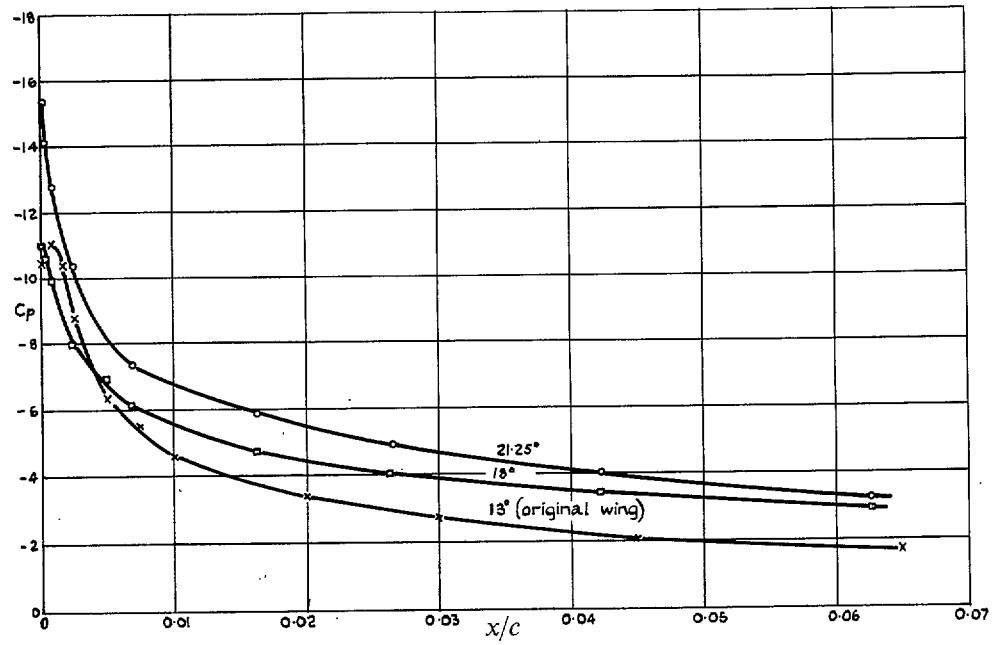

FIG. 32. Upper surface pressure distributions near nose. Station C. First droop nose.

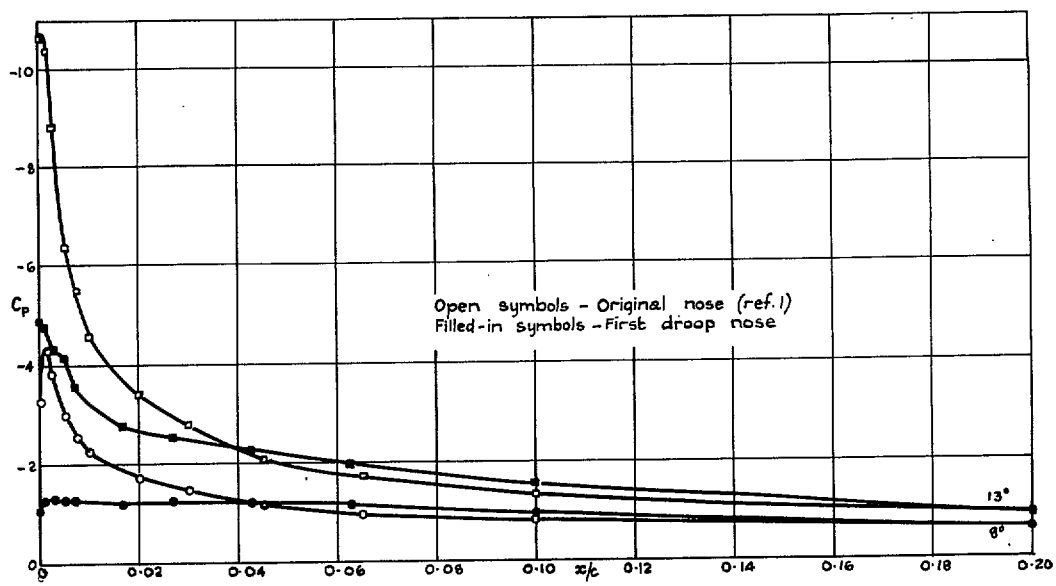

FIG. 33. Upper surface pressure distribution changes near nose with droop. Station C.

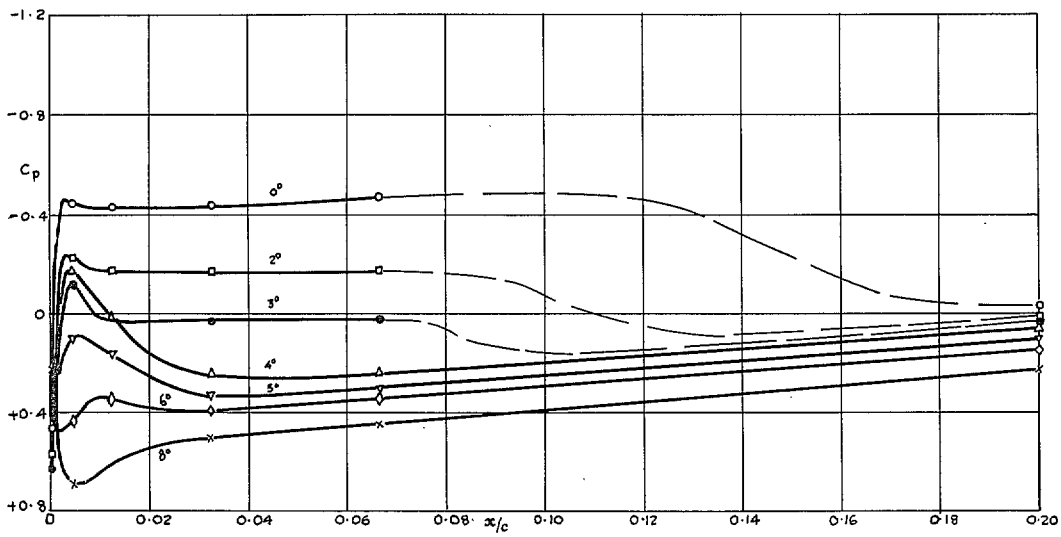

FIG. 34. Lower surface pressure distributions, near nose, showing flow separation at low incidences – Plain wing, Station C. First droop nose.

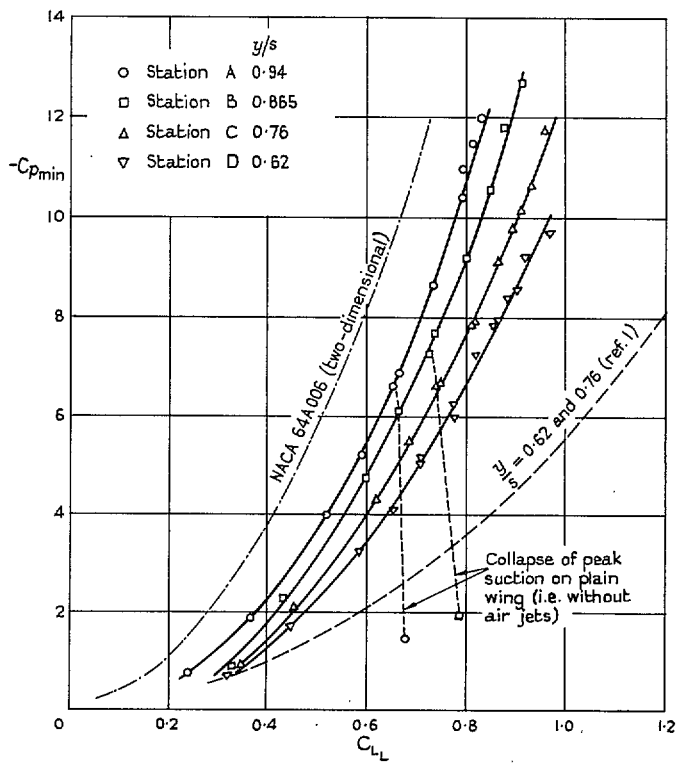

FIG. 35. Minimum pressure coefficient versus local lift coefficient. Original wing.

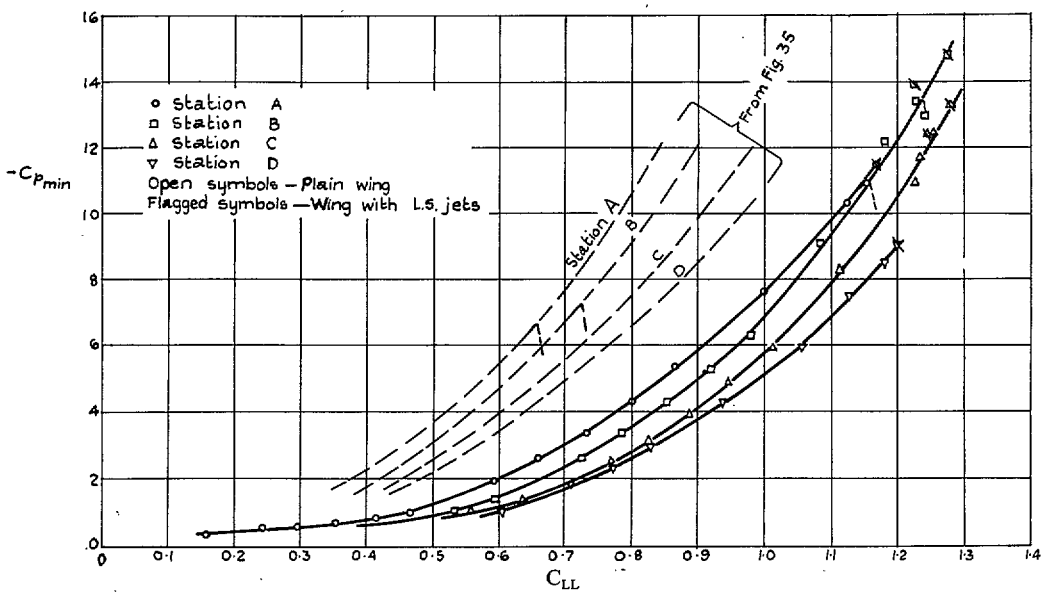

FIG. 36. Minimum pressure coefficient versus local lift coefficient. First droop nose.

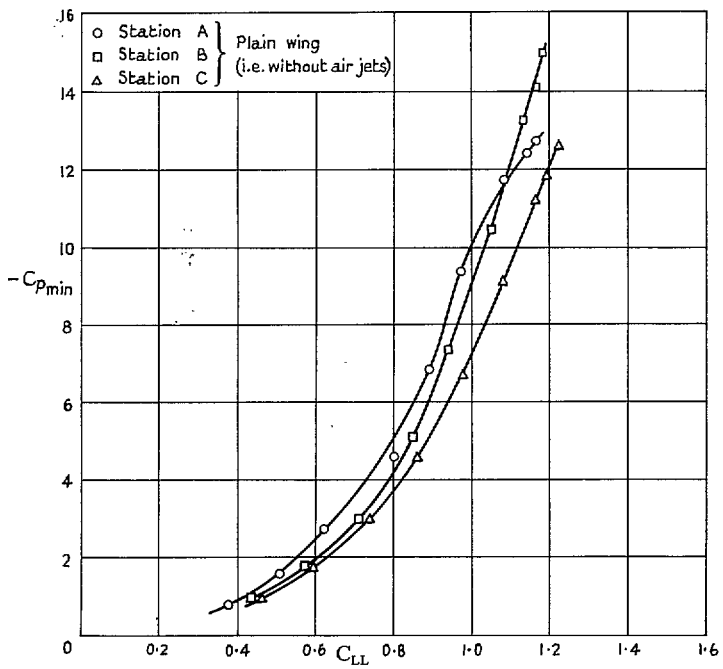

FIG. 37. Minimum pressure coefficient versus local lift coefficient. Second droop nose.

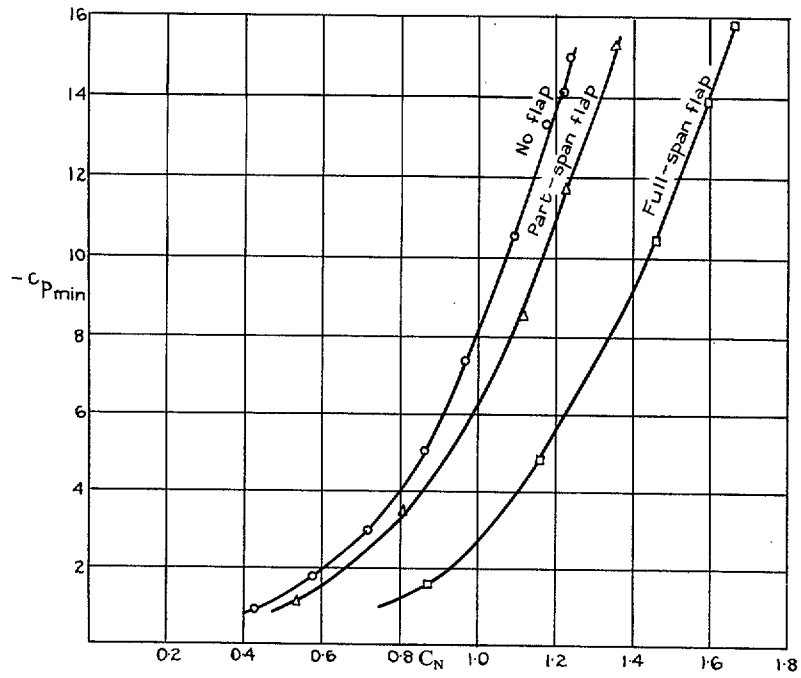

FIG. 38. Effect of flaps on $C_{p\,min}$, at Station B in terms of C_N, for wing without L.E. devices. Second droop nose.

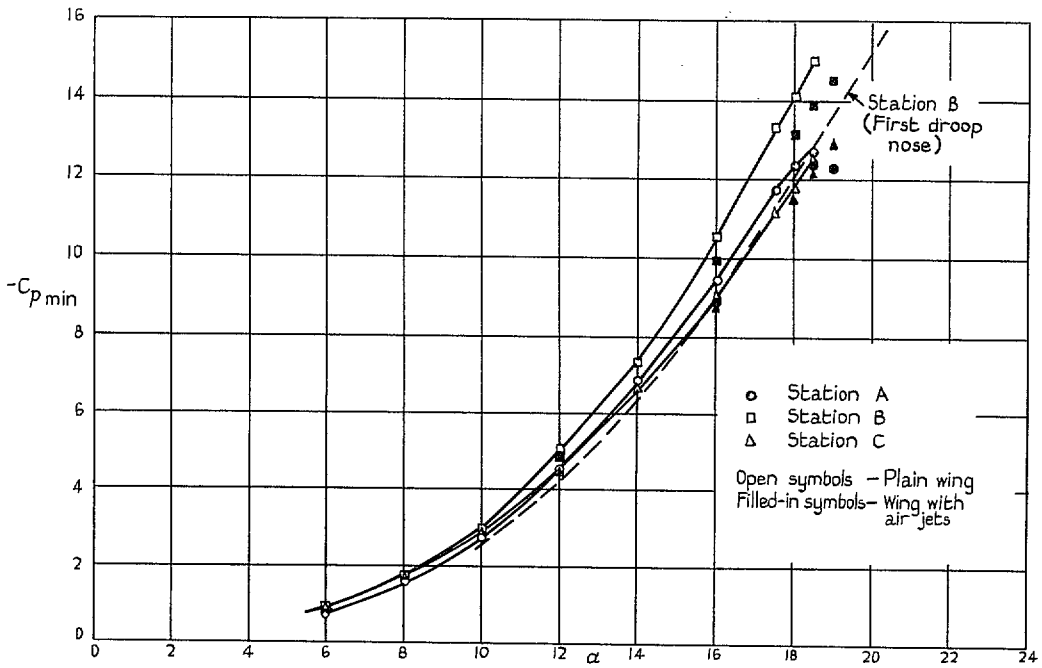

FIG. 39. Minimum pressure coefficient versus incidence. No-flap case. Second droop nose.

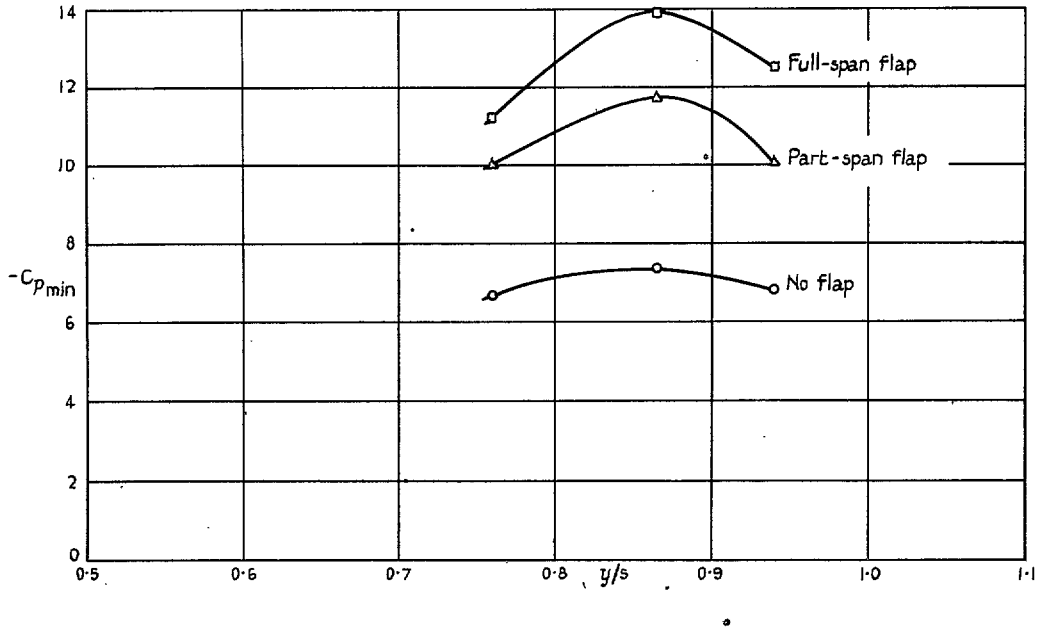

FIG. 40. Spanwise distribution of minimum pressure coefficient at $\alpha = 14°$ for different flap conditions.

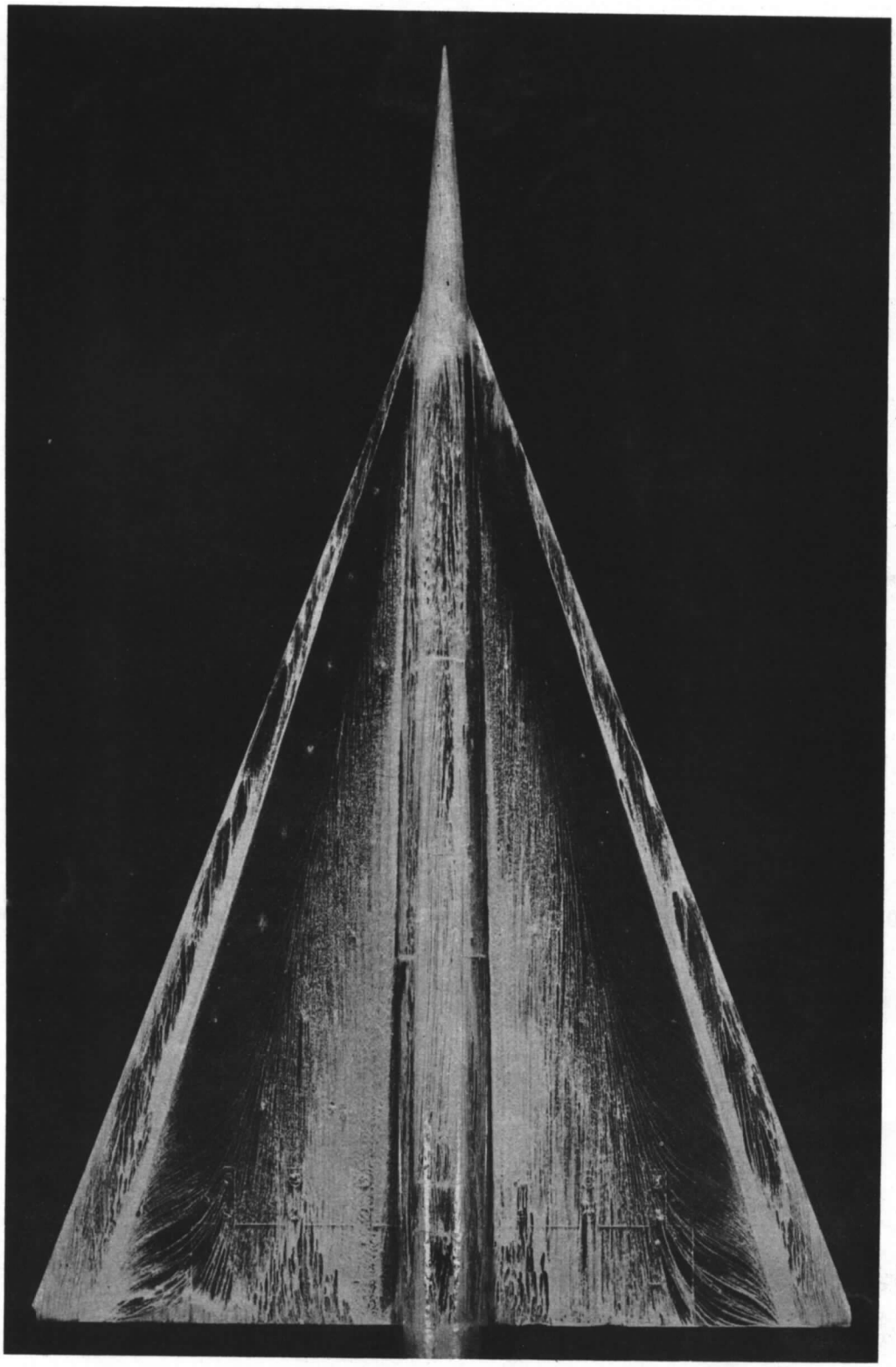

FIG. 41. Type of flow on a highly swept wing at incidence

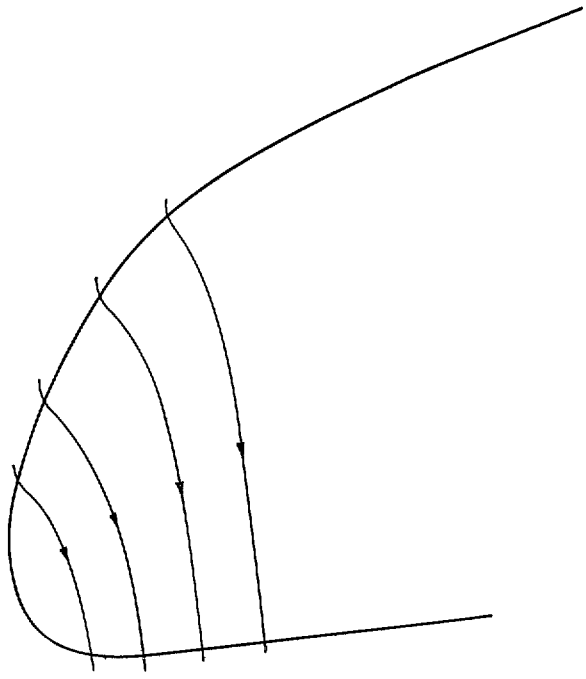

FIG. 42. Postulated flow directions, near surface, for curved wing tip in inviscid flow

Printed in Wales for Her Majesty's Stationery Office by Allens (Cardiff) Limited

Dd 125874 K 5 1/67

Published by
HER MAJESTY'S STATIONERY OFFICE

To be purchased from
49 High Holborn, London W.C.1
423 Oxford Street, London W.1
13A Castle Street, Edinburgh 2
109 St. Mary Street, Cardiff
Brazennose Street, Manchester 2
50 Fairfax Street, Bristol 1
35 Smallbrook, Ringway, Birmingham 5
80 Chichester Street, Belfast 1
or through any bookseller

S.O. Code No. 23-345